To the graduate council:

I am submitting herewith a thesis written by James N. Acree entitled "An Upgrade to the A-10A airplane." I have examined the final copy of this thesis for form and content and recommend that it be accepted in partial fulfillment of the requirements for the degree of Master of Science, with a Major in Aviation Systems.

Mr. Ralph Kimberlin, Major Professor

We have read this thesis
and recommend its acceptance:

Accepted for the Council:

Vice Provost
and Dean of The Graduate School

AN UPGRADE
TO THE
A-10A AIRPLANE

A Thesis

Presented for the

Master of Science

Degree

The University of Tennessee Space Institute, Tullahoma

James N. Acree

December 1990

STATEMENT OF PERMISSION TO USE

In presenting this thesis in partial fulfillment of the requirements for a Master's degree at The University of Tennessee Space Institute, Tullahoma, I agree that the Library shall make it available to borrowers under rules of the Library. Brief quotations from this thesis are allowable without special permission, provided that accurate acknowledgment of the source is made.

Permission for extensive quotation from or reproduction of this thesis may be granted by my major professor, or in his absence, by the Head of Interlibrary Services when, in the opinion of the either, the proposed use of the material is for scholarly purposes. Any copying of use of the material in this thesis for financial gain shall not be allowed without my written permission.

Signature _____

Date 18 November 1990

ABSTRACT

A handling qualities and performance study of the A-10A airplane as applicable to the land-based close air support mission was completed in 1988. Four test flights were conducted with and without external stores, various internal fuel loadings, and center of gravity locations near the center of the recommended operating range. A small sustained maneuvering envelope, as evidenced by poor sustained turn performance, low maximum level airspeed, and slow acceleration capabilities were revealed during these tests. Also low roll rates were displayed. These characteristics are of a serious nature and will make the airplane vulnerable to hostile forces in a high threat environment. Additionally, slow engine response will likely contribute to airplane mishaps during landing evolutions. While the A-10A airplane continued to demonstrate excellent potential for the close air support mission, development of a performance upgrade is recommended.

Engine replacement will offer significant performance improvements with negligible detrimental effects. The proposed General Electric CF34/F7A1 engine will remedy this deficiency. The engine can be available from the manufacturer in the near future and testing can be conducted to verify the predicted performance. A negligible change in center of gravity position due to slightly increased engine weight and a larger fan diameter will not adversely affect flying qualities. However, minimal structural modification due to increased weight and thrust may be necessary for airframe lifetime considerations. Also, several handling quality improvements are recommended and their improvements estimated.

TABLE OF CONTENTS

SECTION		PAGE
1.	INTRODUCTION	1
	1.1 Background	1
	1.2 Purpose of the Study	2
	1.3 Aircraft Description	3
	1.4 Scope and Method of Flight Tests	4
	1.5 Method of Analysis	5
	1.6 Chronology	6
2.	DISCUSSION OF FLIGHT TEST RESULTS	7
	2.1 Aircraft Performance	7
	2.1.1 Takeoff	7
	2.1.2 Climb	7
	2.1.3 Single-engine	8
	2.1.4 Range and Endurance	8
	2.1.5 Acceleration	10
	2.1.6 Maximum Level Airspeed	10
	2.1.7 Sustained Turns	11
	2.1.8 Instantaneous Turns	11
	2.1.9 Maneuvering Envelope	12
	2.1.10 Descent	13
	2.1.11 Landing	13
	2.1.12 Mission Profiles	14
	2.2 Aircraft Handling Qualities	17
	2.2.1 Mechanical Characteristics	17
	2.2.2 Ground Handling	17
	2.2.3 Takeoff	18
	2.2.4 Static Longitudinal Stability	19
	2.2.5 Short Period	20
	2.2.6 Phugoid	21
	2.2.7 Maneuvering Longitudinal Stability	22
	2.2.8 Static Lateral-directional Stability	23
	2.2.9 Dihedral	23
	2.2.10 Sideforce	24
	2.2.11 Longitudinal Characteristics in Sideslips	24
	2.2.12 Aileron Yaw	25
	2.2.13 Spiral Stability	25
	2.2.14 Dutch Roll	26
	2.2.15 Roll Performance	27
	2.2.16 Roll Sensitivity	28
	2.2.17 Trimmability	28
	2.2.18 Roll Coupling	29
	2.2.19 Stall Characteristics	29
	2.2.20 Configuration Changes	31
	2.2.21 Landing	32
	2.2.22 Engine Response	32
	2.2.23 Asymmetric Thrust	33

TABLE OF CONTENTS

SECTION		PAGE
3.	DISCUSSION OF PROPOSED UPGRADES	36
	3.1 Proposed Solutions	36
	3.1.1 Engine	36
	3.1.2 Anti-servo (Leading) Aileron Tabs	38
	3.1.3 Auto-pilot	38
	3.1.4 Turn Coordinator	39
	3.1.5 Takeoff Trim Increase	39
	3.2 Aircraft Performance	40
	3.2.1 General	40
	3.2.2 Takeoff	40
	3.2.3 Climb	42
	3.2.4 Single-engine	41
	3.3.5 Range and Endurance	41
	3.2.6 Acceleration	42
	3.2.7 Maximum Level Airspeed	42
	3.2.8 Sustained Turns	43
	3.2.9 Maneuvering Envelope	43
	3.2.10 Mission Profiles	44
	3.3 Aircraft Handling Qualities	45
	3.3.1 General	45
	3.3.2 Takeoff	45
	3.3.3 Aileron Yaw	46
	3.3.4 Roll Performance	46
	3.3.5 Stall Characteristics	47
	3.3.6 Engine Response	47
	3.3.7 Asymmetric Thrust	47
4.	CONCLUSIONS AND RECOMMENDATIONS	49
	4.1 General	49
	4.2 Specific	49
BIBLIOGRAPHY		51
APPENDICES		52
	APPENDIX A. FLIGHT CONTROL DESCRIPTION	52
	APPENDIX B. ILLUSTRATIONS	55
	APPENDIX C. CURVES	58
	APPENDIX D. ANALYSIS	106
	APPENDIX E. REVISED CURVES	117
	APPENDIX E. LIST OF SYMBOLS	128

LIST OF TABLES

TABLE		PAGE
I.	Takeoff Performance	7
II.	Range Characteristics	9
III.	Endurance Characteristics	9
IV.	Maximum Sustained Turn Performance	11
V.	Maximum Instantaneous Turn Performance	12
VI.	Landing Performance	14
VII.	Close Air Support Profile	15
VIII.	Ferry Profile	15
IX.	Primary Control System Mechanical Characteristics	17
X.	Flight Path Stability	20
XI.	Short Period Characteristics	21
XII.	Dutch Roll Characteristics	26
XIII.	Stall Performance	30
XIV.	Improved Close Air Support Profile	44
XV.	Improved Ferry Profile	44

LIST OF FIGURES

FIGURE		PAGE
1.	A-10A Airplane Overview (General)	56
2.	A-10A Weapon Carriage Stations	57
3.	A-10A Center of Gravity Travel During Flight Tests	59
4.	A-10A Fuel Required to Climb	60
5.	A-10A Time Required to Climb	61
6.	A-10A Distance Required to Climb	62
7.	A-10A Single-Engine Rate of Climb	63
8.	A-10A Single-Engine Angle of Climb	64
9.	A-10A Cruise Fuel Flow	65
10.	A-10A Cruise Specific Range	66
11.	A-10A Cruise Endurance/Angle of Attack Correlation	67
12.	A-10A Cruise Range/Angle of Attack Correlation	68
13.	A-10A Energy Height During a Level Acceleration	69
14.	A-10A Maximum Sustained Load Factor	70
15.	A-10A Maximum Sustained Turn Rate	71
16.	A-10A Minimum Sustained Turn Radius	72
17.	A-10A Maximum Instantaneous Load Factor	73
18.	A-10A Maximum Instantaneous Turn Rate	74
19.	A-10A Minimum Instantaneous Turn Radius	75
20.	A-10A Total Maneuvering Envelope	76
21.	A-10A Fuel to Glide Descend	77
22.	A-10A Time to Glide Descend	78
23.	A-10A Distance to Glide Descend	79
24.	A-10A Fuel for Penetration Descent	80
25.	A-10A Time for Penetration Descent	81
26.	A-10A Distance for Penetration Descent	82
27.	A-10A Ferry Mission Profile	83
28.	A-10A Close Air Support Mission Profile	84
29.	A-10A Longitudinal Control Gradient	85
30.	A-10A Lateral Control Gradient	86
31.	A-10A Directional Control Gradient	87
32.	A-10A Cruise Static Longitudinal Stability	88
33.	A-10A Landing Static Longitudinal Stability	89
34.	A-10A Landing Flight Path Stability	90
35.	A-10A Cruise Short Period Characteristics	91
36.	A-10A Landing Short Period Characteristics	92
37.	A-10A Cruise Phugoid Characteristics	93
38.	A-10A Landing Phugoid Characteristics	94
39.	A-10A Cruise Longitudinal Maneuvering Stability	95
40.	A-10A Landing Longitudinal Maneuvering Stability	96
41.	A-10A Cruise Static Lateral-Directional Stability	97
42.	A-10A Landing Static Lateral-Directional Stability	98
43.	A-10A Cruise Spiral Stability	99
44.	A-10A Landing Spiral Stability	100
45.	A-10A Cruise Dutch Roll Characteristics	101
46.	A-10A Landing Dutch Roll Characteristics	102
47.	A-10A Roll Performance	103
48.	A-10A Cruise Roll Sensitivity	104

FIGURE PAGE

49. A-10A Landing Roll Sensitivity 105
50. A-10A Wingspan efficiency 109
51. A-10A Aircraft Drag 114
52. Improved Fuel to Climb 119
53. Improved Time to Climb 120
54. Improved Distance to Climb 121
55. Improved Single-Engine Rate of Climb 122
56. Improved Single-Engine Angle of Climb 123
57. Improved Cruise Fuel Flow 124
58. Improved Cruise Specific Range 125
59. Improved Maximum Sustained Load Factor 126
60. Improved Maximum Sustained Turn Rate 127
61. Improved Minimum Sustained Turn Radius 128
62. Improved Total Maneuvering Envelope 129

1. INTRODUCTION

1.1 Background

The U. S. Air Force has identified the need to improve the weapons delivery capability, especially through survivability, of their fixed-wing close air support mission aircraft. Currently the service uses the A-7D Corsair and the A-10A Thunderbolt. Significant defense budget cutbacks are inevitable (due to a perceived decreased international threat and current national deficit problems) and will likely influence any decisions. Three options have been proposed to meet this need: the A-16, the A-7F, and an A-10 upgrade.

The close air support mission demands that an aircraft have the capability to either operate from a small and imperfect airstrip close to the battlefield, or travel greater ranges from established airfields. The aircraft must be able to make small radius turns in order to optimize time in the vicinity of the battlefield. It must be capable of rapid energy addition at low altitude, or it must keep its energy level high for evasive maneuvers. Fast ingress and egress from hostile areas is a necessity to minimize vulnerability. It must have good survivability in that it can avoid and/or sustain some degree of combat damage. Finally, it must be able to accurately deliver a variety of weaponry against a variety of target types, in order to provide maximum flexibility in a constantly-changing combat environment.

The General Dynamics F-16 Falcon has displayed an impressive air-to-ground combat capability in addition to its designed air-to-air mission. A derivative, the A-16, would incorporate all of the high-energy and aerodynamic benefits of the F-16 and be fitted with air-to-ground mission systems. But the Falcon exhibits its good performance at high subsonic airspeeds, which results in a large turn radii. It would find effective operation in a confined battlefield environment difficult. Standoff employment of air-to-surface missiles

(such as the Maverick) would be nearly impossible at high airspeeds without subsequent overflight of the target area and unneccessarily exposing the aircraft to hostile return fire. Additionally, the Falcon derives its high energy capabilities from a small airframe, which contains little fuel, and results in very short mission ranges (unrefueled). The development and production costs of the A-16 no doubt, will be expensive as well.

The LTV A-7 Corsair has served both the U. S. Air Force and Navy in the air-to-surface role, but suffers from out-of-date mission avionics technology. An ongoing improvement increases airplane performance by incorporating a new, afterburning engine. The fuselage is lengthened and slightly more streamlined. New mission avionics updates weapon delivery capabilities. Yet the airframe is again optimized at high airspeeds, causing the same difficulty as for the A-16 above. Use of the afterburning engine during the mission phase of the flight would also degrade range capabilities.

The Fairchild A-10A Thunderbolt airplane design reveals energy optimization in the slower airspeed regimes, and associated small turn radii. It has both a short-field launch capability as well as excellent range performance. Its duality of powerplants, flight control systems, and independent flight surfaces offer excellent survivability benfits. Also, it offers a very stable platform for the accurate achievement of weapon release parameters. Unfortunately the airplane exhibits poor overall energy characteristics (maximum level airspeeds, sustained maneuvering performance and energy addition capabilities).

1.2 Purpose

The purpose of this test was to evaluate the handling qualities and performance of the A-10A airplane for the close air support mission and to introduce and predict the effectiveness of proposed improvements.

1.3 Airplane Description

The A-10A, built by the Fairchild Republic Company, is a single-seat, twin turbofan airplane with a low rectangular wing and twin vertical stabilizers. The wing has 7^{o} of dihedral outboard of the main landing gear pods, and has stall strips on the leading edges. Pylon-mounted nacelles, extending laterally from the aft fuselage, support TF34-GE-100/91-100A engines which provide a sea level, standard day, installed static thrust of 9,000 lb. each (maximum). The cockpit has titanium armor protection, is pressurized, and contains a "zero-zero" capable ejection seat escape system. Airplane features include an auxiliary power unit, inflight boom-refueling capability, and forward-retractable tricycle landing gear with steerable nosewheel and anti-skid main wheel brakes. Gear retraction causes the Center of Gravity to move forward 1.7 percent of the Mean Aerodynamic Chord (%MAC). The main landing gear wheels remain partially exposed when retracted, in order to avoid lockup if battle damage is sustained. The primary flight control system is irreversible and consists of conventional ailerons and elevators, and twin rudders. Multiple backup modes are built into the flight control system, including a manual reversion mode (reversible). The controls are powered by two independent hydraulic systems for redundancy and augmentation is provided for rate damping in the pitch and yaw axes. Electrically-operated trim is available in all axes. The ailerons consist of split upper and lower panels that also serve as speedbrakes when selected. Four trailing edge wing flaps and two leading edge slats are hydraulically-operated and electrically-actuated. The flaps are pilot-selectable; the slats are automatically programmed according to angle of attack and Mach number. The airplane has a 30mm gun and and 11 hard points for armament. A Heads Up Display (HUD) provides weapon aiming and flight status information to the pilot. An Inertial Navigation System (INS) is installed. A laser-illuminator detector pod extends down from the right front fuselage in order to alert the pilot to designated targets.

The fuel system consists of 4 internal tanks with a capacity of 10,520 lb. of fuel (JP-4), and the airplane has a capability to hold 22,040 lb. (total) with 3 external tanks mounted. A more detailed description of the airplane is contained in the A-10A Flight Manual. A detailed flight control description is presented in appendix A. Appendix B, figures 1 and 2 show the A-10A airplane.

1.4 Scope and Method of Tests

Handling qualities and performance were evaluated during four daytime flights totalling 6.0 hours under both visual and instrument meteorological conditions. All flights originated and terminated at Truax Airfield in Madison, Wisconsin, where the surface elevation was 850 ft. MSL. Tests were performed at up to 25,000 ft. MSL, 450 KOAS, and load factors of -0.5 to 6.0 g's.

Takeoff loadings for all flights included one pilot, full internal fuel, 9 weapons pylons (stations 2 and 10 removed), and between 620 and 1020 rounds of 30mm ammunition. The ammunition was loaded moderately forward of the center of gravity and each round weighed about one pound. The laser-illuminator detector pod was not installed for any of the test flights. Two flights had empty aircraft weapon pylons (load A). Two test flights were flown with external store loadings (load B) of two maverick missiles (stations 3 and 9) and six BDU-33 practice bombs loaded on two TER-9 racks (stations 4 and 8). Airplane gross weight during the test flights varied between 31,000 and 39,500 lb. and center of gravity varied between 22.6 and 26.3 %MAC. Appendix C, figure 3 presents CG travel for each loading.

Three configurations were tested: takeoff, cruise, and landing. The takeoff condition consisted of landing gear down and maneuver flaps. The cruise condition included gear and flaps up. The landing condition included gear down, flaps down, and

speedbrakes extended approximately one-half of the total available extention (as recommended by the Flight Manual). Thrust levels varied and are defined by individual test. Both pitch and yaw SAS were engaged unless specifically addressed in the conditions for that test.

Tests were oriented to a mission which must include all-weather target ingress and egress, day/VMC close air support, first pass tank kill capability, self-contained survivability in a high threat environment, and the ability to scramble takeoff with minimal delay.

Flight manual recommended speeds for takeoff, climb, cruise, descent, and landing were used in establishing flight conditions for performance data. Test instrumentation consisted of a hand-held force gage, stopwatch, and cloth tape measure. Control stick forces and displacements were measured; rudder pedal forces and displacements were estimated. Sideslip angles were estimated by referencing the directional gyro headings. Angle of attack was measured in units displayed, not by actual degrees. Takeoff and landing distances were estimated by reference to airfield objects, such as runway markers, buildings and towers. Bomb and gunnery impacts were measured by spotters on a scorable target. Data were recorded inflight on kneeboard cards, a portable voice recorder, and on the airplane cockpit television video recorder. The test results are detailed in a DT-IIA Technical Report. Specific test methods are detailed in the U. S. Naval Test Pilot School Flight Test Techniques and Fixed Wing Performance manuals. Tasks were judged according to NASA's Pilot Rating in the Evaluation of Aircraft Handling Qualities.

1.5 Method of Analysis

Numerical analysis was accomplished using the performance equations presented in Appendix D. Basic performance derivations and assumptions are detailed in the U. S.

Naval Test Pilot School's Airplane Performance. In order to simplify performance analysis, the following assumptions were made:

a. Engine thrust remains constant throughout the aircraft's airspeed envelope.

b. Engine thrust remains constant from sea level to 6,000 ft. MSL.

c. Induced drag is negligible at high speeds (V_{max}).

d. c_{do} is constant throughout the aircraft's airspeed envelope (up to 0.7M).

e. The drag polar is parabolic.

1.6 Chronology

Flight testing by the author was accomplished from 17 October to 3 November of 1988. During the following year, defense budget cuts forced the U. S. Air Force to re-evaluate plans to develop expensive replacements to the A-10A airplane for the mission. The author began a search for proposed improvements to the A-10A in January of 1990. The performance improvements were calculated and the first draft of this report written in May of 1990. Assistance from various sources helped to formulate this final document.

2. DISCUSSION OF FLIGHT TEST RESULTS

2.1 Performance

2.1.1 Takeoff

Takeoff performance was evaluated during three takeoffs. The runway was dry and level. Takeoff performance characteristics are presented in table I.

Table I
TAKEOFF PERFORMANCE

Gross Wt./Load (lb / A or B)	Headwind (kt.)	Altitude (ft. MSL)	Air Temperature (^{O}F.)	Ground Roll Distance (ft.)	Takeoff Speed (KOAS)
37,500 / A	11	730	45	2,000	138
39,000 / B	0	880	30	2,000	140
39,000 / B	0	1,050	40	2,000	140

The fuel used during the ground roll and acceleration to the recommended climb airspeed (200 KOAS) was minimal (65 lb.), being less than 1 % of the total capacity. The average takeoff distance was 2,000 ft. This was well within the average short field runway length (4,000 ft.) to be expected during forward-deployed operations. This short ground roll provides ample margin for safe aborts. The takeoff performance was satisfactory.

2.1.2 Climb

Climb performance was evaluated in the cruise condition and at maximum thrust. Climb schedule was as recommended by the flight manual, and varied with altitude at between 175 and 200 KOAS. A climb from 5,000 to 25,000 ft. MSL (load A, 37,000 lb.) and a climb from 3,000 to 15,000 ft. MSL (load B, 38,500 lb.) were performed. Appendix C, figures 4, 5, and 6 show climb fuel, time, and distance for both loadings.

Both climbs consumed less than 6% (600 lb.) of the total fuel capacity and required less than 10 minutes. The altitudes of 15,000 and 25,000 ft. MSL are representative of transit altitudes for the respective flight loadings as fuel efficiency is adequate (section 2.1.4) at those flight conditions. The fuel expended to climb to optimum cruising altitudes and the climb performance were satisfactory.

2.1.3 Single-engine

Single-engine performance was evaluated during three climbs in the normal takeoff configuration. Climb airspeeds were a constant 120, 135, and 150 KOAS. The climbs were performed at 5,000 ft. MSL and at a free air temperature 20^{o} lower than that for standard day. Average gross weight was 33,000 lb. with load A. Appendix C, figures 7 and 8 show climb rate and angle versus airspeed. Maximum rate of climb under the conditions of test was 490 ft./min. at 133 KOAS. Maximum angle of climb in this condition was 2.1 degrees at 120 KOAS. Upon engine failure at takeoff, the angle of climb will be insufficient to clear ground obstacles near the runway. The low single-engine climb angle was unsatisfactory.

2.1.4 Range and Endurance

Range and endurance performance was evaluated at various stabilized airspeeds during level flight at 5,000, 15,000, and 25,000 ft. MSL in loads A and B in the cruise condition. The.average gross weight was 36,700 lb. Flight conditions were favorable for engine performance, being approximately 30^{o} Fahrenheit below standard day temperatures. Appendix C, figures 9 and 10 show test day fuel flow and specific range versus Mach. Figures 11 and 12 show fuel flow and specific range versus AOA. Table II presents

maximum range characteristics and table III presents test day maximum endurance characteristics from the appendix data.

Table II
RANGE CHARACTERISTICS

Altitude (ft. MSL)	Maximum Specific range (nm./lb.)	Optimum Mach (#)	Optimum Angle of Attack (units)
5,000	0.101	0.33	15.5
15,000	0.112	0.40	16.3
25,000	0.142	0.47	15.9

Table III
ENDURANCE CHARACTERISTICS

Altitude (ft. MSL)	Minimum Fuel Flow (lb./hr.)	Optimum Mach (#)	Optimum Angle of Attack (units)
5,000	2,000	0.25	18.5
15,000	1,850	0.30	20.0
25,000	1,700	0.35	21.0

Best cruise specific range displayed a significant increase between 15,000 and 25,000 ft. MSL (18%) and it was expected that cruise performance increased significantly above the highest test altitude of 25,000 ft. MSL. Overall, cruise specific ranges were high, and allowed for flexibility of mission operations. Optimum cruise angle of attack was consistant, being 15.9 $\pm$0.4 units; there were negligible fuel penalties (less than 2%) for flight at a constant AOA of 15.9 units. As a result, the pilot will find maximum range cruise conditions easy to fly, as he may reference a constant angle of attack. The cruise performance was satisfactory.

Maximum endurance fuel flows did not vary significantly between 5,000 and 25,000 ft. MSL (15 %). The fuel flows were low, and allowed for time flexibility during all test flight profiles. The optimum endurance AOA was consistant, being 19.8 $\pm$1.3 units

and offered a comfortable stall margin (5 units AOA). Flight at a constant angle of attack of 19.8 units did not yield significant fuel flow penalties (less than 5 %). During holding delays, the pilot will find optimum endurance flight easy to fly, as he may reference a constant angle of attack. The maximum endurance characteristics were satisfactory.

2.1.5 Acceleration

Excess energy characteristics were evaluated during a level acceleration at 5,000 ft. MSL in the cruise configuration, load A, and using maximum thrust. Average gross weight was 35,100 lb. and the free air temperature was 30^{o} Fahrenheit lower than that for standard day conditions. Appendix C, figure 13 presents energy height and excess power characteristics. Maximum excess power occured at less than 0.27 Mach/160 KOAS. Time to accelerate from 200 to 300 KOAS (0.33 to 0.49 Mach) was a slow 45 seconds. Between engagements, the airplane will be slow to accelerate or will gradually lose energy, and will be an easy target for hostile forces. The slow level acceleration capability is a serious deficiency which must be corrected.

2.1.6 Maximum Level Airspeed

The maximum level airspeed was determined during the test of section 2.1.5 above. Maximum sustained level airspeed was a slow 342 KOAS (0.56 Mach) at 5,000 ft. MSL. During target ingress and egress, a slow airplane will be easily acquired and fired upon by hostile forces. The low maximum level flight airspeed is a serious deficiency.

2.1.7 Sustained Turns

Sustained turn performance was evaluated in the cruise configuration, with maximum thrust and load A. Tests were conducted at 6,000 ft. MSL between 200 and 350 KOAS and at an average gross weight of 34,400 lb. Appendix C, figures 14, 15, and 16 present maximum sustained load factor, turn rate, and turn radius. Sustained turn performance is summarized in table IV.

Table IV
MAXIMUM SUSTAINED TURN PERFORMANCE

Mach/Airspeed (#/KOAS)	Load factor (g)	Turn Rate (^{o}/sec.)	Turn Radius (nm.)
0.33/200	2.6	13.0	0.3
0.42/250	2.9	11.5	0.4
0.51/300	2.7	9.0	0.7
0.55/325	2.1	6.0	1.0
0.57/337	1.0	0	(level flight)

Maximum sustained turn rate was 13 ^{o}/sec. at 200 KOAS. Minimum sustained turn radius was 0.3 nm, also at 200 KOAS. This was at a low airspeed, from which the airplane would be easily targeted from the ground. At more survivable mission airspeeds of more than 300 KOAS, the turn rate and radius were less than 9 ^{o}/sec. and more than 0.7 nm. The low sustained turn rate is a serious deficiency.

2.1.8 Instantaneous Turns

Instantaneous turns were evaluated under the same conditons as for sustained turns in section 2.1.7 above. Load factors, turn rates, and turn radii are presented in appendix C, figures 17, 18, and 19, respectively. Instantaneous turn performance is summarized in table V.

Table V
MAXIMUM INSTANTANEOUS TURN PERFORMANCE

Mach/Airspeed (#/KOAS)	Load factor (g)	Turn Rate (°/sec.)	Turn Radius (nm.)
0.33/200	3.2	15.0	0.23
0.42/250	4.6	18.5	0.23
0.51/300	6.5	22.0	0.25
0.55/350	6.8(1)	20.0	0.28

Maximum instantaneous turn rate was 22 °/sec. at 300 KOAS. The maximum instantaneous turn rate throughout the test airspeed envelope was high (over 15°/sec.). Maximum instantaneous turn radius was less than 0.30 throughout most of the airspeed envelope (200 to 370 KOAS). Upon detection of hostile missile launch at high airspeeds, the pilot should be able to generate the necessary turn rate to force missile overshoot. The instantaneous turn performance was satisfactory.

2.1.9 Maneuvering Envelope

The total sustained operating envelope was evaluated using turn and excess power performance results from above. Appendix C, figure 20 shows the test day, 33,000 lb. gross weight, airplane capability at 6,000 ft. MSL. The sustained envelope represents less than 50 % of the aerodynamic and structural limit envelope, and therefore reflects engine/airframe incompatibility. The sustained maneuvering envelope was small, and restricted close air support maneuvering. During extended defensive maneuvering in a low altitude, high threat environment, the pilot will have to keep flight conditions to within the sustained parameters (use low turn rates and low airspeeds), which can result in easy aquisition by enemy fire control. The small sustained operating envelope is a serious deficiency.

2.1.10 Descent

Maximum range descent performance was first evaluated in the cruise condition, at idle thrust, and from 25,000 to 15,000 ft. MSL at an average gross weight of 36,200 lb. Airspeed was held constant at 155 KOAS as recommended by the flight manual. Appendix C, figures 21, 22, and 23 show fuel, time, and distance to descend. Total fuel flow was less than 4 lb. per 1,000 ft. of altitude. The rate of descent was consistant at 2,000 ft. per minute. Average distance travelled per 1,000 ft. of altitude loss was 1.8 miles, and at a fuel usage of only 1.9 lb. per mile. During a maximum range flight profile, the pilot will be able to significantly extend the range by the use of the glide descent. The maximum range descent performance was satisfactory.

Penetration descent performance was evaluated from 15,000 to 5,000 ft. MSL in the cruise condition with idle thrust, and speedbrakes extended 40% as recommended by the flight manual. Airspeed was held constant at 250 KOAS and average gross weight was 35,500 lb. Appendix C, figures 24, 25, and 26 show fuel, time, and distance to descend. Fuel to descend was less than 60 lb. and the rate of descent (9,000 ft./min.) was adequate to meet typical published approach altitude restrictions. The penetration descent performance was satisfactory.

2.1.11 Landing

Landing performance was evaluated during three landings with gear down, flaps full down, and speedbrakes at 40% on the approach as recommended by the flight manual. The runway was dry, and anti-skid braking was utilized. Landings were flared to 120 KOAS and speedbrakes were deployed to 100% extension upon touchdown. Moderate braking was applied at 100 KOAS until the airplane was stopped. Table VI presents landing data.

Table VI
LANDING PERFORMANCE

Gross Wt./Load (lb./ A or B)	Headwind (kt.)	Air Temperature (^{O}F.)	Pressure Altitude (ft.)	Landing Distance (ft.)
32,000 / A	9	45	730	1,500
33,500 / B	0	40	1,050	1,500
32,000 / B	0	40	1,050	1,500

Rollout distances were short. Moderate braking force did not cause unusually hot brake disks. During landing on a short runway, the pilot will be able to safely stop the airplane without increasing the risk of hot brakes or blown tires. The landing performance was satisfactory.

2.1.12 Mission Profiles

The airplane was evaluated for the close air support and ferry profiles using the performance test results presented above. Fuel required for all but the cruise portion of the flight was first established. The remaining fuel was allocated to the optimum cruise condition to determine available ranges. Loading B was used in determining ferry profile performance as an approximation for the carriage of three external fuel tanks. With respect to close air support, loading B was used until the ground attack phase, then load A for the return. Appendix C, figures 27 and 28 display each mission by profile and by percentage of fuel used. Table VII presents ferry profile characteristics and table VIII presents close air support profile characteristics.

Table VII
CLOSE AIR SUPPORT PROFILE

Event	Flight Condition		Fuel Usage
	Altitude (ft. MSL)	Airspeed (KOAS)	(lb.)
Start, taxi, takeoff	0	0 to 200	300
Climb	0 to 15,000	200 to 185	400
Cruise	15,000	180	3,200
Max range descent	15,000 to 5,000	155	50
Holding at IP (5 min.)	5,000	155	500
Weapons employment	0	300 to 350	600
Climb	0 to 25,000	200 to 175	600
Cruise	25,000	180	2,600
Max range descent	25,000 to 15,000	155	50
Holding delay (10 min.)	15,000	150	350
Penetration descent	15,000 to 5,000	250	50
Approach, landing	5,000 to 0	130	300
Emergency reserve	0	0	1,500

Table VIII
FERRY PROFILE

Event	Flight Condition		Fuel Usage
	Altitude (ft. MSL)	Airspeed (KOAS)	(lb.)
Start, taxi, takeoff	0	0 to 200	300
Climb	0 to 25,000	200 to 175	600
Cruise	25,000	180	18,850
Max range descent	25,000 to 15,000	155	50
Holding delay	15,000	150	350
Penetration descent	15,000 to 5,000	250	50
Approach, landing	5,000 to 0	130	300
Emergency reserve	0	0	1,500

Maximum ferry range was approximately 2,700 nm. with 3 external fuel tanks. This was an exceptionally long range which provided mission flexibility. The airplane will be capable of deploying to forward airfields with minimal enroute delays or tanking support. The airplane was satisfactory for the ferry mission profile.

Maximum combat range was approximately 400 nm. This was a long range, which provided mission flexibility. The airplane will have the fuel capability to strike deeply into enemy territory and was satisfactory for the close air support mission profile.

2.2 Handling Qualities

2.2.1 Mechanical Characteristics

The mechanical characteristics of the primary flight control system were evaluated on the ground with both engines running, and verified inflight in the cruise configuration (loading A) at 250 KOAS and 15,000 ft. MSL. Inflight gross weight was 37,500 lb. and center of gravity was 24.6 %MAC. Longitudinal, lateral, and directional control force gradients are presented in appendix C, figures 29, 30, and 31. Table IX presents the mechanical characteristics.

Table IX
PRIMARY CONTROL SYSTEM MECHANICAL CHARACTERISTICS

Axis	Breakout, including friction (lb.)	Damping Ratio	Force Freeplay (in.)	Control Centering (in.)
Pitch	< 1	0.3	1/8	< 0.2
Roll	< 1	0.3	1/8	< 0.2
Yaw	< 5	0.2	< 0.5	< 0.5

Control forces and displacements were moderate and predictable, and control friction was not excessive. Breakout and freeplay were acceptable, and control centering was positive. Sharp control raps in all axis produced multiple control oscillations, but did not result in detectable airplane responses. The pilot will not find the mechanical characteristics of the primary control system objectionable. The mechanical characteristics of the primary control system were satisfactory.

2.2.2 Ground Handling

Ground handling was evaluated during four preflight and postflight taxi periods with and without nosewheel steering engaged. Test conditions included wind speeds of 7

to 17 kt. from all quadrants and surface temperatures of 30^{o} to 47^{o} Fahrenheit. All surfaces were paved, level, and dry. Tests were conducted at idle thrust. Taxiways were 75 ft. wide; the runway was 150 ft. wide.

Nosewheel steering provided the means to maintain centerline within 1 ft. using only casual inputs. Maintaining taxiway centerline using only differential braking (with nosewheel steering deactivated) was not difficult, requiring infrequent (every 2 to 3 seconds) small (10 lb.) pedal depressions. Turns with one wheel brake locked could be easily accomplished, due to the wide main wheelbase and sufficient residual thrust at idle throttle settings. Idle thrust was more than sufficient to provide normal taxi speeds. The ground handling characteristics of the airplane were satisfactory as the pilot will be able to taxi as required.

2.2.3 Takeoff

Handling qualities were evaluated during four dry surface takeoffs with headwinds of between 0 and 11 knots and with crosswinds of between 0 and 17 kt. Loadings were 38,000 lb. (26.3 %MAC) and 39,500 lb. (26.0 %MAC). Directional control during the initial portion of the takeoff roll (to 70 KOAS) was accomplished with nosewheel steering and then with rudder, as recommended by the flight manual. Rotation was performed at 125 KOAS.

During the initial part of the roll, nosewheel steering made centerline control easy, requiring only gentle pedal pressure (less than 10 lb.) against crosswinds. During the remainder of the roll, rudder control authority provided equally effective tracking and with equal ease of operation. However, the longitudinal control force required to set the normal takeoff attitude was excessive, requiring 15 lb. aft stick. Application of any less aft stick force increased flyoff speed 20 to 25 kt., and increased the takeoff roll distance up to 700

ft. The heavy aft stick force required for takeoff rotation is a minor deficiency.

2.2.4 Static Longitudinal Stability

Apparent static longitudinal stability, as evidenced by longitudinal control force and displacement variation with airspeed was evaluated at 8,000 ft. MSL. Tests were done in the cruise configuration (35,500 lb., 24.0 %MAC) from trim airspeeds of 200 and 295 KOAS and in the landing configuration (32,300 lb., 24.7 %MAC) from a trim airspeed of 130 KOAS. Flight path stability was concurrently evaluated in the landing configuration as well. Control force and displacement with airspeed variation from 130 and 295 KOAS are presented in appendix C, figures 32 and 33.

With gear and flaps up, slightly positive apparent stability was indicated by slight increases in stick forces and displacements required with deviation from trim airspeed when operating below 270 KIAS. Above 270 KOAS, neutral apparent stability was indicated by no variation in control forces or displacements required with deviation from trim airspeed. The trim speed band was 15 KIAS at 200 KOAS and increased in size as trim airspeed increased to 270 KOAS (where neutral apparent static stability was present). When disturbed from trim airspeed during normal cruise airspeeds (250 KOAS or less), apparent static stability tended to return the airplane toward trim airspeed. During diving accelerations to normal weapons delivery airspeeds (275 to 350 KOAS), little or no trim was required to keep longitudinal control forces light and manageable. This allowed the pilot to easily make small target tracking corrections. The combination of low speed positive and high speed neutral apparent static longitudinal stability was an enhancing characteristic.

With gear and flaps extended, moderately strong positive apparent stability was

indicated by increases in stick forces and displacements required with deviation from 130 KOAS (2 lb. and 1/2 in. per 10 kt. deviation). The trim speed band was small (4 to 5 KOAS). The airplane was easily trimmed and displayed the tendency to return towards trim airspeed whenever disturbed. The apparent static longitudinal stability was satisfactory.

Landing configuration flight path stability, as evidenced by flight path angle variation with airspeed deviation from trim, is presented in appendix C, figure 34. Rate of climb/descent versus indicated airspeed is presented in table X, as corrected to level flight at 130 KOAS. Flight path angle increased gradually as airspeed decreased from trim, and decreased gradually as airspeed increased from trim. There were no abrupt flight path angle changes with airspeed changes. During landing approaches, the pilot did not tend to experience excessive rates of descent prior to stall warning. The flight path stability characteristics in the landing configuration were satisfactory.

Table X

FLIGHT PATH STABILITY

Airspeed (KOAS)	Vertical Velocity (ft./min.)
110	+250
120	+200
130	(level flight)
140	-290
150	-510

2.2.5 Short Period

Short period characteristics were evaluated in the cruise configuration at 15,000 ft. MSL and at 150, 200, 250, and 300 KOAS (35,800 lb., 24.0 %MAC). They were evaluated in the landing configuration at 130 KOAS and 8,000 ft. MSL (33,500 lb.,

25.0 %MAC). Appendix C, figures 35 and 36 show the airplane response to pitch doublets with SAS on and SAS off. Short period characteristics are presented in table XI.

Table XI
SHORT PERIOD CHARACTERISTICS

Airspeed (KOAS)	Damping Ratio SAS on	SAS off	Natural Frequency (rad./sec.) SAS on	SAS off
150	Deadbeat	0.31	Deadbeat	1.4
200	Deadbeat	0.28	Deadbeat	1.6
250	Deadbeat	0.20	Deadbeat	2.3
300	Deadbeat	0.09	Deadbeat	2.9
130	Deadbeat	Deadbeat	Deadbeat	Deadbeat

The short period motion was completely deadbeat with SAS engaged. Intentional pitch attitude changes were solid and predictable, and displayed no tendency for oscillatory motion. With SAS disengaged, the short period was positively damped and adequate as a backup mode for cruise flight attitude control (although easily excited due to the low natural frequency) and deadbeat in the landing configuration. During target tracking (SAS on), the pilot did not have to correct for uncommanded pitch attitude overshoots, allowing precision aiming. In the landing pattern, intentional pitch attitude changes were solid, and with SAS engaged were very predictable. The short period characteristics were satisfactory.

2.2.6 Phugoid

Long period characteristics were evaluated in the cruise configuration at 15,000 ft. MSL and from 215 KOAS trim (36,500 lb., 24.2 %MAC) and in the landing configuration at 8,000 ft. MSL and from 135 KOAS trim (33,000 lb., 24.9 %MAC). Appendix C, figures 37 and 38 present indicated airspeed versus time data. In the landing configuration, the period was 39 seconds, the damping ratio was 0.09, and the motion was

not easily excited. During controls-free (trimmed) flight in the landing pattern, the airplane maintained airspeed and attitude for over 30 seconds. However, the long period in the cruise configuration at 200 and 250 KOAS was easily excited (due in part, to the decreased longitudinal static stability, revealed in section 2.2.4). The period was 68 seconds and the damping ratio was 0.10. Maintaining altitude (±100 ft.) was difficult, requiring constant monitoring and numerous (at least every 10 seconds) small (1 to 2 lb.) corrections. During target area ingress, the pilot was fatigued by the requirement to constantly monitor altitude. The easily excited long period in the cruise configuration is a minor deficiency.

2.2.7 Longitudinal Maneuvering Stability

Longitudinal maneuvering stability, as evidenced by the variation of longitudinal control stick force and position gradients with load factor, was evaluated in the cruise configuration (load A) at 8,000 ft. MSL and 325 KOAS (34,500 lbs., 23.6 %MAC), and in the landing configuration (load B) at 8,000 ft. MSL and 130 KOAS (33,000 lb., 24.9 %MAC). Longitudinal control force versus load factor is presented in appendix C, figures 39 and 40. In the cruise configuration, pull forces were light to moderate (4 lb./g) and varied consistently with load factor. Push forces were moderate (8 lb./g) and were consistent. Pitch control force per unit of displacement was comfortable (3 lb./in.), providing 1.2 g per inch of control displacement. In the landing configuration, average pull forces were moderately strong (16 lb./g) and varied consistently with load factor. Dynamic control force characteristics, as qualitatively tested by sudden pull-ups did not indicate significant differences in stick force per unit load factor in any flight condition. The pilot could predictably, and aggressively maneuver the airplane throughout its envelope due to the comfortable and natural maneuvering control forces and displacements. The longitudinal maneuvering stability characteristics were satisfactory.

2.2.8 Static Lateral-directional Stability

Static lateral-directional stability characteristics in the cruise configuration (load A) were evaluated during a steady heading left sideslip at 17,000 ft. MSL and 270 KOAS (36,000 lb., 24.1 %MAC) and in the landing configuration during a steady heading left sideslip at 8,000 ft. MSL and 140 KOAS (32,900 lb., 24.9 %MAC). Appendix C, figures 41 and 42 show rudder pedal force and position versus sideslip angle. Apparent static directional stability, as indicated by the variation of rudder pedal position with sideslip angle, was positive in both cases. Smooth, increasing rudder pedal deflection and force with increasing sideslip angle reflected moderate apparent directional stability. Full rudder pedal deflection generated 5^{o} of sideslip in cruise flight, and 20^{o} of sideslip in the landing configuration. This allowed the pilot to directionally correct airplane track over ground during landing approaches with 15 to 17 kt. right crosswinds. There was no requirement for rudder coordination during steady turns at any bank angle in either configuration. The static lateral-directional stability characteristics were satisfactory.

2.2.9 Dihedral

Dihedral characteristics in the cruise configuration (load A) were evaluated during a steady heading left sideslip at 17,000 ft. MSL and 270 KOAS (36,000 lb., 24.1 %MAC), and in the landing configuration (load A) during a steady heading left sideslip at 8,000 ft. MSL and 140 KOAS (32,900 lb., 24.9 %MAC). Appendix C, figures 41 and 42 show lateral control force and position versus sideslip angle. Lightly increasing lateral control stick force and displacement with increasing sideslip angle reflected low, but positive dihedral characteristics in both configurations. Full rudder in cruise (5^{o} sideslip) required less than one lb. and less than 0.5 in. of lateral control stick input to maintain balanced flight. Full rudder on landing (20^{o} sideslip) required only a 3 lb. and 0.5 in. of lateral

control stick input to maintain balanced flight. In summation, rudder inputs did not result in significant roll rates. During air-to-ground gunnery, the pilot was able to lay a spray pattern side-to-side without undesirable airplane roll responses, resulting in the capability to strafe multiple targets in a single diving run. The dihedral characteristics were satisfactory.

2.2.10 Sideforce

Sideforce characteristics in the cruise configuration were evaluated during a steady heading left sideslip at 17,000 ft. MSL and 270 KOAS (36,000 lb., 24.1 %MAC) and in the landing configuration at 8,000 ft. MSL and 140 KOAS (32,900 lb., 24.9 %MAC). Appendix C, figures 41 and 42 show bank angle versus sideslip angle. The variation of bank angle with sideslip indicated positive sideforce in both conditions. Sideforce was strong in cruise flight, requiring over 2^{o} of bank angle for each 1^{o} of sideslip to maintain balanced flight. Sideforce was moderate during landing, requiring 0.75^{o} of bank angle for each 1^{o} of sideslip to maintain balanced flight. During air-to-ground target tracking, sideforce cues were strong, alerting the pilot to out-of-balance, and incorrect aiming conditions. During landing approaches in 17-kt. crosswinds, the wing down, top rudder technique for runway alignment and centerline tracking did not produce an excessive bank attitude, allowing the wingtip to safely clear the runway surface. The sideforce characteristics were satisfactory.

2.2.11 Longitudinal Characteristics in Sideslips

Longitudinal control forces were evaluated during steady heading left sideslips in the cruise configuration at 17,000 ft. MSL and 270 KOAS (36,000 lb., 24.1 %MAC) and landing configuration at 8,000 ft. MSL and 140 KOAS (32,900 lb., 24.9 %MAC).

Appendix C, figures 41 and 42 show longitudinal control force required to maintain airspeed and attitude in sideslips. Longitudinal control forces were negligible in both configurations (less than 1 lb. at full rudder deflection). During intentional sideslip to refine an aiming solution, the pilot did not have to counter airplane pitching moments (due to sideslip). The longitudinal characteristics in sideslips were satisfactory.

2.2.12 Aileron Yaw

Aileron yaw was evaluated throughout the flight envelope (SAS on). Tests were conducted in the cruise configuration, and during two approaches to land. In the landing configuration, normal lateral control inputs (for up to 45^{o} angle of bank changes) did not produce significant aileron yaw, although the detected response was slightly adverse (up to 1/2 balance ball deflection). Lateral control inputs in the landing pattern did not require rudder coordination and the pilot was able to command landing pattern turns without rudder coordination. However, during cruise flight, rapid lateral control inputs (faster than 1 in./sec). generated considerable adverse yaw (the balance ball was displaced by up to 2 ball widths). The large adverse yaw made aggressive target tracking corrections difficult, as roll commands contaminated the directional tracking solution. The yaw tendency had to be neutralized with coordinated rudder. The strong adverse yaw in the cruise configuration was a minor deficiency.

2.2.13 Spiral Stability

Spiral stability characteristics were evaluated in the cruise configuration (load A) at 15,000 ft. MSL and 250 KOAS (36,500 lb., 24.2 %MAC) and in the landing configuration (load B) at 8,000 ft. MSL and 130 KOAS (33,000 lb., 24.9 %MAC). Appendix C, figures 43 and 44 present bank angle change with time, from a controls-free

condition at 20° of initial bank angle in each direction. Spiral stability, as evidenced by the variation of bank angle with time, was slightly positive in cruise flight, as the wings returned to level from the right turn, and did not increase in bank from the left turn. It was slightly negative in the landing configuration. However, time to double amplitude was never reached as the test was terminated at 30 seconds with only 10° to 15° increases in bank. During steady turns in the visual landing pattern, bank angle did not tend to vary significantly from trimmed conditions. In cruise flight, the pilot was not fatigued by the requirement to constantly correct for strong rolling tendencies. The spiral stability characteristics were satisfactory.

2.2.14 Dutch Roll

Dutch roll characteristics were evaluated in the cruise configuration at 15,000 ft. MSL and 150, 200, 250, and 300 KOAS (35,800 lb., 24.0 %MAC) and in the landing configuration at 130 KOAS and 8,000 ft. MSL (33,500 lb., 25.0 %MAC). Appendix C, figures 45 and 46 show the airplane response to rudder doublets with SAS on and SAS off. Table XII presents dutch roll characteristics.

Table XII
DUTCH ROLL CHARACTERISTICS

Airspeed	Damping Ratio		Natural Frequency (rad./sec.)	
(KOAS)	SAS on	SAS off	SAS on	SAS off
150	Deadbeat	0.20	Deadbeat	1.2
200	Deadbeat	0.10	Deadbeat	1.5
250	Deadbeat	0.10	Deadbeat	1.6
300	Deadbeat	0.10	Deadbeat	2.4
130	Deadbeat	0.40	Deadbeat	1.2

The dutch roll motion was completely deadbeat in cruise flight with SAS engaged, and essentially so in the landing phase. Airplane yaw quickly (less than 1 sec.) disappeared, and allowed for predictable heading control. The motion was purely directional; it did not excite rolling tendencies. With SAS disengaged, the dutch roll was positively damped and adequate as a failure mode for cruise and landing flight directional control (although easily excited by gusts in both phases). During target tracking (SAS on), the pilot did not have to correct for uncommanded directional oscillations, allowing for smooth weapons aiming. The dutch roll characteristics were satisfactory.

2.2.15 Roll Performance

Roll performance in the cruise configuration was evaluated during several maximum lateral control displacement rolls of 360^{o} at 5,000 ft. MSL and between 198 and 340 KOAS (37,000 lb., 24.2 %MAC). Roll performance in the landing configuration was evaluated during maximum lateral control displacement rolls of 30^{o} at 5,000 ft. MSL and at 130 KOAS (37,000 lb. and 25.9 %MAC). Time to roll is shown as a function of indicated airspeed in appendix C, figure 47. Time to roll 30^{o} in the landing configuration was 0.9 seconds which was adequate for landing pattern turn requirements. In cruise, time to complete the roll varied from 3.2 seconds at 340 KOAS to 4.9 seconds at 198 KOAS. Average roll rates were very slow, especially at the slow airspeeds (72 ^{o}/sec. at 198 KOAS). During pop-up attacks, the pilot was not consistantly able to roll the airplane quickly enough to place his lift vector as needed for target acquisition, resulting in target undershoots, aiming errors, and degraded weapons placement. The slow roll rate in the cruise configuration is a serious deficiency which should be corrected.

2.2.16 Roll Sensitivity

Roll sensitivity in the cruise configuration was evaluated at 15,000 ft. MSL and 250 KOAS (36,500 lb., 24.2 %MAC) and in the landing configuration at 10,000 ft. MSL and 130 KOAS (33,000 lb., 24.9 %MAC). Roll rate versus lateral control force is presented in appendix C, figures 48 and 49. Roll sensitivity was low near trim, being less than 5^{o}/sec.-lb. below 4 lb. of stick force for the cruise condition, and less than 3^{o}/sec.-lb. for the landing condition. Roll sensitivity increased smoothly and predictably to 13^{o}/sec.-lb. and 5^{o}/sec.-lb. at 8 lb. of stick force for the cruise and landing configurations, respectively. Precise angle of bank holding was easily accomplished, with no lateral pilot induced oscillation tendencies. During target tracking, the pilot was able to control angle of bank easily, and devote most of his time to pitch and directional aiming corrections. The roll sensitivity was satisfactory.

2.2.17 Trimmability

The ease and effectiveness of trimming the airplane was qualitatively evaluated in the cruise and landing configurations throughout the flight envelope. The airplane was trimmed laterally and longitudinally with the trim hat on the control stick, and trimmed directionally with the trim switch on the flight control panel. The directional trim was not required during normal flight operations. Lateral trimmability was easy and quick. Longitudinal trimmability in the cruise configuration was difficult, especially at the high airspeeds (above 230 KOAS) where static longitudinal stability approached and then become neutral. The large pitch trim rate (no trim gage with which to measure) caused frequent overshoots of the desired trim position. During cruise flight at 15,000 ft. MSL and 250 KIAS, numerous back and forth trim operations were required to attain proper trim setting. The high pitch trim rate which causes oversensitivity and trim precision difficulties

is a minor deficiency.

2.2.18 Coupled Rolls

Roll coupling characteristics in the cruise configuration (loading A only), were evaluated during maximum lateral deflection 360° rolls at 1.7 and 2.0 g. The maneuvers were performed at 15,000 ft. MSL and 250 KOAS. Gross weight and CG was 37,000 lb. and 24.2 %MAC. During the 1.7 g roll, a maximum of 2.0 g was recorded. During the 2.0 g roll, a maximum of 3.0 g was recorded. No abrupt airplane motions were observed. The pilot was able to perform rolling pullouts (low g) after target tracking without airplane departure. The coupled rolls were satisfactory.

2.2.19 Stall Characteristics

Stall, stall warning, and stall recovery characteristics were evaluated in the cruise configuration at 15,000 ft. MSL (37,000 lb., 24.3 %MAC) and landing configuration at 10,000 ft. MSL (34,500 lb., 25.2 %MAC). An accelerated (2g in cruise, and 30° bank angle in landing) and unaccelerated (1g) stall was performed in each configuration. Constant load factor, decreasing airspeed was used for the stall approach. Trim airspeeds were 170 KOAS and 130 KOAS in cruise and landing, respectively. Recovery consisted relaxation of aft stick force, full thrust with angle of attack (AOA) below stall, a roll to wings level, and peak performance pull (23 units AOA) to a climbing condition (as recommended by the flight manual. The recovery was considered complete with the airplane in a stabilized climb at less than 23 units AOA. Stall warning devices included steady and chopped audio tones in both configurations, and a stick shaker in the landing configuration. Table XIII presents stall performance.

Table XIII
STALL PERFORMANCE

Load Factor (g)	Solid Tone (KOAS/AOA)	Chopped Tone (KOAS/AOA)	Stick Shaker (KOAS/AOA)	Buffet (KOAS/AOA)	Stall (KOAS/AOA)
(Cruise configuration)					
1.0	135/23	130/24	Not applicable	127/24.5	125/25
2.0	185/23	175/24	Not applicable	Not apparent	170/25
(Landing configuration)					
1.0	120/23	117/24	117/24	113/24.5	110/25
1.2	130/23	127/24	127/24	123/24.5	119/25

Stall warning was evaluated for effectiveness of pilot cueing and margin of onset. Natural stall warning, in the form of very light buffet, was almost imperceptible and occurred almost coincidentally with the stall (less than 5 KOAS prior). Furthermore, in the landing configuration stall buffet was masked by speedbrake buffet and the stick shaker caused the control stick to vibrate at such a small magnitude, that it was not sufficient to alert the pilot. However, artificial warning, in the form of audio tones, was loud and unmistakeable (with volume controls near maximum), and provided a sufficient margin of warning, being 2 units AOA and at least 10 KOAS prior to the stall. Control position was natural, with increasing aft stick force and displacement required for increasing AOA. Both aileron and rudder surfaces were effective throughout the approach to stall in the cruise and landing conditions. During low altitude maneuvering flight at high angles of attack, the pilot was adequately alerted to near stalled conditions, and had adequate control authority to prevent inadvertently stalling the airplane. The stall warning characteristics were satisfactory.

Stalls were evaluated for objectionable characteristics. The unaccelerated and accelerated stalls were both marked by a mild g-break, and a mild right roll at 25 units AOA. A small left rudder input (1 in.) was effective in controlling the roll in both configurations. There was no tendency for departure. Aileron control was reduced, but all

control surfaces were effective. Aft stick force (at least 10 lb.) was required to keep the airplane stalled; no pitchup tendencies were observed. Rate of descent was less than 1,000 ft./min. in the stall. When stalled, the pilot was not disoriented by unusual attitudes which might have complicated the recovery procedures and increased recovery altitude. The stall characteristics were satisfactory.

Stall recovery was evaluated for ease and altitude loss. Altitude loss in both the accelerated and unaccelerated stalls was insignificant (less than 100 ft.), and time for a complete recovery was short (less than 5 sec.). The recovery was easy to perform and natural in sequence, requiring steady aft stick (4 to 7 lb.) to maintain a steady warning tone and thrust addition. No reference to cockpit instrumentation was necessary. No tendency for progressive stall entry was apparent. Upon stalling the airplane during aggressive maneuvering, the pilot was able to easily recover the airplane without a significant loss of altitude. The stall recovery characteristics were satisfactory.

2.2.20 Configuration Changes

The effects of thrust changes and landing gear, speedbrake, and flap movement were evaluated in both open loop (hands off) tests and during closed loop (task oriented) tests. The evaluation was conducted at 6,000 ft. MSL and at 23.3 to 25.0 % MAC and 32,500 to 34,100 lb. gross weight with both pitch and yaw SAS on. Landing gear retraction forced no apparent change in pitch attitude, while extention caused a very slight pitchdown, requiring only 1.5 lb. of aft stick force to maintain level flight. Flap extension caused a mild pitchup which was easily countered with 5 lb. of forward stick force; retraction caused a mild pitchdown which required six pounds of aft stick force to neutralize. Speedbrake extension and retraction caused no apparent change in airplane

attitude. Increasing thrust from idle to maximum caused a slight pitchup; decreasing thrust caused a mild pitchdown. All control forces required to maintain steady flight during configuration changes were small and there was no tendency for airplane overcontrol. The airplane configuration changes were satisfactory.

2.2.21 Landing

Landing handling qualities were evaluated in loadings A and B with antiskid braking on. Landing weights varied from 32,000 to 33,500 lb. and CG from 24.6 to 25.0 %MAC. Surface wind conditions varied with headwinds of 0 to 12 kt. and right crosswinds of 0 to 17 kt. Approach airspeeds of 130 to 150 KOAS were flown to a flare, and landing rollout directional control was maintained with rudder until below 100 KOAS when differential braking was utilized. Crosswind effects were effectively controlled by the wing-down, top rudder technique, and lineup was easily achieved and maintained. The flare required less than 15 lb. aft stick and attitude was easily set. Centerline tracking ($\pm$ 10 ft.) during landing rollout was easy, requiring infrequent (every 3 to 5 sec.) small (1 in.) rudder pedal displacements. There was no requirement for aileron or elevator, as airplane pitch and roll attitude remained constant. The landing characteristics were satisfactory.

2.2.22 Engine Response

Engine response characteristics were evaluated during a waveoff from a low approach at 1,000 ft. MSL. Smooth steady backstick (5 to 10 lb.) was required for optimum rotation to a best climb and engine thrust produced no adverse pitching moments. However, engine response time from the approach setting (80 %RPM) to maximum was excessive, being 3 to 5 seconds. Engine response time from flight idle to maximum was over 8 seconds. During low waveoffs for a simulated fouled runway, the pilot was not

able to generate the immediate thrust required to avoid ground contact. The slow engine response during waveoffs is a serious deficiency.

2.2.23 Asymmetric Thrust

Asymmetric thrust was evaluated from 9,000 to 10,000 ft. MSL. Loading was B, and average gross weight was 37,200 lb. The left engine was determined to be the critical engine, due to the loss of gear and flap retraction capability with its failure. The simulations were performed with the left engine at idle. With a true left engine failure, rudder forces would have been higher than for the simulation, due to the hydraulic backpressure in the left rudder actuator (appendix A, page 54), but there should have been no difference in controllability or flight characteristics.

Static minimum controllable airspeed ($V_{mc(s)}$) was evaluated in the takeoff configuration for compatibility with airplane flight requirements. Trim was set for normal takeoff as per the flight manual. The limiting factor was wing stall at 127 KOAS, and so $V_{mc(s)}$ was undefined. The stall was marked by a mild g-break and a right roll. Control positions prior to the stall were 70% right rudder pedal deflection, very light left stick, and 5 to10 lb. of backstick. $V_{mc(s)}$ was less than the best single-engine climb speed of 133 KOAS (section 2.1.3). Following a simulated left engine failure in the takeoff, configuration the pilot was able to control the airplane at the optimum single-engine rate of climb airspeed. The static minimum controllable airspeed characteristics were satisfactory.

Dynamic minimum controllable airspeed ($V_{mc(d)}$) was evaluated in the takeoff configuration as well. Trim was set as above. Sudden loss of takeoff thrust was simulated by quickly retarding the left throttle to idle. The simulated reaction time was determined to be 3 seconds due to the slow spooldown characteristics of the TF34 engine. Natural cueing to the failure was provided by airplane yaw to the left. $V_{mc(d)}$ was 135 KOAS,

and was defined by the requirement to quickly lower the pitch attitude in order to avoid quickly decelerating into the stall. In addition, significant (80%) right rudder deflection was required to maintain directional control and keep the heading change to 5^{o} or less. Recovery to original heading and to the best single engine rate of climb airspeed of 133 KOAS required 2 to 4 seconds. $V_{mc(d)}$ was at or less than the normal takeoff airspeed of 135 to 145 KOAS. During a simulated engine failure at takeoff, the pilot was able to safely maintain control of the airplane. The dynamic minimum controllable airspeed characteristics were satisfactory.

Minimum trim airspeed was evaluated in the cruise configuration for compatibility with airplane cruise flight characteristics. The minimum trim airspeed in wings-level, balanced flight, was 136 KOAS, and was limited by full right rudder trim authority. No significant pitch or roll trim changes were made from balanced engine flight. Minimum best range and endurance single-engine airspeeds, as recommended by the flight manual, was 180 KOAS and 165 KOAS (for 37,000 lb. gross weight and loading A). Because the minimum trim airspeed was less than best range and endurance airspeeds, the pilot will be able to trim out all control forces and not be fatigued. The minimum trim airspeed was satisfactory.

Asymmetric thrust approach characteristics were verified during a visual approach and waveoff from the landing configuration at 150 KOAS. Surface winds were down the runway at 16 kt,. and the approach was flown to a low waveoff at 10 ft. AGL. Rudder pedal forces were high during the approach (75 lb.), but could be trimmed out completely. Runway lineup and heading control were maintained as desired. Shallow turns (less than 30^{o} bank) were easily accomplished for lineup corrections. The slow thrust response of the TF34 engine (3 seconds from 80% RPM to maximum) made control requirements smooth, predictable, and easy; increasing right rudder with right engine spoolup provided a

waveoff capability with less than 2^{o} of heading change. The single engine approach characteristics were satisfactory.

3. DISCUSSION OF PROPOSED UPGRADES

3.1 Proposed Solutions

3.1.1 Engine

Inflight performance can be improved by either reducing drag or increasing thrust. Drag reductions considered were major airframe redesign, reduction of skin anomalies (antennas, pods, etc.) and removal of weapons pylons. The purpose of this proposed upgrade is to offer the most cost-effective solutions to deficiencies without impairing aircraft capabilities. Any major airframe redesign offers little confidence in improvement and cannot be performed economically. Removal of surface anomalies or weapons pylons decreases aircraft capabilities in one way or another. Therefore, drag reduction was discounted. It was decided that the inflight performance deficiencies can best and most easily be accomplished by increasing the airplane's available thrust.

The selection of a replacement for the TF-34 engine was based upon several factors. These included simplicity of retrofit, aircraft fit and weight penalties, thrust available, and specific fuel consumptions. Simply adding thrust augmentation (afterburner) was discounted due to the significant fuel and vulnerability sacrifices. The aircraft's capability to operate at great ranges without inflight tanker support must not be sacrificed and the nearly continuous use of the afterburner required for adequate performance in the high-threat areas would consume an inordinate percentage of onboard fuel. Additionally, a turbofan design offers a low observable infrared signature to suface-to-air homing weapons; this advantage would be lost if thrust augmentation was utilized.

A General Electric engine upgrade was chosen. Designated the CF-34, it will offer approximately 50% more thrust than the current TF-34 (13,500 lb. static at sea level, on standard day) and do so without a fuel penalty. While a slight total fuel consumption

reduction is advertised (generally 5%), the fuel consumption will be assumed to be the same. The basic engine will be 20 inches longer due to the addition of two turbine stages and the fan will be 4 inches wider in diameter. Updated blade technology provides most of the performance improvement, with core materials capable of sustaining higher operating temperatures accounting for the rest. Engine weight will increase by less than 300 pounds, and will be assumed negligible for weight and center of gravity concerns. This information was made available through the TF-34 program office of General Electric.

An optional feature of the CF34 engine that should be incorporated will provide a better engine response time. This is achieved by increasing the gas generator idle speed through a relatively simple redesign of the compressor section. A variable guide vane section restricts airflow at low power settings (near inflight idle) and force a higher engine core speed, keeping idle thrust the same. While this optional feature produces a higher idle fuel flow than the basic design, this penalty will be insignificant to the mission because of the limited time spent at flight idle. The benefit is almost instant engine response forward of the throttle idle setting, because the engine is already operating at a higher speed. Opening of the new variable guide vanes can be accomplished quickly to force a simultaneous thrust increase. Designed properly, this will not impact total available thrust.

It will be assumed that the same accessory section can be utilized, minimizing the complexity of the retrofit. Because the engine is mounted externally to the fuselage, the minimal increase in length will not be an installation problem. In order to avoid any unknown boundary layer effects, the intake should be kept the same distance from the fuselage, necessitating an increase in pylon length of two inches (one-half of the overall diameter increase). Unless wind tunnel tests reveal unexpected interference effects, the drag increase from the new pylon will be negligible. Nacelle drag will be assumed to stay the same. The impact of engine replacement wil be discussed in sections 3.2 and 3.3.

3.1.2 Anti-servo (Leading) Aileron Tabs

Airplane roll rate can be improved by increasing lateral control surface effectiveness or decreasing the effects of inertia in that axis. As inertia changes would require extensive redesign, the lateral controls were analyzed. An increase in aileron size or addition of spoiler panels was discounted due to the complexity of wing structure redesign. Either modification would entail wing structural analyses and potentially introduce new load paths. There might be an impact on fuel tank placement as well. Additionally, spoiler panels might also introduce a degradation in stall qualities. Spoiler deflection during accelerated stalls can induce sharp rolls at the stall. During aggressive low-altitude maneuvering (essential for the mission) such a roll-off could prove fatal. Lastly, increasing total aileron displacement was investigated. Realizing that increasing the available displacement angle alone would not offer significant benefits (as the full travel is already about 25^{o}), aileron anti-servo (leading) tabs were selected.

The tabs will not only replace the existing balance tabs, but should travel the full length of the aileron trailing edge for maximum effectiveness. Like the existing tabs, they will have to work in the split aileron- speedbrake mode as well. This will require some redesign of the aileron structure itself. The tabs should be rigged to remain conformal until one-half aileron deflection is achieved. At that point they can be geared such that full tab deflection is acheived with full aileron deflection. In this fashion the roll sensitivity around center will not increase and possibly cause other handling problems. The impact of the modification will be discussed in section 3.3.

3.1.3 Auto-Pilot

The long period and trimmability problems encountered during enroute flight in cruise conditions can best be remedied by an auto-pilot system. Changing trim rates or

altering flight control design might provide improvement in this area, but are more extensive (and expensive) than the addition of a strap-on system such as this. An auto-pilot offers fatigue relief for long ferry missions; of special concern because the airplane is single-piloted. Compensation for the easily excitable long period mode is needed.

3.1.4 Turn Coordinator

The adverse yaw generated during large lateral control inputs in cruise flight can best be remedied by an improved turn coordinator. Reducing roll control (aileron) effectiveness would make the already poor roll performance worse. Adding spoilers to induce proverse yaw effects would have the same unfavorable effects as discussed in section 3.1.2 (degrading stall character). Altering the basic airframe would be beyond the scope of a cost-effective upgrade. However, a turn coordinator change is not recommended. The deficiency is a minor one, and the oscillations do not persist after lateral inputs are removed because of the excellent damping provided by the yaw SAS system. A change would require significant rudder deflections in order to offset the large adverse yaw effects that the large ailerons are capable of producing (which may be larger after the addition of anti-servo tabs as recommended in section 3.1.2). This may degrade high angle of attack characteristics.

3.1.5 Takeoff Trim Increase

The excessive control input required to rotate the aircraft at takeoff can most easily be remedied by increasing noseup trim (any other solution, such as changing landing gear position on the airplane is vastly more complicated). However the airplane flies away comfortably when airborne (section 2.2.20). Increasing takeoff pitch trim will only degrade this aspect and is therefore not recommended.

3.2 Aircraft Performance

3.2.1 General

Of the proposed changes, only the new engine will affect airplane performance. Instantaneous turn, descent, and landing performance will not be readdressed, as no significant changes will be expected in these areas. Idle thrust will remain essentially unchanged for descents and landing rollout considerations. Instantaneous turn performance is dependant only upon maximum lift available, as A-10A thrust is applied in-line with the longitudinal axis.

3.2.2 Takeoff

The length of the takeoff roll will decrease significantly with the new engines. Appendix D, section 2, shows the method of calculation for the improved takeoff performance. Given the same conditions as those during testing, only 1,300 ft. of runway distance, will be required. This is only 65% of the original 2,000 ft. required. This will allow the A-10A to operate from very short runways, even those surfaces with some portions disabled due to battle damages.

3.2.3 Climb

Fuel, time and distance to climb will improve significantly with the new engine. Appendix D, section 3, shows the method of calculation for the improved climb performance. While the best climb speeds should increase slightly with the new upgrade, the original climb profile will be assumed for the new rate, time, and distance computations. Appendix E, figures 52, 53, and 54 show fuel, time and distance to climb under the same conditions tested on the original airplane. Climbs shown are in both loadings and from 3,000 to 25,000 ft. MSL. Fuel to climb, time to climb, and distance to

climb all decrease by 65% over the original model. The improved climb performance will be more than satisfactory, because the original A-10A climb performance is adequate.

3.2.4 Single-engine

Single-engine climb performance will improve dramaticaly with the new engine. Appendix D, section 4, shows the method of calculation for improved single-engine performance. Appendix E, figures 55 and 56 show takeoff configuration rate and angle of climb versus airspeed under the same conditions as tested in the original airplane. The airspeed for the best rate and angle of climb remain the same at 120 and 133 KOAS, respectively. The best climb angle will be 3.2^{o} (50% improvement) in the improved airplane, which will offer the pilot satisfactory ground clearance in the event of a failed engine. The best rate of climb will be 710 ft./min. (50% improvement) which will get the airplane away from ground obstacles quickly, and allow the pilot to concentrate on procedure. The single-engine performance will be satisfactory with the new engine.

3.2.5 Range and Endurance

Enroute performance will significantly improve with the new engine. Appendix D, section 5, shows the method of calculation for the improved range performance. Appendix E, figures 57 and 58 show the improved cruise fuel flow and specific ranges. (Best endurance speeds will remain the same as they are drag dependant only, however fuel flow will drop somewhat with the increased thrust for the same fuel consumption.) Best range speed will increase from 0.47M to 0.55M, and specific range will increase by 41% to 0.20 nm./lb. (at 25,000 ft. MSL). The range and endurance characteristics of the airplane will be excellent upon incorporation of the new engine.

3.2.6 Acceleration

The ability of the airplane to recover expended energy at low altitude will dramatically increase with the new engine. Appendix D, section 6, shows the method of calculation for the improved acceleration. Given the same conditions as tested at 5,000 ft. MSL, the new engines will accelerate the aircraft from 200 KOAS to 300 KOAS in less than 10 seconds, just 21% of the original model's 45 seconds. The new acceleration capability will be adequate to meet the mission needs.

3.2.7 Maximum Level Airspeed

The maximum level airspeed with the new engine will increase by 21% to 415 KOAS (453 KTAS) at 5,000 ft. MSL, at the test conditions. Appendix D, section 7, shows the method of calculation. The higher airspeed available will offer the ability to quickly enter and exit the enemy environment, substantially increasing the chance of surviving and fighting again. Additionally, the aircraft will have a higher energy state at the higher airspeeds, offering more maneuvering options if engaged by enemy air threats. The new maximum level airspeed will be satisfactory.

3.2.8 Sustained Turns

Sustained turn performance with the new engine will be significantly increased. Appendix D, section 8, shows the method of calculation for the improved sustained turn performance. The new maximum sustained load factor, turn rate, and turn radius are displayed in appendix E, figures 59, 60, and 61 (for the same ambient conditions as tested in the original model). The new maximum sustained load factor will be 4.2g (45% improvement). Whereas 3 g's sustained was unavailable, it will now be available at 180 to

360 KOAS at 5,000 ft. MSL. The maximum sustianed turn rate will be 16 degrees/second (33% improvement). The minimum sustained turn radius will be 0.55 nm. (45% improvement). These offer the pilot the ability to maneuver as required over the target area, and maintain the high energy state needed to quickly exit the area or engage the enemy further. The new sustained turn performance will be excellent.

3.2.9 Maneuvering Envelope

The revised total maneuring envelope is displayed in appendix E, figure 62. The improved sustained performance when compared to the instantaneous performance and airframe limitations reveal much better overall engine/airframe compatibility than in the original model. The size of the improved sustained envelope will be approximately 70%, of the available envelope, and the maximum level airspeed will be 90% of the redline airspeed. This will offer the pilot greatly increased speeds and turning capabilities for mission accomplishment, without the need to constantly keep energy in reserve for self defense. The new envelope will be satisfactory.

3.2.10 Mission Profiles

Improved ranges will be available to the pilot with the upgraded airplane. Using the improved performance information derived in appendix D, new profiles reveal increased total mission ranges. Tables XIV and XV display typical close air support and ferry profiles.

Table XIV
CLOSE AIR SUPPORT PROFILE

Event	Flight Condition		Fuel Usage
	Altitude (ft. MSL)	Airspeed (KOAS)	(lb.)
Start, taxi, takeoff	0	0 to 200	300
Climb	0 to 15,000	200 to 185	150
Cruise	15,000	260	3,700
Max range descent	15,000 to 5,000	155	50
Holding at IP (5 min.)	5,000	155	500
Weapons employment	0	300 to 350	600
Climb	0 to 25,000	200 to 175	250
Cruise	25,000	255	2,700
Holding delay (10 min.)	15,000	150	350
Penetration descent	15,000 to 5,000	250	50
Approach, landing	0	150	300
Emergency reserve	0	0	1,500

Table XV
FERRY PROFILE

Event	Flight Condition		Fuel Usage
	Altitude (ft. MSL)	Airspeed (KOAS)	(lb.)
Start, taxi, takeoff	0	0 to 200	300
Climb	0 to 25,000	200 to 175	250
Cruise	25,000	180	19,200
Max range descent	25,000 to 15,000	155	50
Holding delay	15,000	150	350
Penetration descent	15,000 to 5,000	250	50
Approach, landing	5,000 to 0	130	300
Emergency reserve	0	0	1,500

The close air support mission range will be 550 nm., a 37% improvement over the basic airplane. The ferry mission range will be 3,900 nm., a 44% improvement. The airplane will be capable of travelling great ranges without the need for inflight refueling. Furthermore, the aircraft will be capable of higher airspeeds at the same fuel flow as the original design. These characteristics will further reduce dependency on other units and

offer unit independence, resulting in more employment options. The new mission profile performance will be excellent, and should be typical of future designs.

3.3 Aircraft Handling Qualities

3.3.1 General

The new engine, aileron anti-servo tabs, and auto-pilot will affect general airplane handling qualities to some degree. Some aspects will not be readdressed, as no significant changes will be expected (the center of gravity remains essentially unchanged). These aspects include ground handling, static and dynamic longitudinal and maneuvering stability, static lateral-directional stability, sideforce, spiral stability, dutch roll, configuration changes, and landing considerations. Flight control mechanical characteristics should remain unchanged. The effects of the phugoid will be compensated for by the auto-pilot (also solving the trimmability concern) and will not be discussed. Sprial stability was evaluated to be neutral, but will be made less relevant by an auto-pilot system. Roll sensitivity near trim should remain unchanged, as the anti-servo tabs will not become active until lateral control reaches one-half throw. The remaining areas of concern are addressed in this section.

3.3.2 Takeoff

The takeoff handling qualities will change only as a result of the increased engine thrust. Because the thrust increase causes a slight noseup pitching moment, the new engine should assist slightly during rotation. This will help offset the minor deficiency noted in section 2.2.3 (large stick input required for takeoff rotation). The slight thrust effect on pitching moment should not (at least not significantly) degrade trimmability during the

configuration change following takeoff. The takeoff handling qualties will be essentially unchanged and will be satisfactory.

3.3.3 Aileron Yaw

Adverse yaw due to aileron deflection will increase due to the increased lateral control power provided by the anti-servo tabs. As indicated by the flight tests of the basic airplane, this will continue to be significant only during large lateral control inputs. As the landing pattern seldomly requires large roll control inputs, this should not affect flight in the landing condition. Aggressive lateral inputs will continue to aggravate target tracking solutions and will require coordinated rudder. This will require that A-10 pilots train to avoid making large lateral control inputs and avoid this situation. Post-modification flight tests will have to verify that the existing deficiency will continue to be minor.

3.3.4 Roll Performance

The aileron anti-servo tabs will increase roll performance. As the anti-servo tabs become effective beyond one half lateral control input, the roll rate will improve. The solution to the slow rate deficiency is the total available rate at maximum stick deflection. This will lessen the need for the pilot to assist rapid rolls with rudder inputs and reduce the possibility of directionally aggravating an unintentional stall at low altitude. Available roll rate will increase at all airspeeds and offer the pilot the ability to place his lift vector where required for rapid target acquisition. The improved roll rate will be adequate for the A-10A mission.

3.3.5 Stall Characteristics

Stall characteristics will have to be verified after the modifications are incorporated. More than sufficient nosedown control authority exists to counter the pitchup due to increased engine thrust during power-on stalls. However, the effects of the aileron modification must be investigated. In particular, stalls with full lateral control inputs will be affected, and could be aggravated by the increased adverse yaw. This effect is expected to be insignificant, because the current stall characteristics are excellent and show no adverse tendencies. Additionally, both aileron and rudder surfaces will continue to be effective throughout the stall, allowing for ease of recovery. The pilot will be able to continue to easily recover from the stall without a significant loss of altitude. The overall stall characteristics should continue to be satisfactory.

3.3.6 Engine Response

Engine response will be more rapid because of the suggested design of the compressor section. The time from flight idle to maximum thrust response will be considerably less than the existing 8 seconds, with 3-4 seconds being likely. This will provide the pilot with the ability to execute close-in waveoffs from an underpowered condition. The engine resonse time should be satisfactory.

3.3.7 Asymmetric Thrust

The static minimum controllable airspeed will likely remain undefined as only 70% rudder deflection was required at the stall during flight tests. This will allow significant remaining yaw control power to offset the effects of the increased thrust The best single-engine climb speed (rate) with the new engine (section 3.2.4) will be essentially unchanged at 133 KOAS and will continue to be higher than the static limit, offering plenty of airspeed

margin to the pilot. The asymmetric approach characteristics will remain unaffected as well, the normal approach airspeed being 150 KOAS which is also higher than the best single-engine climb speed (133 KOAS). The static minimum controllable airspeed and asymmetric approach characteristics should remain satisfactory.

Yaw cueing for an engine failure will remain unchanged, the spooldown characteristics of the new engine being assumably similar. The dynamic minimum controllable airspeed may increase slightly due to increased asymmtric thrust and the existing requirement for over 80% rudder input in the original model. Yet, the average mission takeoff weight will require takeoff rotations at only up to 140 KOAS, and it is unlikely that the pilot will find the new dynamic limit to be greater than this (was 135 KOAS). The new dynamic minimum controllable airspeed should remain satisfactory.

Minimum trim airspeed, which was limited during flight tests to 136 KOAS, was limited by rudder trim authority. This was significantly less than the minimum best range and endurance single-engine airspeeds of 180 KOAS and 165 KOAS (from the flight manual for 37,000 lb. gross weight and loading A). Because the minimum trim airspeed was far less than best range and endurance airspeeds, the new engine is not expected affect the optimum single-engine flight profile. The minimum trim airspeed should continue to be satisfactory.

4. CONCLUSIONS AND RECOMMENDATIONS

4.1 General

The A-10A airplane demonstrated excellent potential for continuing close air support missions for many years. It will be satisfactory upon correction of the serious deficiencies as delineated herein. Furthermore, it will offer the military the best platform, at the best price.

4.2 Specific

The improved engine should be incorporated and tested as soon as possible. This engine will solve all of the performance deficiencies noted in the basic airframe, and will result in a very capable platform, even by tomorrow's standards. The aileron anti-servo (leading) tabs will increase available roll rates to an acceptable level without compromising handling qualities. The engine will also not adversely affect airplane handling qualities.

An auto-pilot will provide relief from pilot fatigue during the long missions that the airplane can achieve. However, a stronger turn coordinator to solve the adverse yaw deficiency is not recommended because of the possible adverse effect on stall characteristics.

BIBLIOGRAPHY

BIBLIOGRAPHY

Flight Manual A-10A Aircraft, TO 1A-10A-1, dated 20 February 1983, updated to 23 August 1988.

Acree, James N. Phase DT-IIA Developmental Testing of the A-10A Airplane, dated 30 November 1988.

USNTPS FTM-103, Fixed Wing Stability and Control Theory and Flight Test Techniques, dated October 1984.

USNTPS FTM-104, Fixed Wing Performance, dated July 1977.

NASA Technical Note D-5153, The Use of Pilot Rating in the Evaluation of Aircraft Handling Qualities, dated April 1969.

USNTPS Course Outline, Airplane Performance, as printed in 1988.

APPENDIX A

FLIGHT CONTROL DESCRIPTION

FLIGHT CONTROL DESCRIPTION

I. Normal Mode

Ia. General

The primary flight controls consist of twin ailerons, twin elevators, and twin rudders. All are operated through a conventional center stick and rudder pedal arrangement in the cockpit. These surfaces are hydraulically operated and provide control irreversibility. Elecrical trim is provided in all three axes. Trailing edge wing flaps and leading edge slats are hydraulically powered and electrically operated. Speedbrakes and pitch and yaw augmentation systems are incorporated.

Ib. Support Systems

The dual hydraulic systems are completely independent. Each engine supports a system offering single-engine hydraulic capability. The left system powers the left rudder, left elevator, left and right ailerons, and trailing edge flaps. The right system powers the right rudder, right elevator, speedbrakes, wing slats, and powers both ailerons as well. Cockpit gages and warning lights alert the pilot to any problems with either system.

Electrical control is required for cockpit gage indications and the flap, trim, speedbrake, and stability augmentation systems. This could be provided by a single engine or APU generator and either of two inverters.

Ic. Primary Controls

The flight controls are rigged through two independent linkage systems for elevator and aileron control, and a single system for rudder control. The cockpit is enclosed by titanium shielding, through which control cables for each axis pass. The cables run directly to the elevator, aileron, and rudder actuators. Within the cockpit, pushrods connect the control stick and pedals to the cable connectors.

Artificial feel is provided by a spring on each elevator, aileron, and rudder actuator input arm; electrical trim motors act to adjust the neutral position of these feel springs. A separate trim button offers the pilot a means of automatically trimming for takeoff in pitch. A bobweight is attached forward of the base of the control stick to provide longitudinal maneuvering force feedback. The elevators, ailerons, and rudders are all mass-balanced, presummably to reduce hinge loads.

The elevator range of travel is approximately 30^{o} trailing edge up to 10^{o} trailing edge down. The ailerons have a range of travel of approximately $\pm 25^{o}$. The rudders are stop-limited to $\pm 25^{o}$ at airspeeds below 240 KOAS, and $\pm 8^{o}$ at higher airspeeds.

Id. Augmentation System

Rate damping augmentation is provided in the pitch and yaw axis. The pitch and yaw Stability Augmentation Systems (SAS) consist of two independent circuits (channels), each for redundancy, and each controls one of the two control surfaces in that axis. Automatic disconnect is designed to occur in the event of a substantial difference in commands between the channels in each axis. The systems are manually selected from the cockpit, and display current status to the pilot. Control stick and pedal authority overrides SAS commands. Additionally, the pitch SAS command a minor compensation with speedbrake employment to assist the pilot with pitch attitude (nosedown command with extension, noseup command with retraction). The yaw SAS provides rate damping with $\pm 7^{o}$ rudder authority, offers yaw trim with $\pm 10^{o}$ rudder authority, and provides an aileron-rudder interconnect with $\pm 10^{o}$ rudder authority.

Ie. Auxiliary Systems

Each aileron splits to create top and bottom wingtip spoilers to act as speedbrakes. Full extension is approximately 70° deflection of top and bottom panels. Up to 80% of that amount is available inflight, 100% only on deck. Full extension or retraction requires only 3 seconds and overspeed protection is incorporated to allow blowback at high airspeeds. Control is provided through a switch on the inboard throttle, however there is no artificial indication of speedbrake position. The position has to be verified visually.

Four trailing edge wing flaps are inboard of the ailerons and offer three position selection. They are up (no extension) for cruise flight, set to the maneuver position for takeoffs (7° extension), and set to the down position for landing (20° extension). Electrical selection is through a control lever, and a gage displays position to the pilot. Each flap is positioned by an independent hydraulic motor, and is designed to blow back during overspeed conditions at approximately 200 KOAS.

Two slats are on the inboard leading edge of the wings and are designed to improve high angle of attack airflow over the wings to the engine intakes. They operate automatically with weight off wheels and are only two position, fully extended or up. Each slat has an independant hydraulic actuator which programs extension as a function of mach number and angle of attack. The angle of attack is measured by a lift transducer located under the left wing leading edge. No slat controls or indicators are provided in the cockpit.

II. Flight Control Degradations

IIa. Hydraulic Failure

A single hydraulic failure will isolate certain control surfaces, and offer at least partial pitch and yaw authority in the powered mode. A single SAS channel is lost with a single hydraulic failure. Also, depending on which hydraulic system fails, flaps, speedbrakes, or slat operation may be lost. If the flaps lose hydraulic support when extended, a pilot-selectable option exists to port trapped fluid and allow aerodynamic trailing of the flaps; this results in the flaps retracting to a nearly retracted position. If the speedbrakes lose hydraulic power while extended, a similar option allows the speedbrakes to close via airloads to a fully closed position.

A dual hydraulic failure will require use of a manual reversion mode of operation. This mode is electrically-selectable from the cockpit and ports hydraulic fluid from the actuators in order to somewhat reduce control forces such that they may be manageable in this unboosted mode. Additionally, this mode is automatically enabled in pitch and yaw when hydraulic pressures drop below approximately 500 psi. An emergency trim system directly drives elevator and aileron trim tabs; rudder trim remains unchanged.

IIb. Electrical Failure

As long as one of the three generators remains functioning, no flight control or related system degradation will occur. Total electrical failure will result in loss of trim, flap, slat, and speedbrake control, as well as loss of SAS operation. The slats will fail to the extended position upon loss of all electrical power.

IIc. Path Jams

In the event that a linkage in the elevator or aileron system becomes damaged and jams, it may be isolated from the other redundant cable path through electrical deselection by the pilot. As yaw control is through one non-redundant system, this option does not exist for rudder controls. However, if a rudder were to become jammed, there is enough slack in the interconnecting cables to offer limited opposite rudder movement.

APPENDIX B

ILLUSTRATIONS

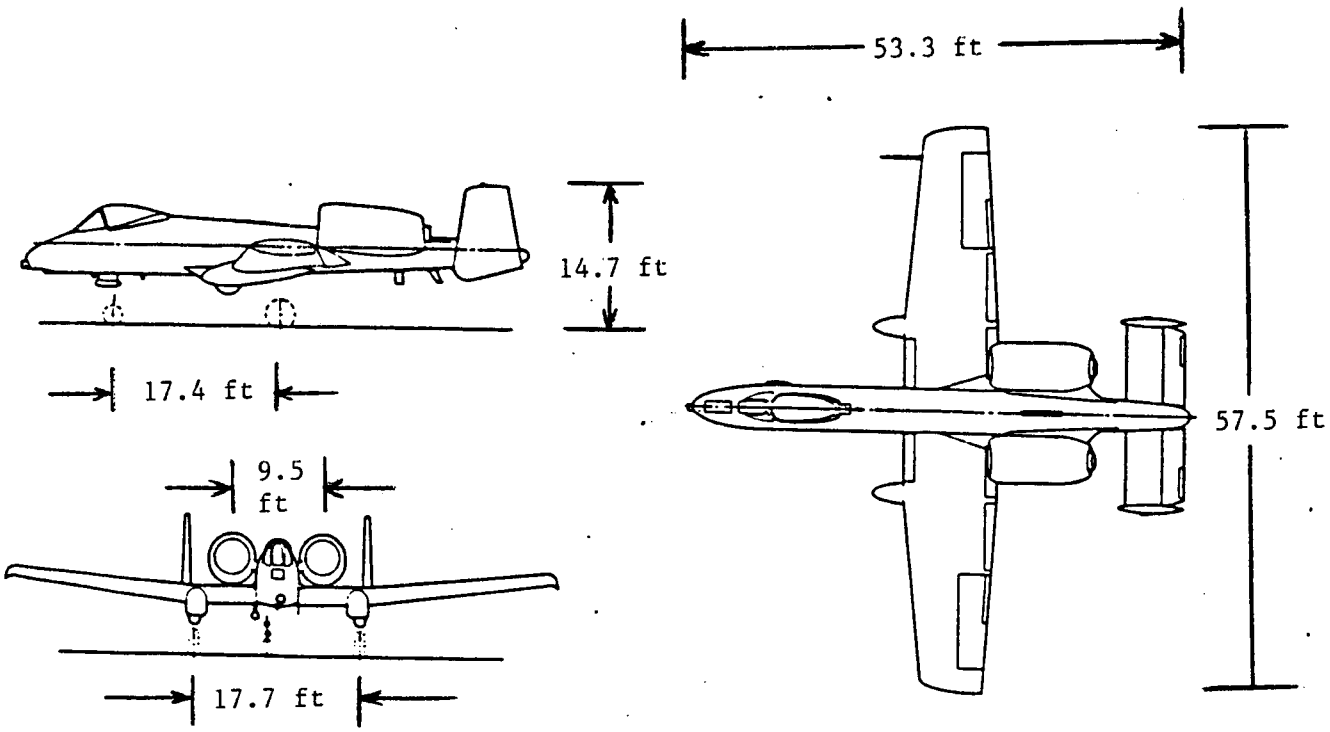

Figure 1
A-10A AIRPLANE OVERVIEW (General)

View Looking
Forward

▽ - Multiple Stores
Capability

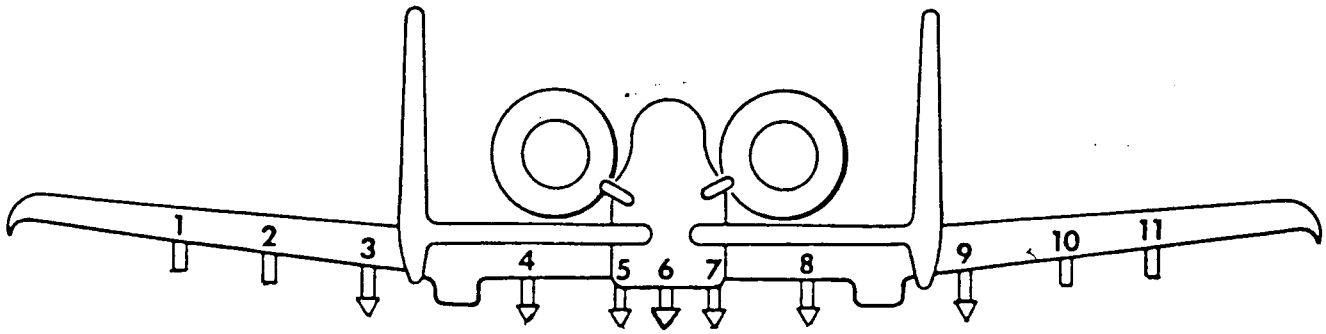

Figure 2
A-10A WEAPON CARRIAGE STATIONS

APPENDIX C

CURVES

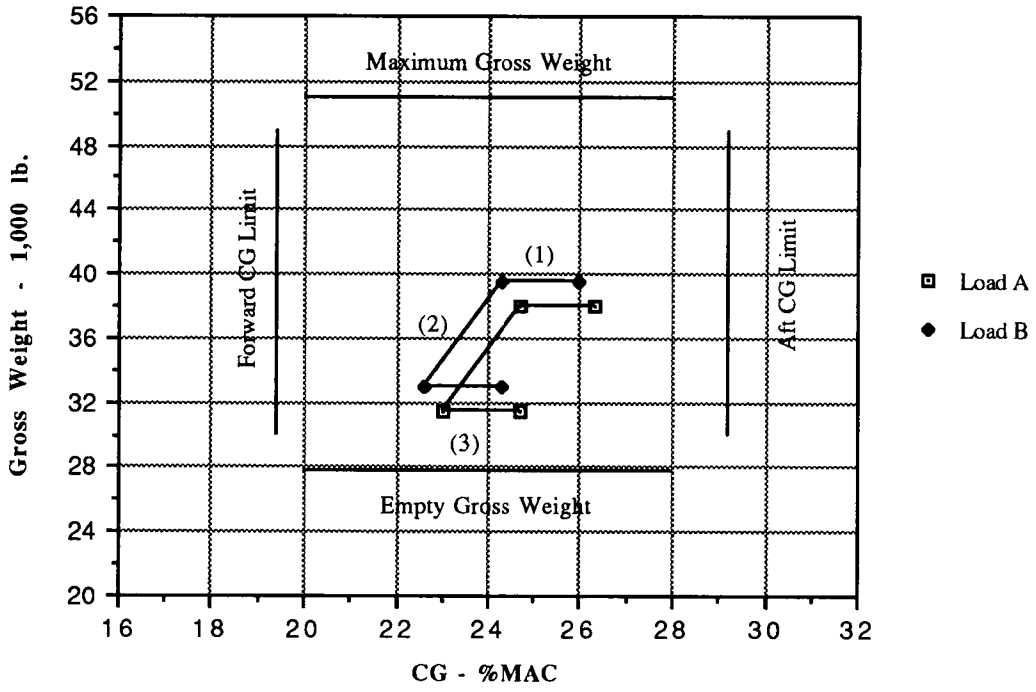

Notes: (1) Landing Gear Retraction
(2) Fuel Burndown
(3) Landing Gear Extension

Load A did not include external stores. Load B included 2 Maverick missiles and 2 triple ejector racks with 6 Mk-76 practice bombs.

Figure 3
A-10A CENTER OF GRAVITY TRAVEL DURING FLIGHT TESTS

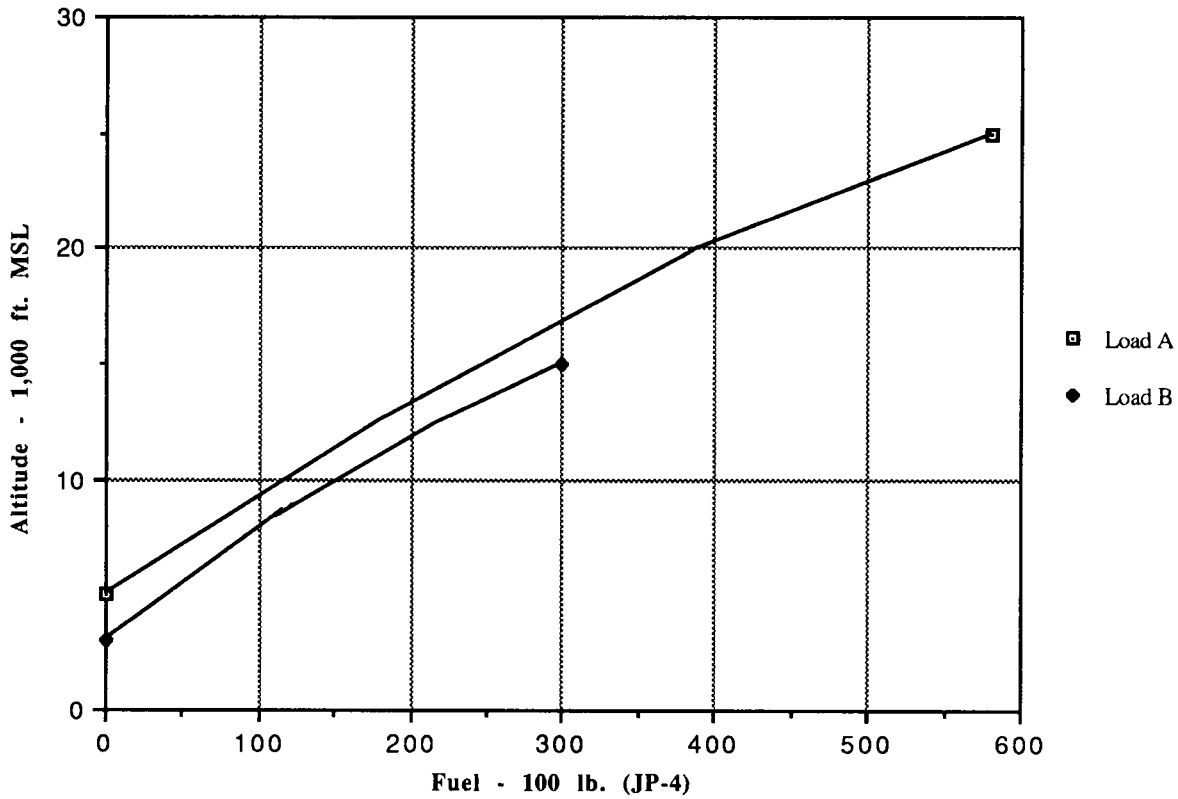

The climb matched the profile recommended by the A-10A Flight Manual. Climb airspeed was between 175 and 200 KOAS. The average gross weights were 37,000 lb. for load A, and 38,500 lb. for load B. The free air temperature was approximately 30° F. lower than standard day.

Figure 4
A-10A FUEL REQUIRED TO CLIMB

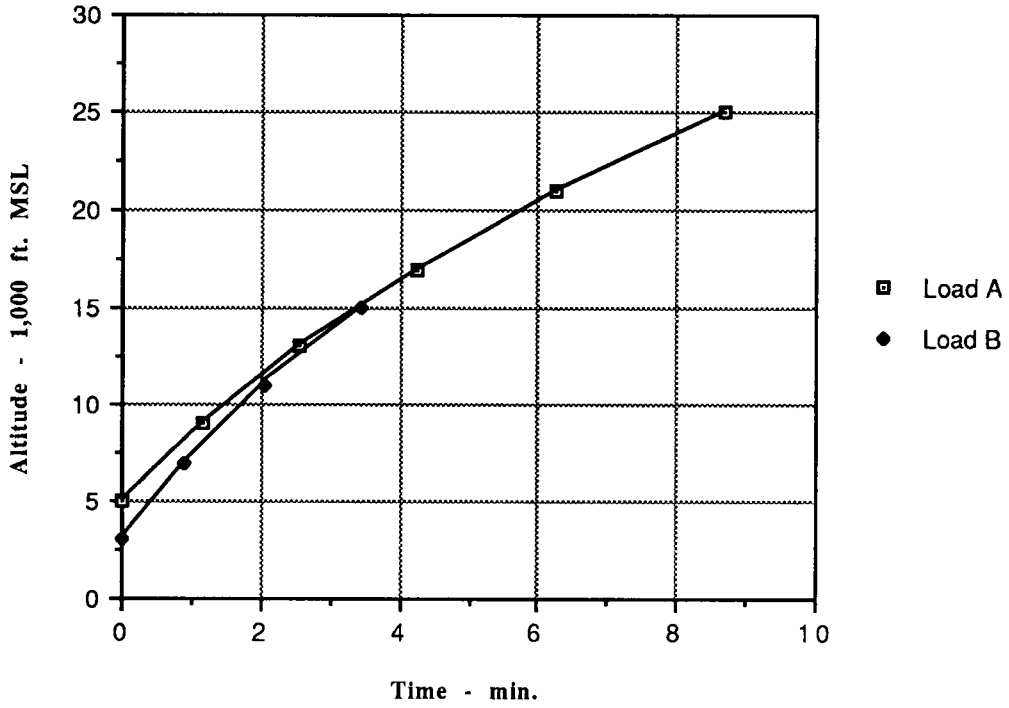

The climb matched the profile recommended by the A-10A Flight Manual. Climb airspeed was between 175 and 200 KOAS. The average gross weights were 37,000 lb. for load A, and 38,500 lb. for load B. The free air temperature was approximately 30^{o} F. lower than standard day.

Figure 5
A-10A TIME REQUIRED TO CLIMB

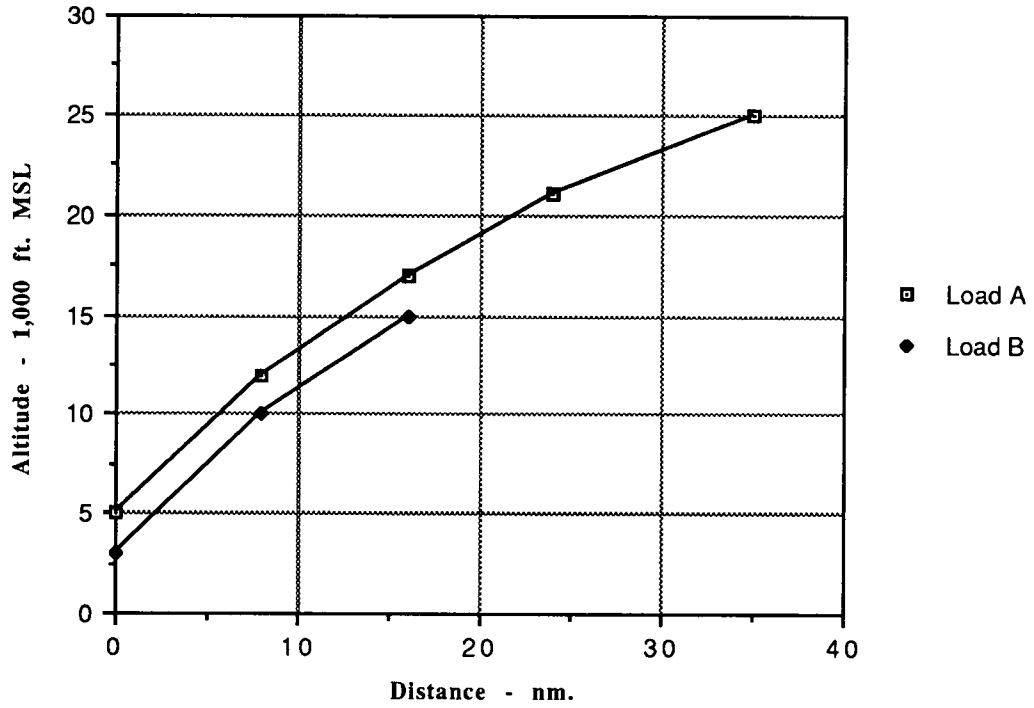

The climb matched the profile recommended by the A-10A Flight Manual. Climb airspeed was between 175 and 200 KOAS. The average gross weights were 37,000 lb. for load A, and 38,500 lb. for load B. The free air temperature was approximately 30^{o} F. lower than standard day.

Figure 6
A-10A DISTANCE REQUIRED TO CLIMB

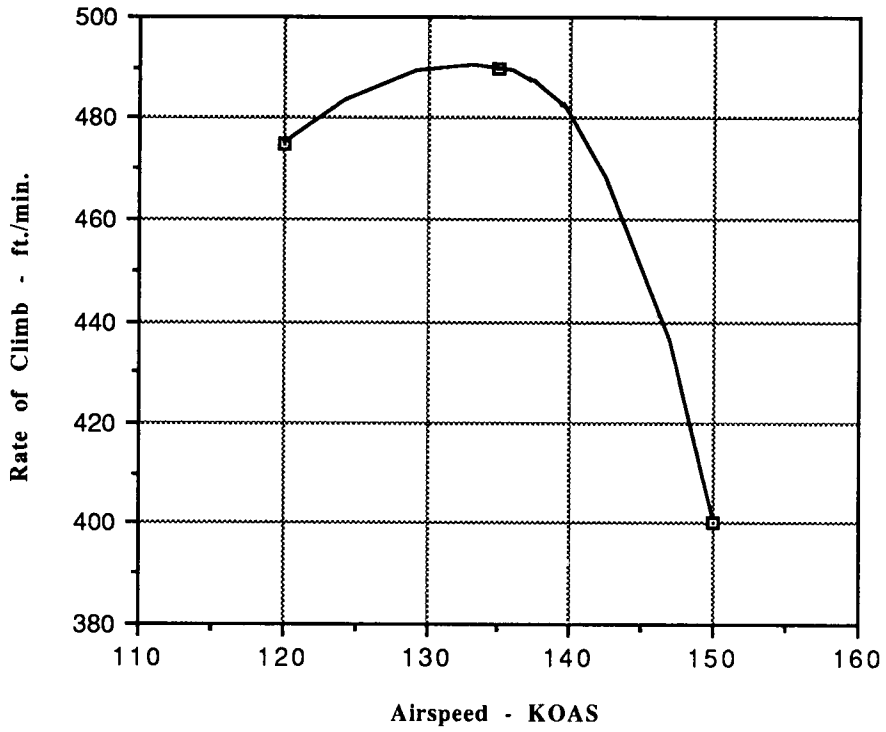

Results were obtained by measuring three climbs at 5,000 ft. MSL and using maximum thrust on the left engine, and idle thrust on the right engine. The takeoff condition was duplicated, with gear down and flaps at the maneuver position. Average gross weight was 33,000 lb. and only load A was used. The free air temperature was approximately 20° F. below standard day conditions.

Figure 7
A-10A SINGLE-ENGINE RATE OF CLIMB

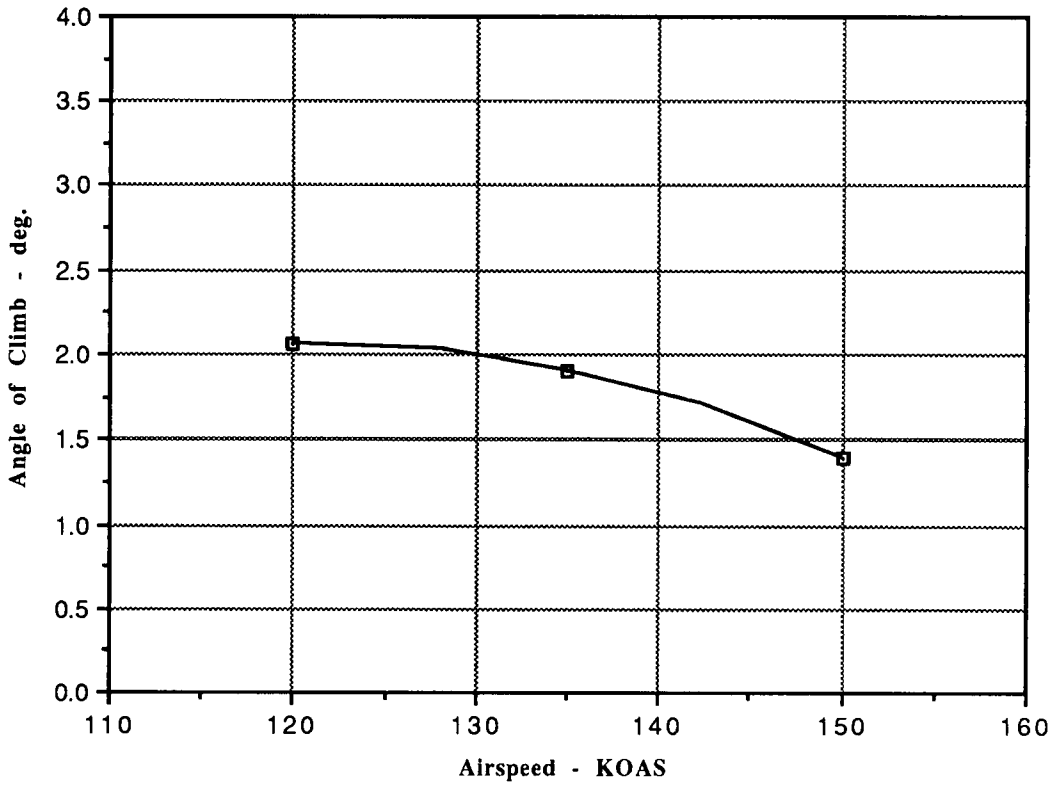

Results were obtained by measuring three climbs at 5,000 ft. MSL and using maximum thrust on the left engine, and idle thrust on the right engine. The takeoff condition was duplicated, with gear down and flaps at the maneuver position. Average gross weight was 33,000 lb. and only load A was used. The free air temperature was approximately 20° F. below standard day conditions. Angle of climb was determined by comparing rate of climb to true airspeed.

Figure 8
A-10A SINGLE-ENGINE ANGLE OF CLIMB

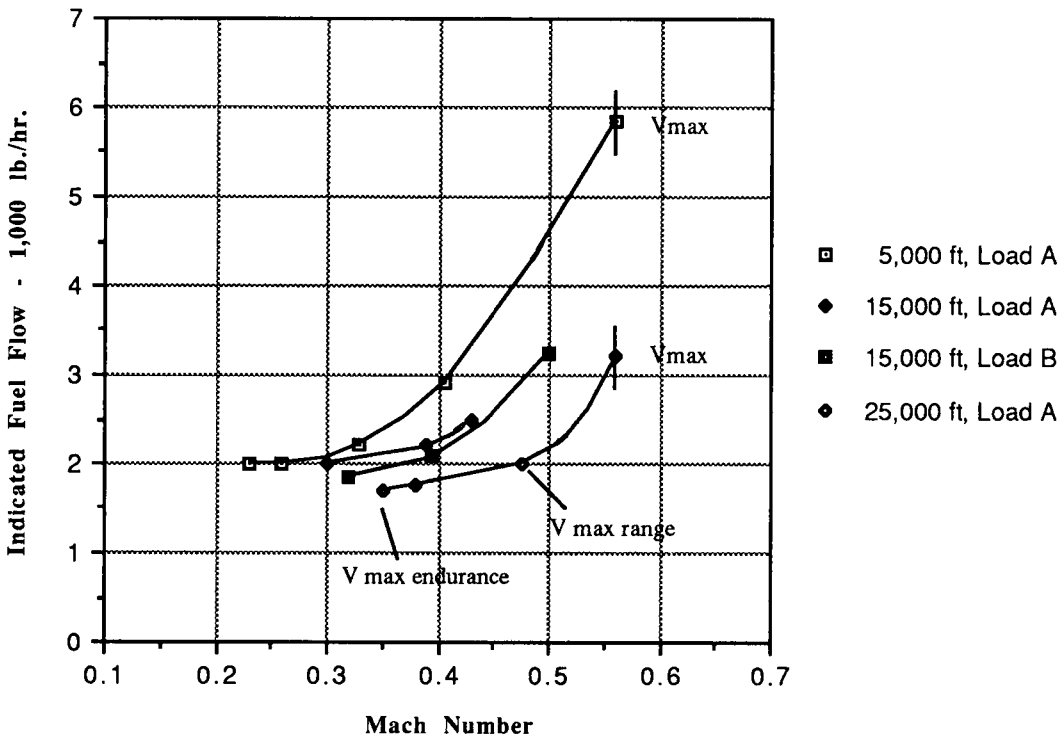

Range and endurance data was obtained while at stabilized airspeeds and in level flight at 5,000, 15,000, and 25,000 ft. MSL. The average gross weight was 36,700 lb. and the free air temperature was approximately 30^{o} F. lower than standard day.

Figure 9
A-10A CRUISE FUEL FLOW

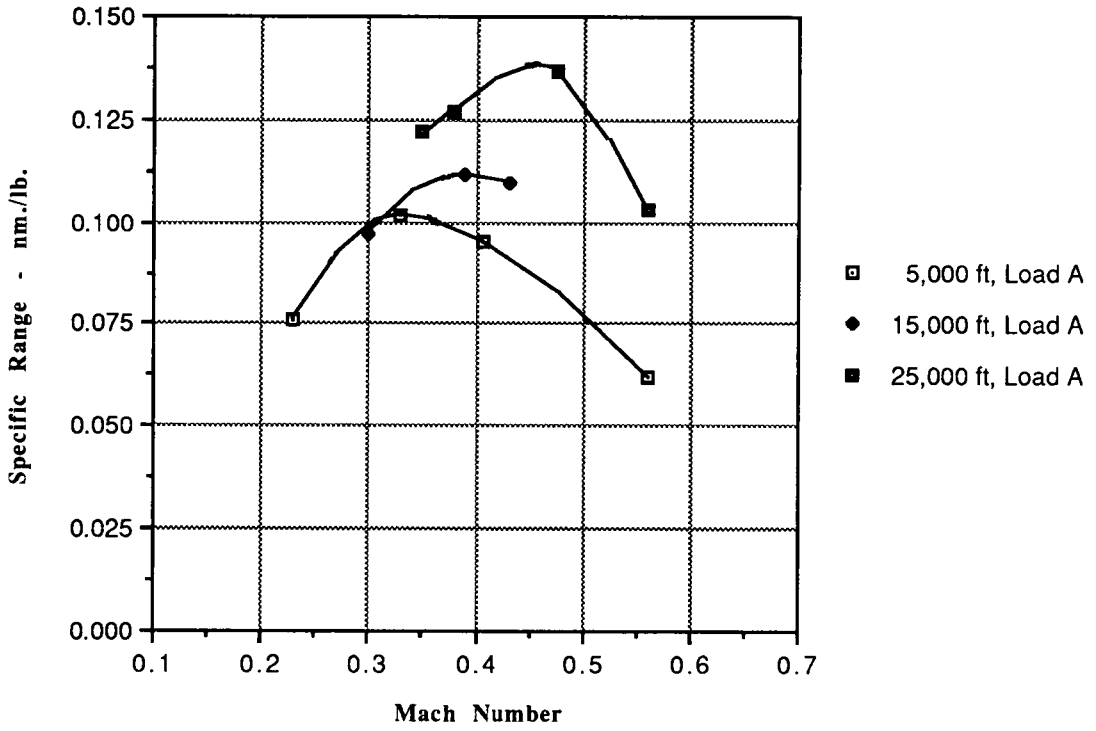

Range and endurance data was obtained while at stabilized airspeeds and in level flight at 5,000, 15,000, and 25,000 ft. MSL. The average gross weight was 36,700 lb. and the free air temperature was approximately 30° F. lower than standard day.

Figure 10
A-10A CRUISE SPECIFIC RANGE

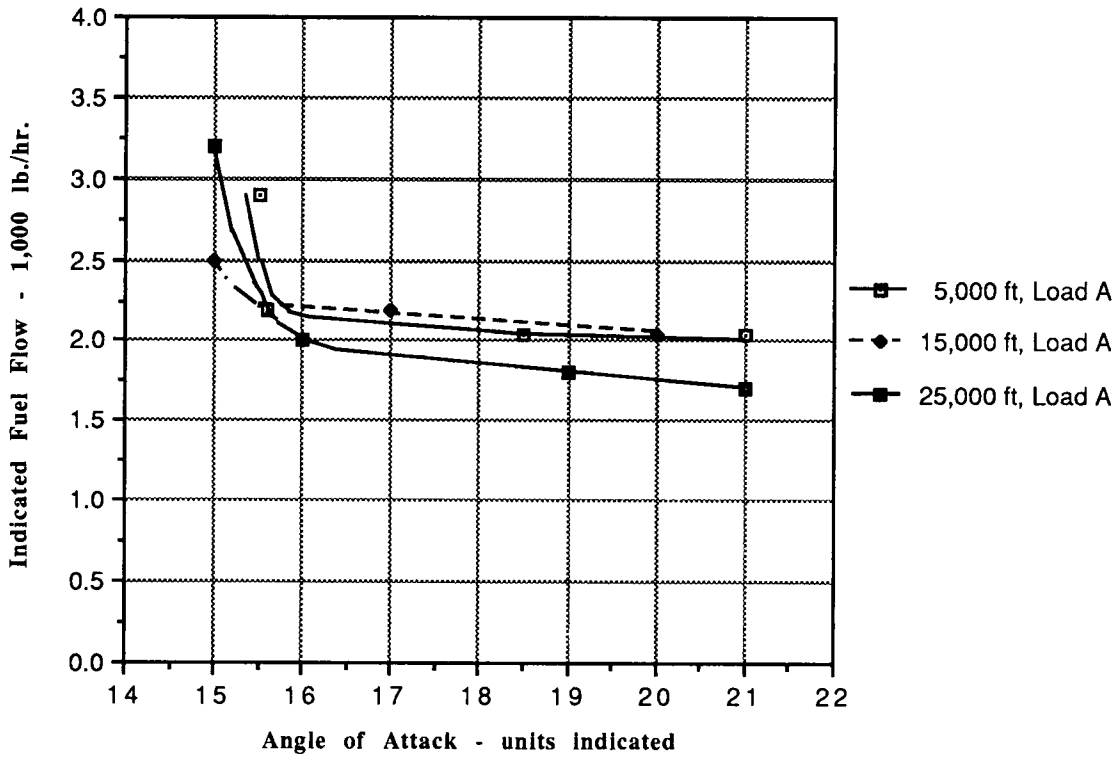

Range and endurance data was obtained while at stabilized airspeeds and in level flight at 5,000, 15,000, and 25,000 ft. MSL. The average gross weight was 36,700 lb. and the free air temperature was approximately 30° F. lower than standard day.

Figure 11
A-10A CRUISE ENDURANCE/ANGLE OF ATTACK CORRELATION

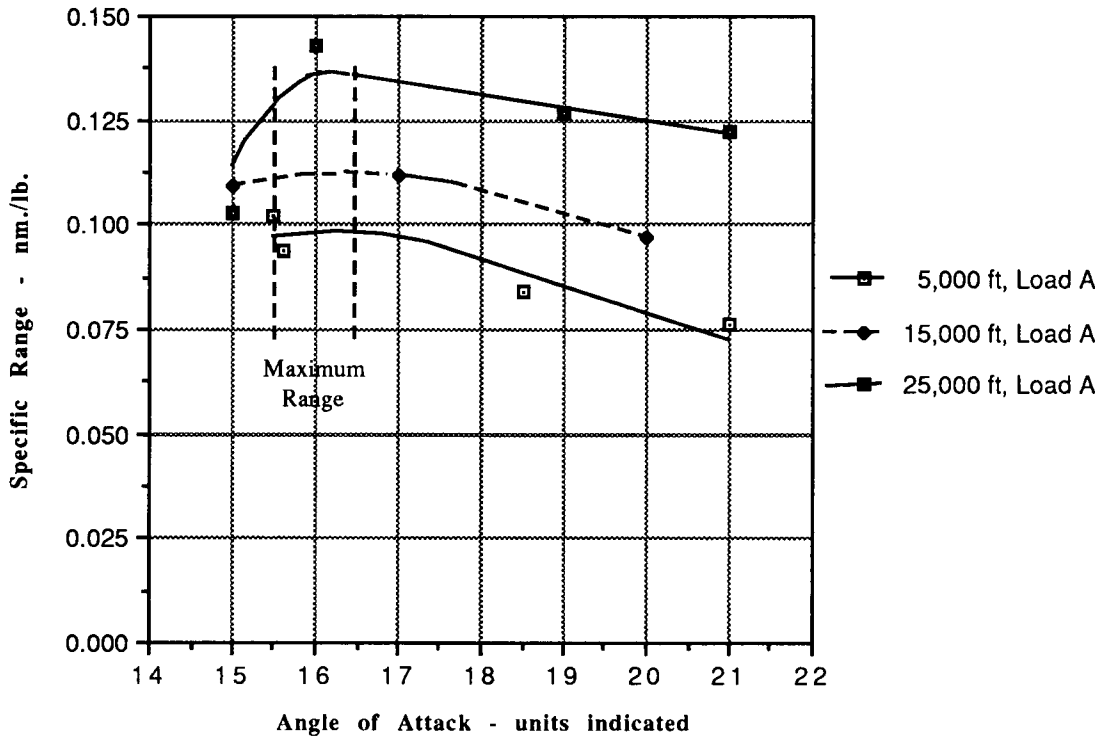

Range and endurance data was obtained while at stabilized airspeeds and in level flight at 5,000, 15,000, and 25,000 ft. MSL. The average gross weight was 36,700 lb. and the free air temperature was approximately 30^{o} F. lower than standard day.

Figure 12
A-10A CRUISE RANGE/ANGLE OF ATTACK CORRELATION

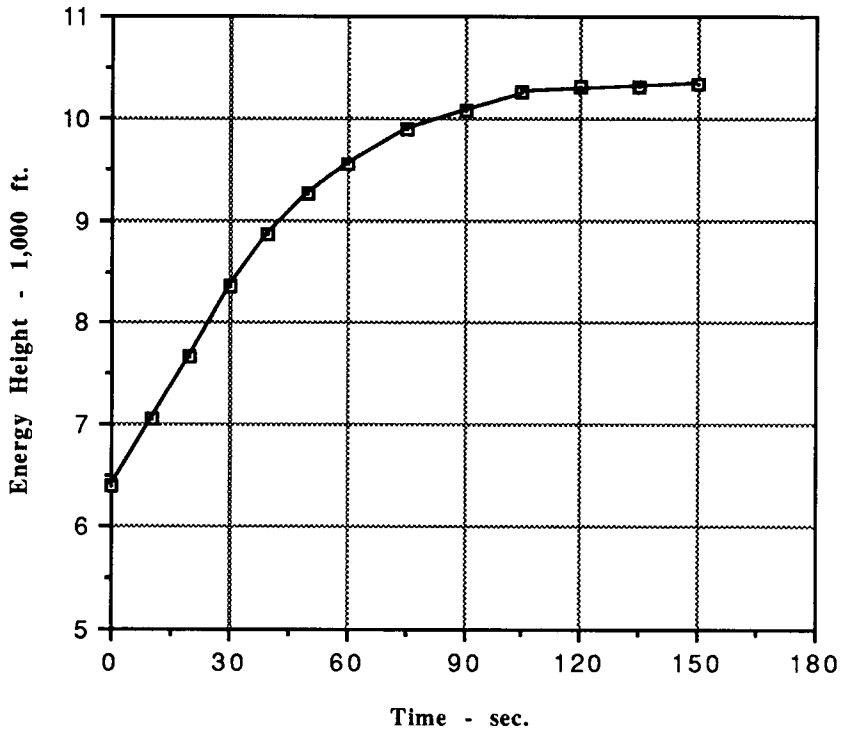

A level acceleration was conducted using maximum thrust at 5,000 ft. MSL. Airspeed versus time data produced this energy height plot. Average gross weight was 35,100 lb. and load A was used. The free air temperature was approximately 30° F. lower than standard day.

Figure 13
A-10A ENERGY HEIGHT DURING A LEVEL ACCELERATION

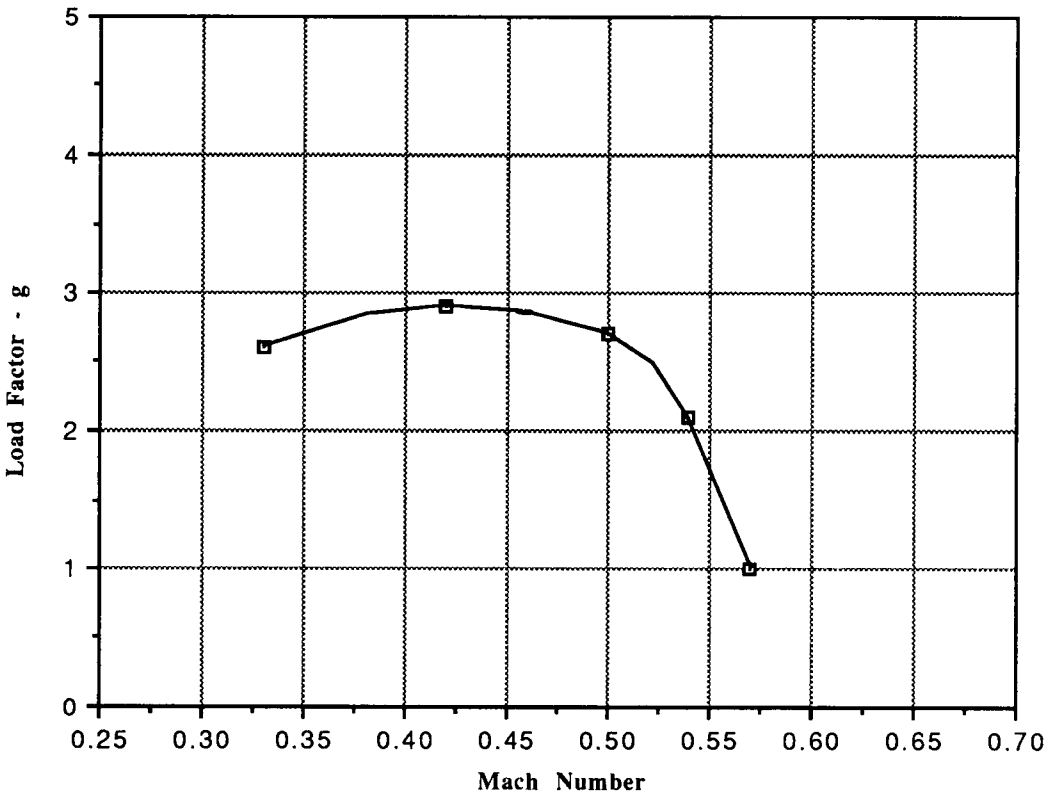

Sustained turns were evaluated at 6,000 ft. MSL and at an average gross weight of 34,400 lb. in load A. Free air temperature was 20° F. lower than standard day.

Figure 14
A-10A MAXIUM SUSTAINED LOAD FACTOR

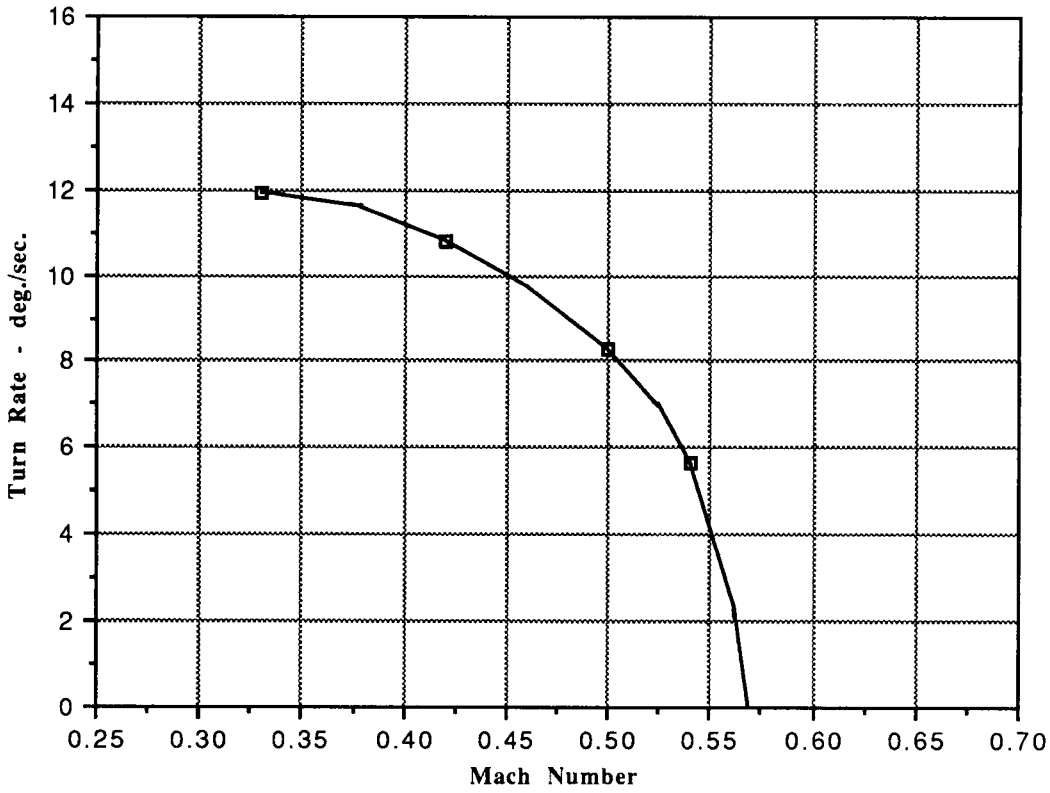

Sustained turns were evaluated at 6,000 ft. MSL and at an average gross weight of 34,400 lb. in load A. Free air temperature was 20° F. lower than standard day.

Figure 15
A-10A MAXIMUM SUSTAINED TURN RATE

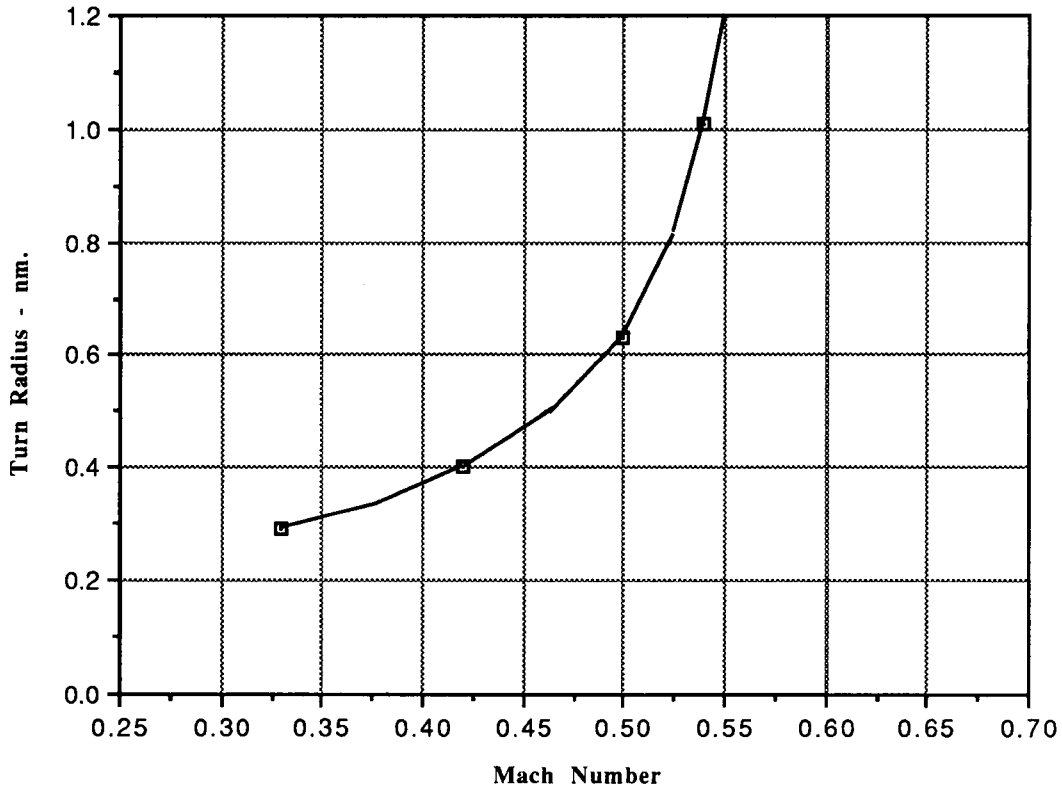

Sustained turns were evaluated at 6,000 ft. MSL and at an average gross weight of 34,400 lb. in load A. Free air temperature was 20° F. lower than standard day.

Figure 16
A-10A MINIMUM SUSTAINED TURN RADIUS

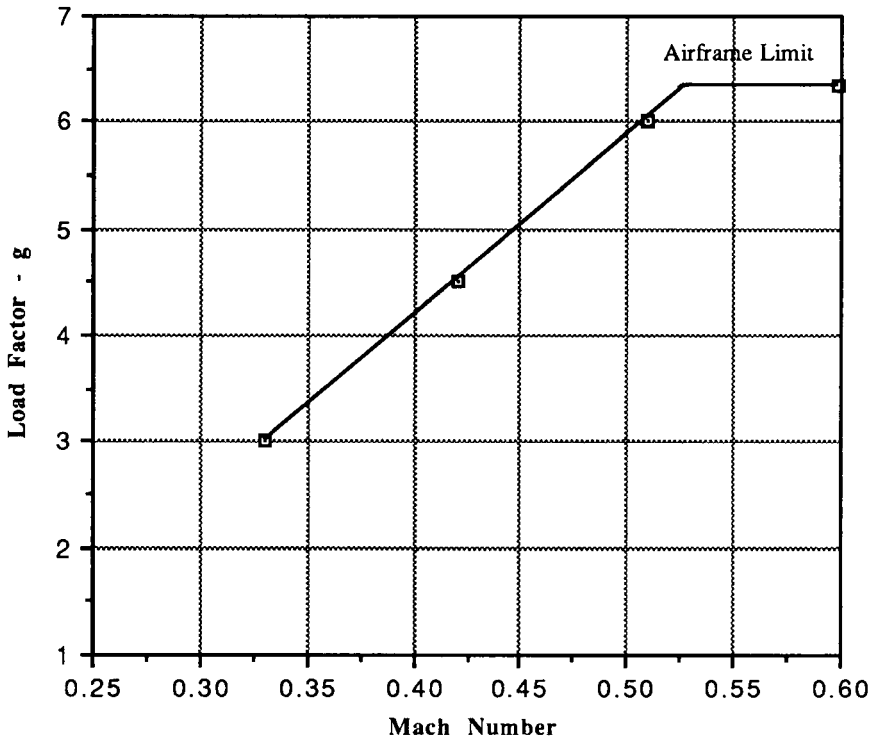

Instantaneous turns were evaluated at 6,000 ft. MSL and at an average gross weight of 34,400 lb. in load A.

Figure 17
A-10A MAXIMUM INSTANTANEOUS LOAD FACTOR

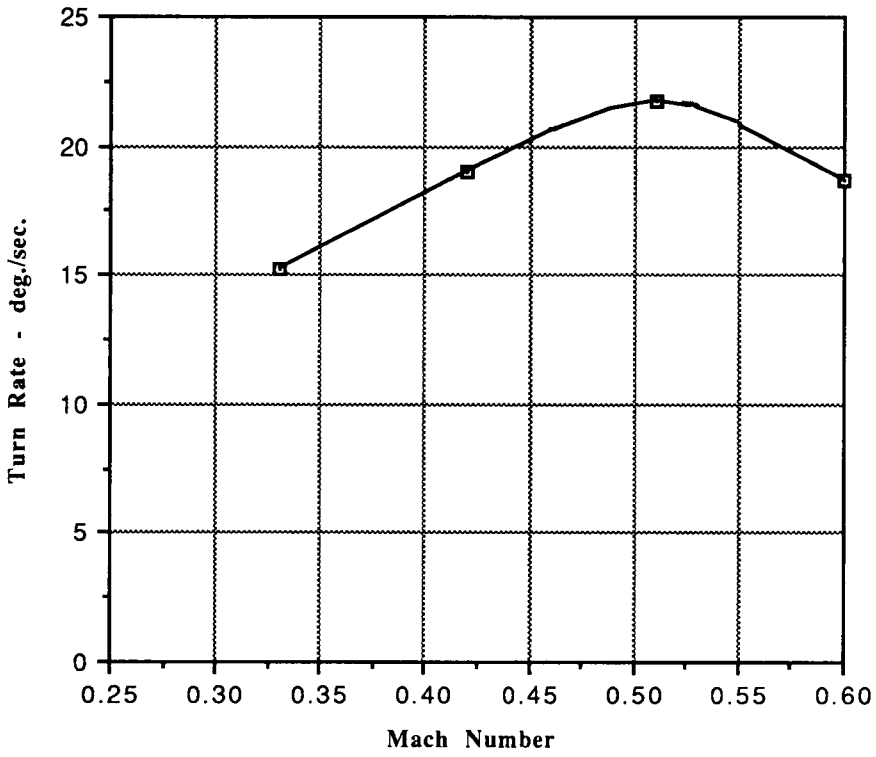

Instantaneous turns were evaluated at 6,000 ft. MSL and at an average gross weight of 34,400 lb. in load A.

Figure 18
A-10A MAXIMUM INSTANTANEOUS TURN RATE

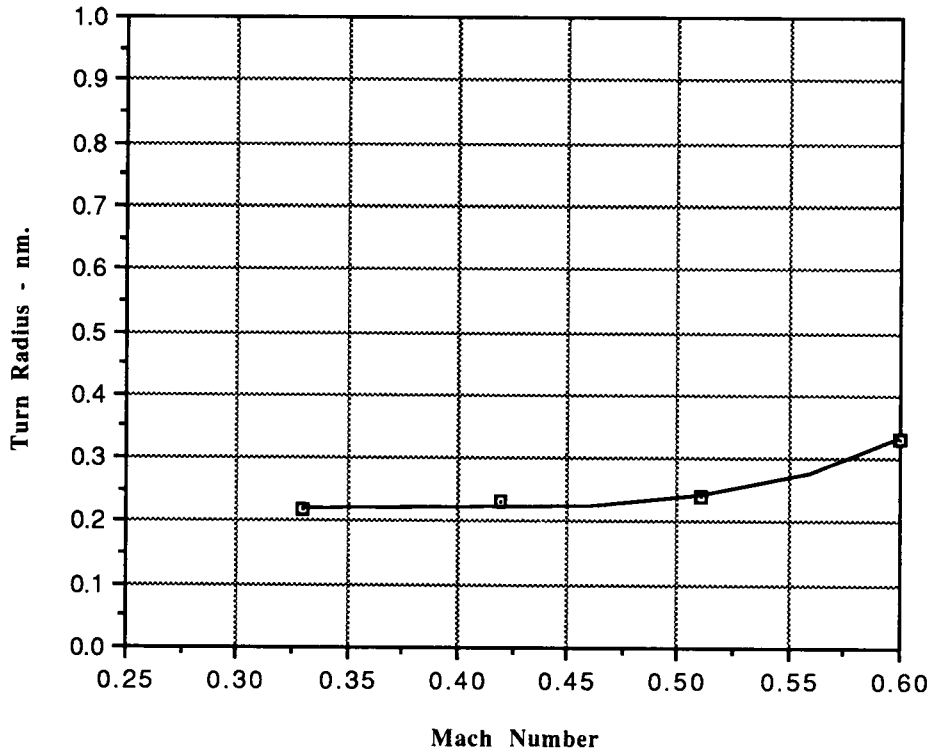

Instantaneous turns were evaluated at 6,000 ft. MSL and at an average gross weight of 34,400 lb. in load A.

Figure 19
A-10A MINIMUM INSTANTANEOUS TURN RADIUS

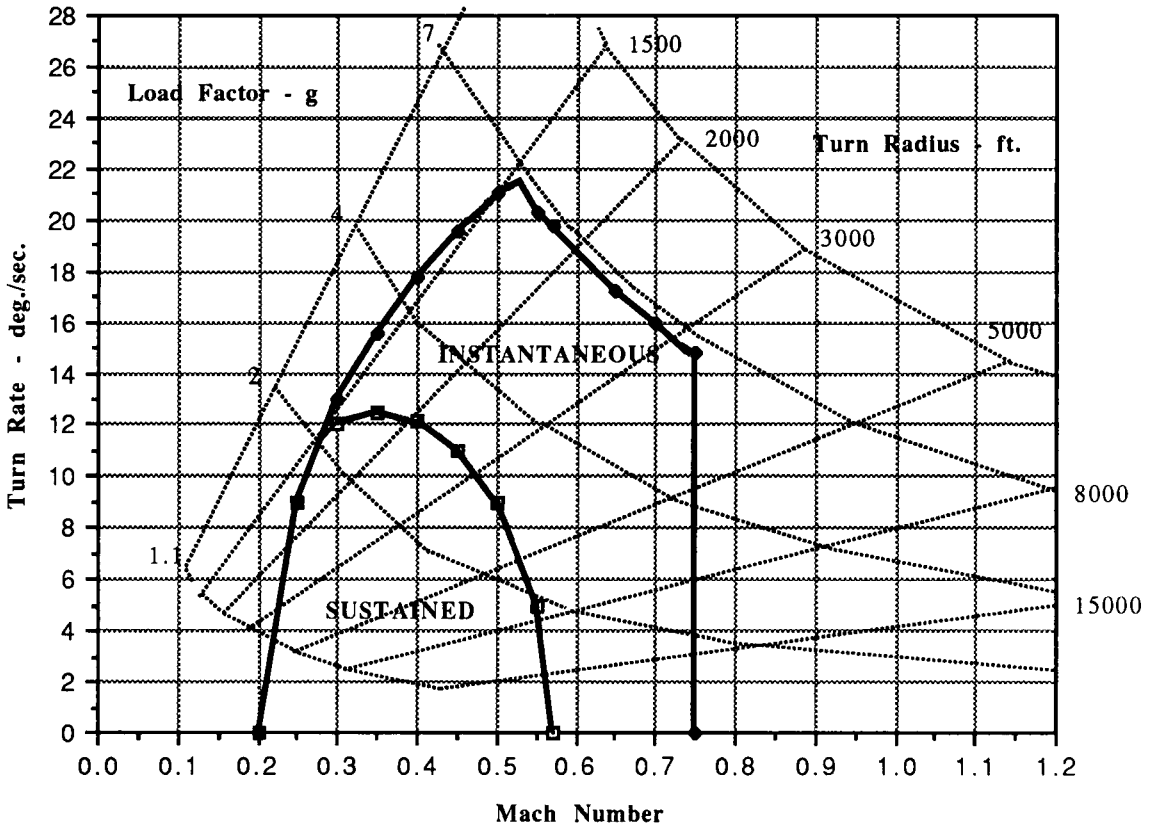

The total envelope presented is based upon the data collected during the turn performance tests conducted at 6,000 ft. MSL. Average gross weight represented is 34,400 lb.

Figure 20
A-10A TOTAL MANEUVERING ENVELOPE

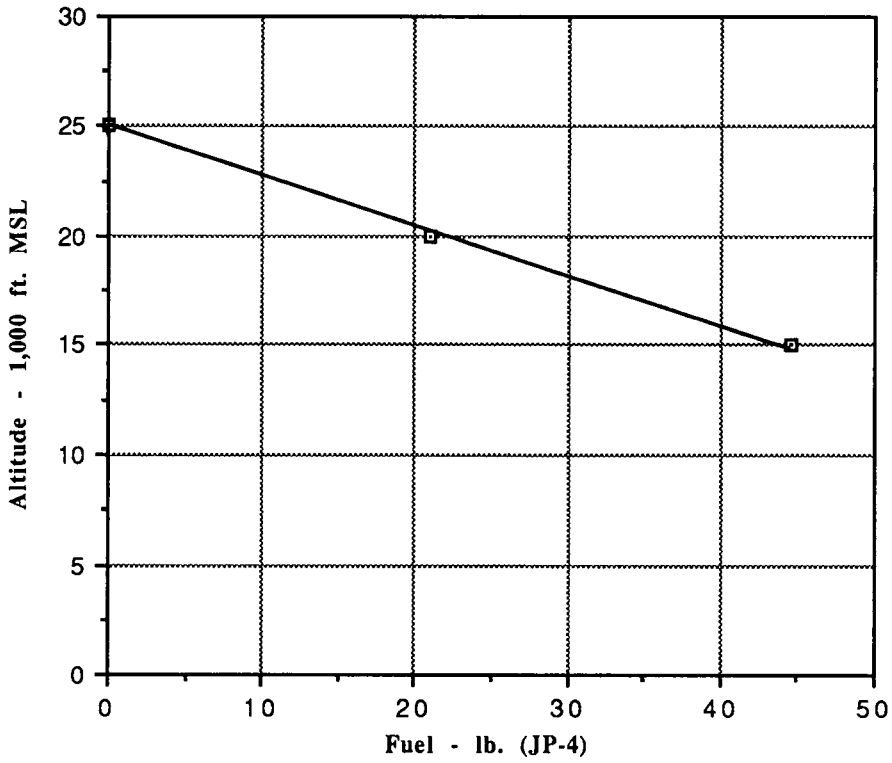

The glide descent was conducted at idle thrust and 155 KIAS, as recommended by the A-10A Flight Manual. The average gross weight was 36,200 lb.

Figure 21
A-10A FUEL TO GLIDE DESCEND

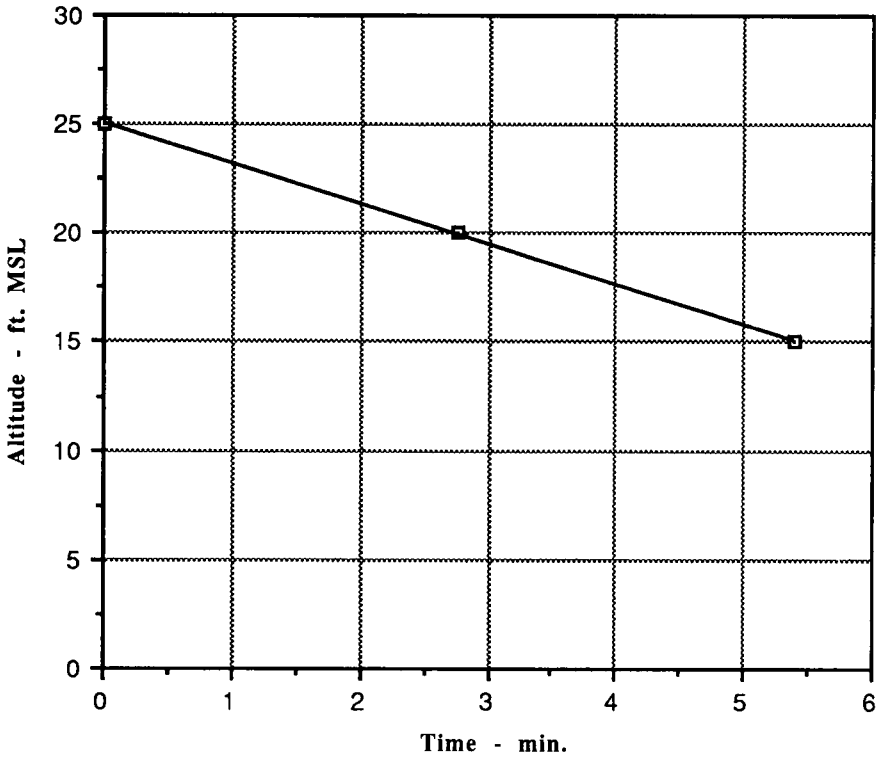

The glide descent was conducted at idle thrust and 155 KIAS, as recommended by the A-10A Flight Manual. The average gross weight was 36,200 lb.

Figure 22
A-10A TIME TO GLIDE DESCEND

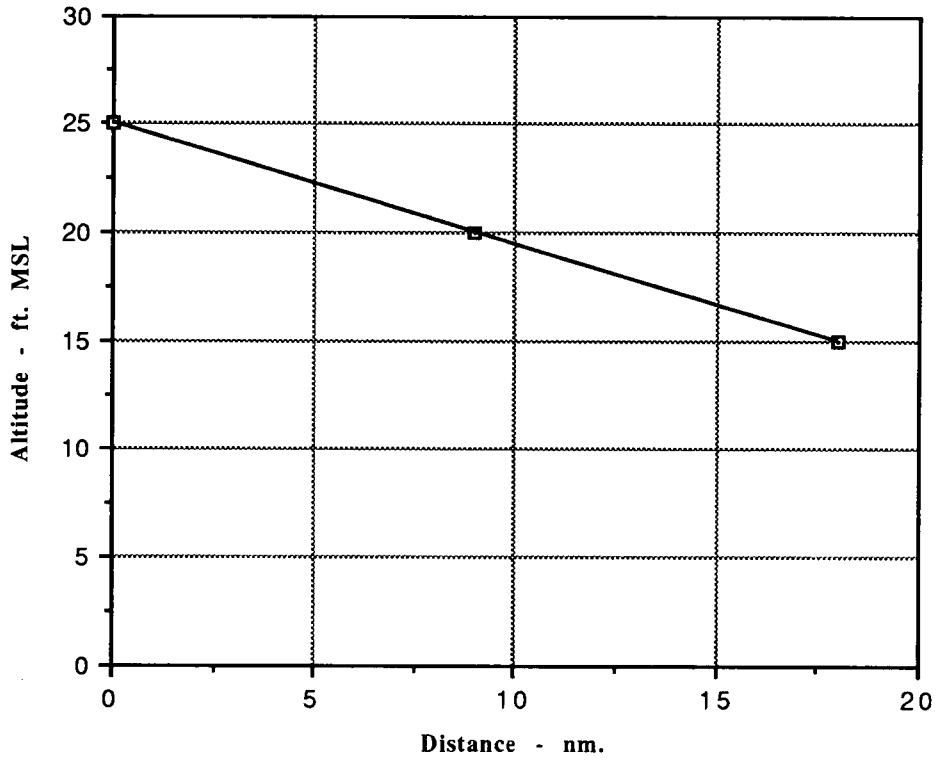

The glide descent was conducted at idle thrust and 155 KIAS, as recommended by the A-10A Flight Manual. The average gross weight was 36,200 lb.

Figure 23
A-10A DISTANCE TO GLIDE DESCEND

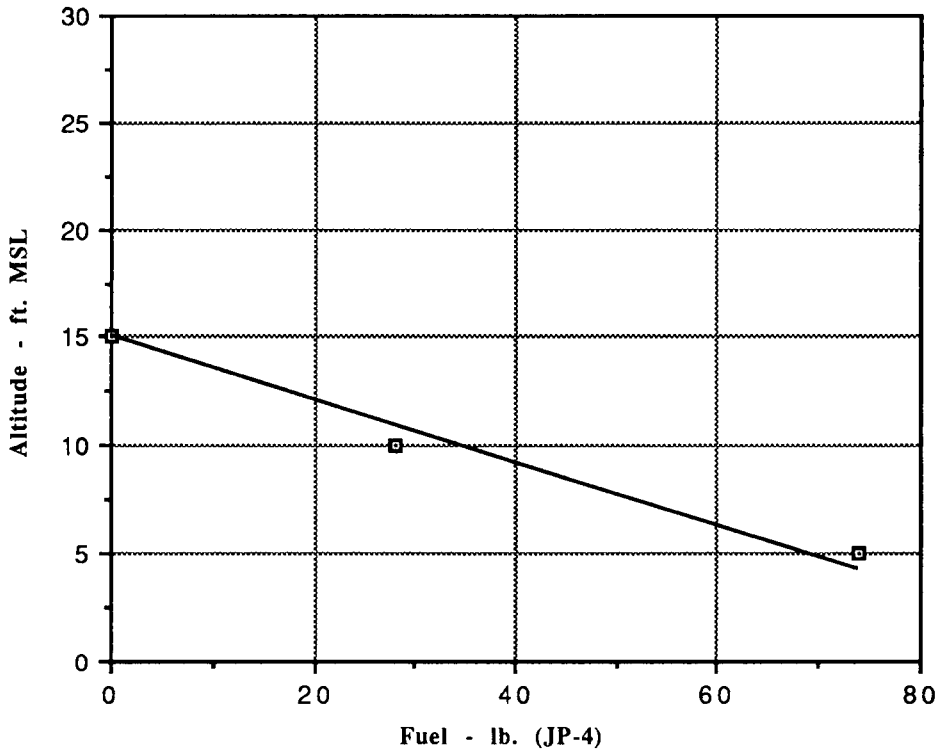

The penetration descent was conducted at idle thrust, 40% speedbrake extension, and 250 KIAS, as recommended by the A-10A Flight Manual. The average gross weight was 35,500 lb.

Figure 24
A-10A FUEL FOR PENETRATION DESCENT

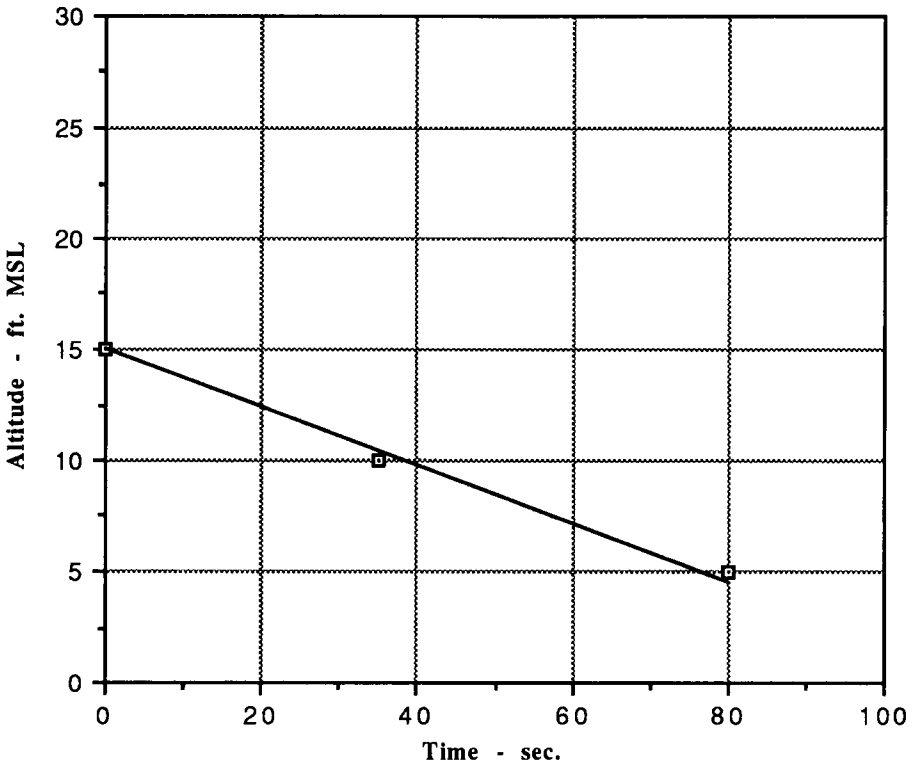

The penetration descent was conducted at idle thrust, 40% speedbrake extension, and 250 KIAS, as recommended by the A-10A Flight Manual. The average gross weight was 35,500 lb.

Figure 25
A-10A TIME FOR PENETRATION DESCENT

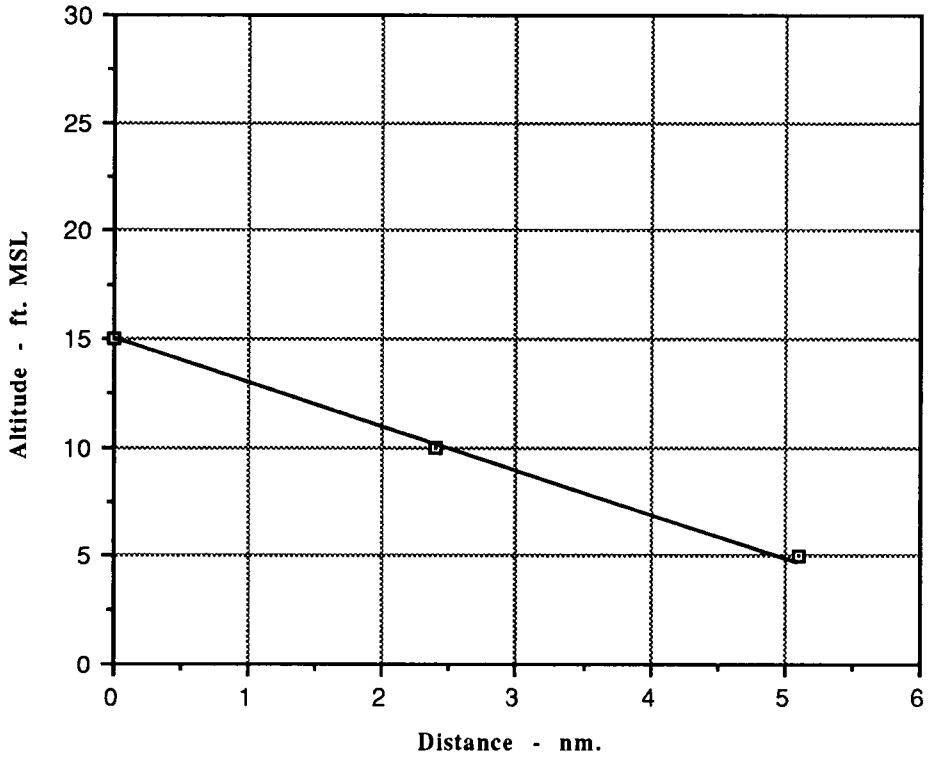

The penetration descent was conducted at idle thrust, 40% speedbrake extension, and 250 KIAS, as recommended by the A-10A Flight Manual. The average gross weight was 35,500 lb.

Figure 26
A-10A DISTANCE FOR PENETRATION DESCENT

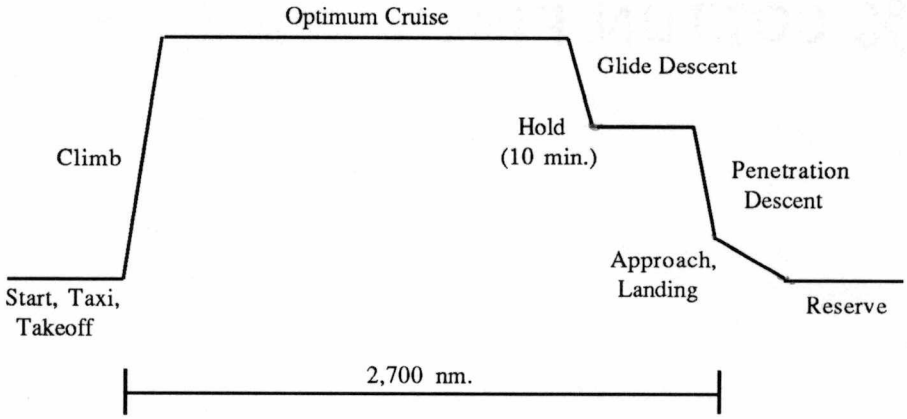

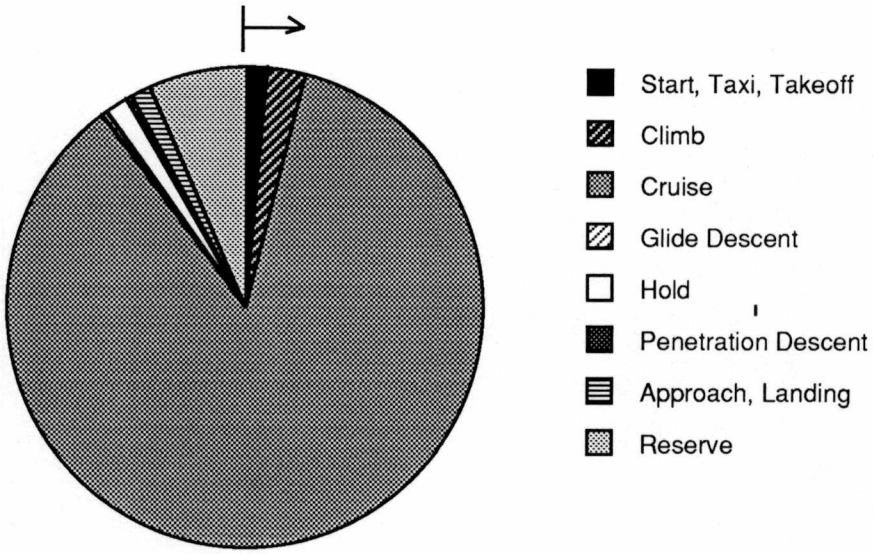

Assuming 22,000 lb. of JP-4 fuel is available (3 external fuel tanks) and load B fuel consumption figures are used from the flight test results herein, maximum distance, one-way flight is depicted. The assumption is made that no significant fuel savings are available by flight above 25,000 ft. MSL (highest tested).

Figure 27
A-10A FERRY MISSION PROFILE

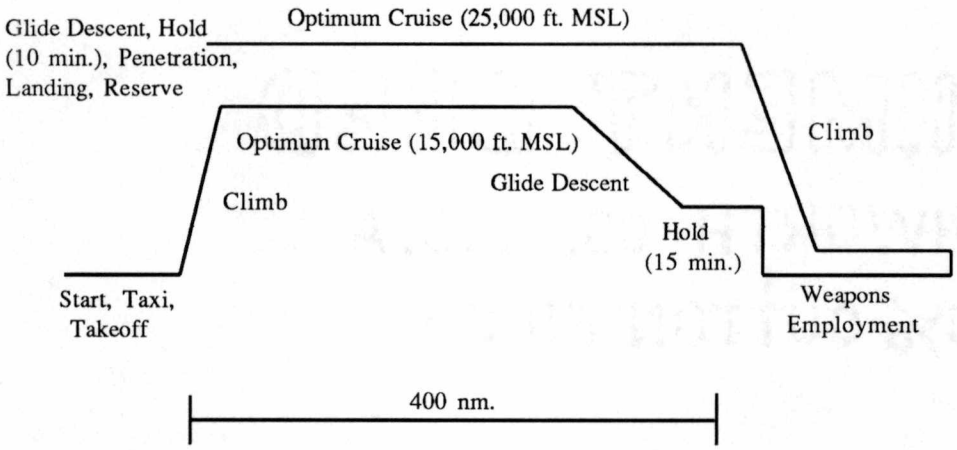

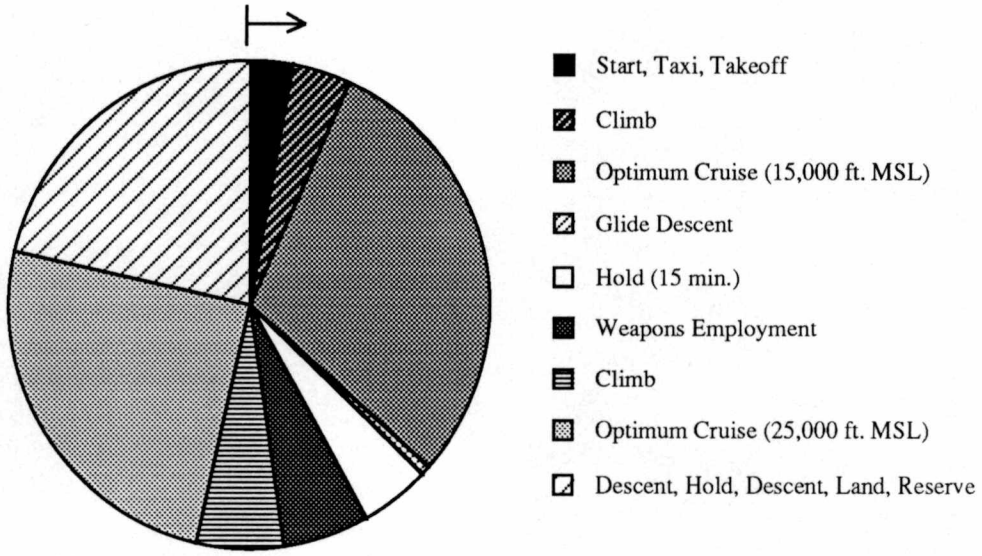

Assuming 10,500 lb. of JP-4 fuel is available and both load A and B fuel consumption figures are used as appropriate, from the flight test results herein, maximum distance, two-way flight is depicted. The assumption is made that no significant fuel savings are available by flight above 25,000 ft. MSL (highest tested).

Figure 28
A-10A CLOSE AIR SUPPORT MISSION PROFILE

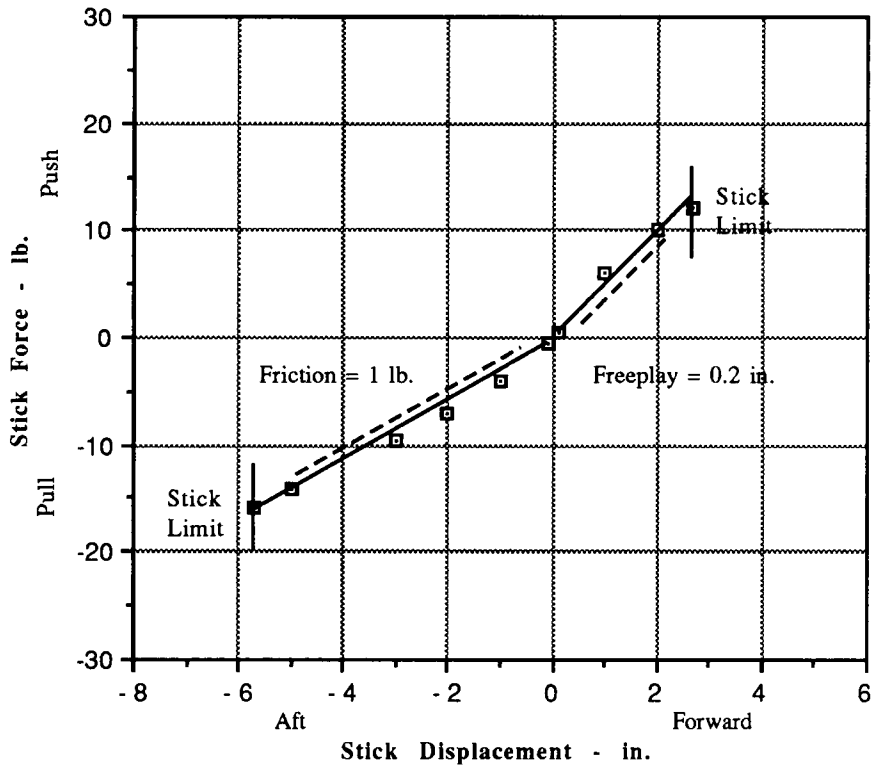

Control measurements were made during a two-engine turn on deck. They were spot verified inflight at 15,000 ft. MSL in load A and at a gross weight and CG of 37,500 lb. and 24.5 %MAC.

Figure 29
A-10A LONGITUDINAL CONTROL GRADIENT

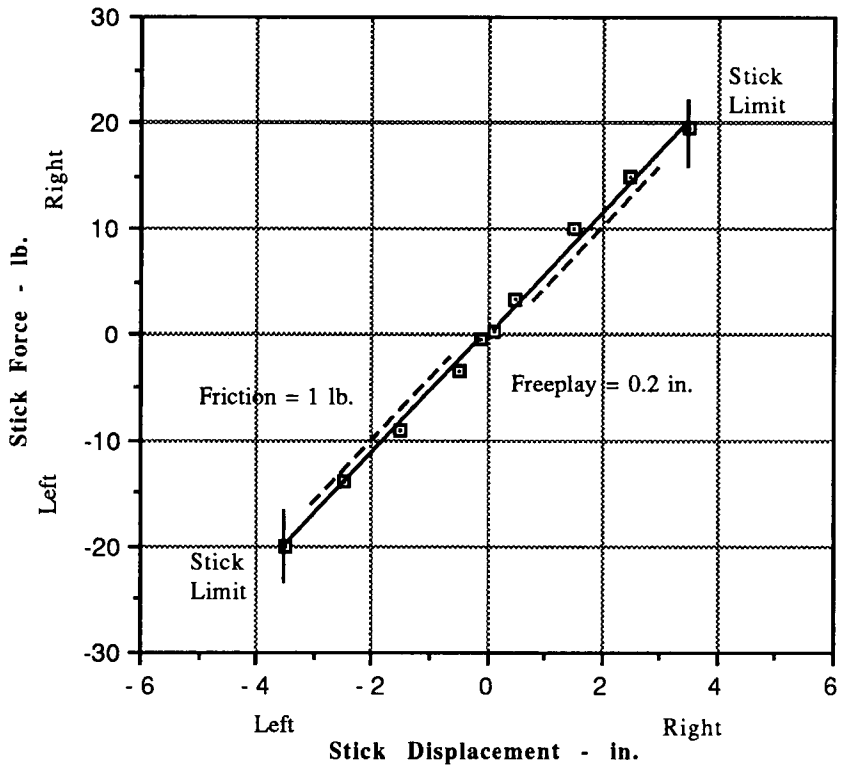

Control measurements were made during a two-engine turn on deck. They were spot verified inflight at 15,000 ft. MSL in load A and at a gross weight and CG of 37,500 lb. and 24.5 %MAC.

Figure 30
A-10A LATERAL CONTROL GRADIENT

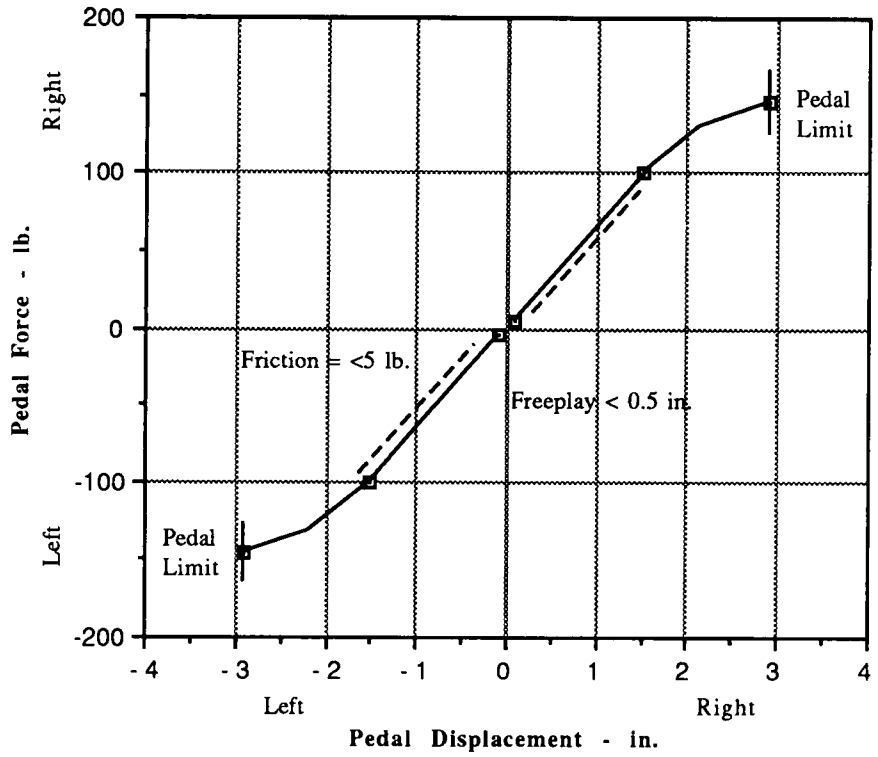

Control measurements were made during a two-engine turn on deck. They were spot verified inflight at 15,000 ft. MSL in load A and at a gross weight and CG of 37,500 lb. and 24.5 %MAC.

Figure 31
A-10A DIRECTIONAL CONTROL GRADIENT

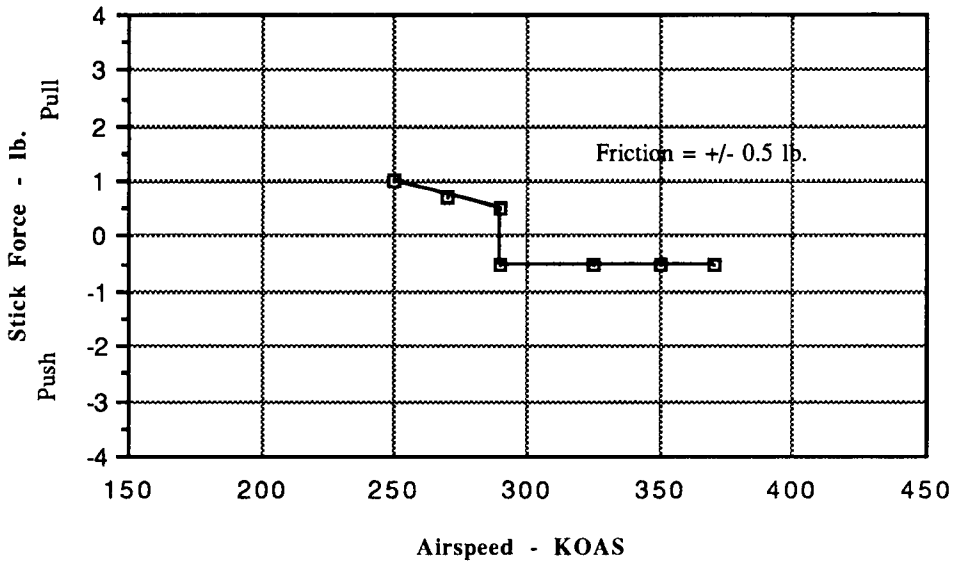

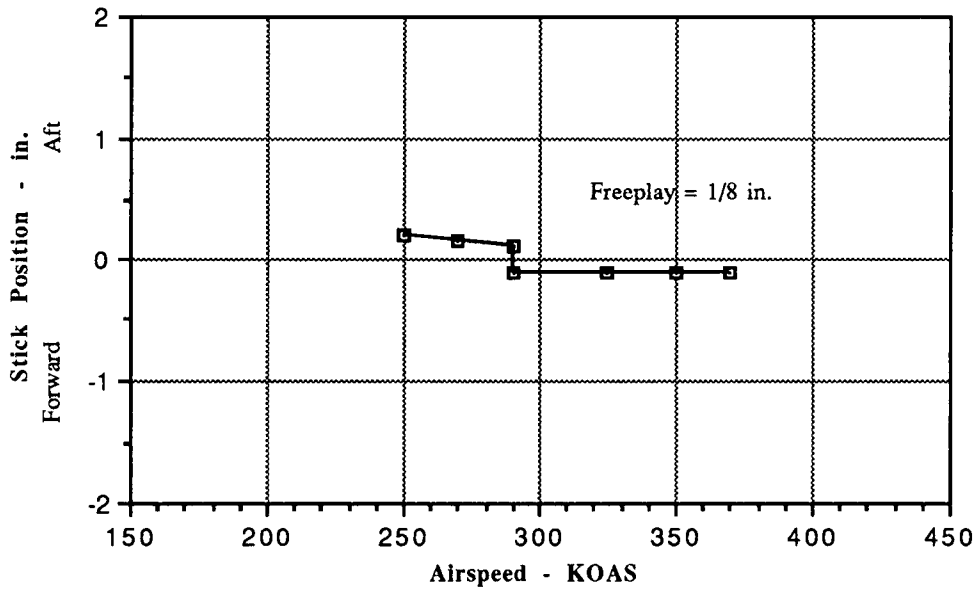

Cruise static longitudinal stability was measured inflight at 8,000 ft. MSL and from a trim airspeed of 295 KOAS. The average gross weight and CG was 35,500 lb. and 24.0 %MAC.

Figure 32
A-10A CRUISE STATIC LONGITUDINAL STABILITY

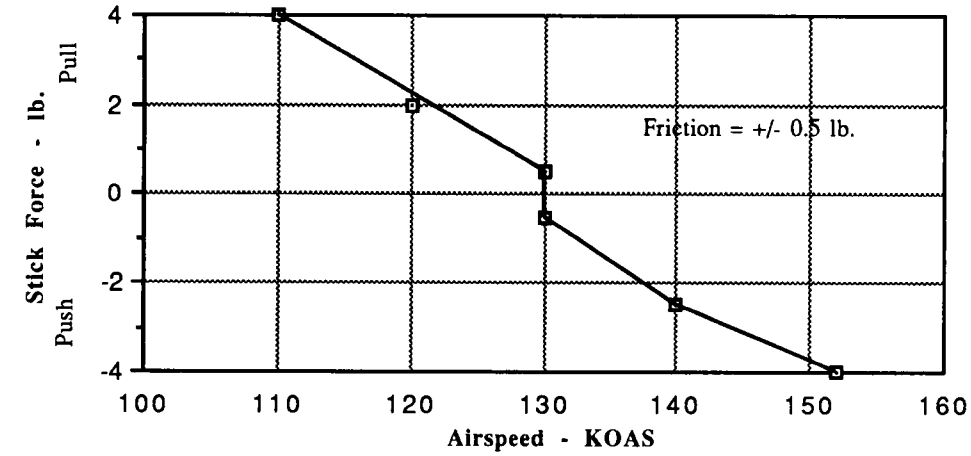

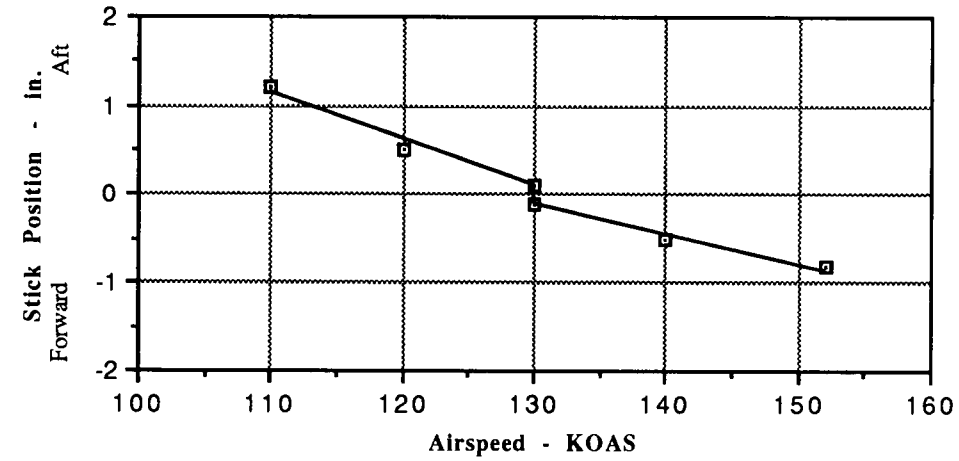

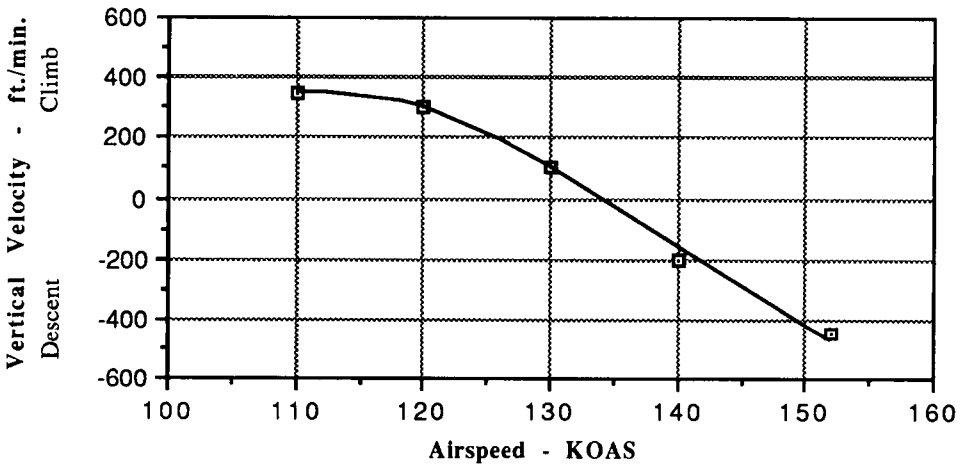

Landing static longitudinal stability was measured inflight at 8,000 ft. MSL and from a trim airspeed of 130 KOAS. The average gross weight and CG was 32,300 lb. and 24.7 %MAC.

Figure 33
A-10A LANDING STATIC LONGITUDINAL STABILITY

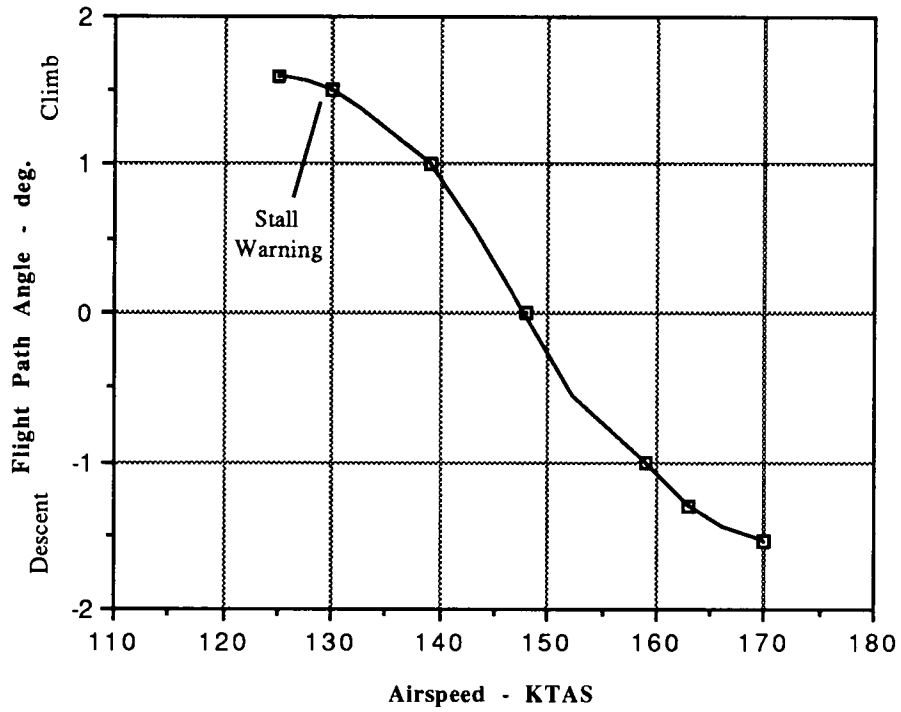

Landing flight path stability was measured inflight at 8,000 ft. MSL and from a trim airspeed of 130 KOAS. The average gross weight and CG was 32,300 lb. and 24.7 %MAC. Data was converted from rate of climb/descent to flight path angle, and it should be noted that it is presented with respect to true airspeed.

Figure 34
A-10A LANDING FLIGHT PATH STABILITY

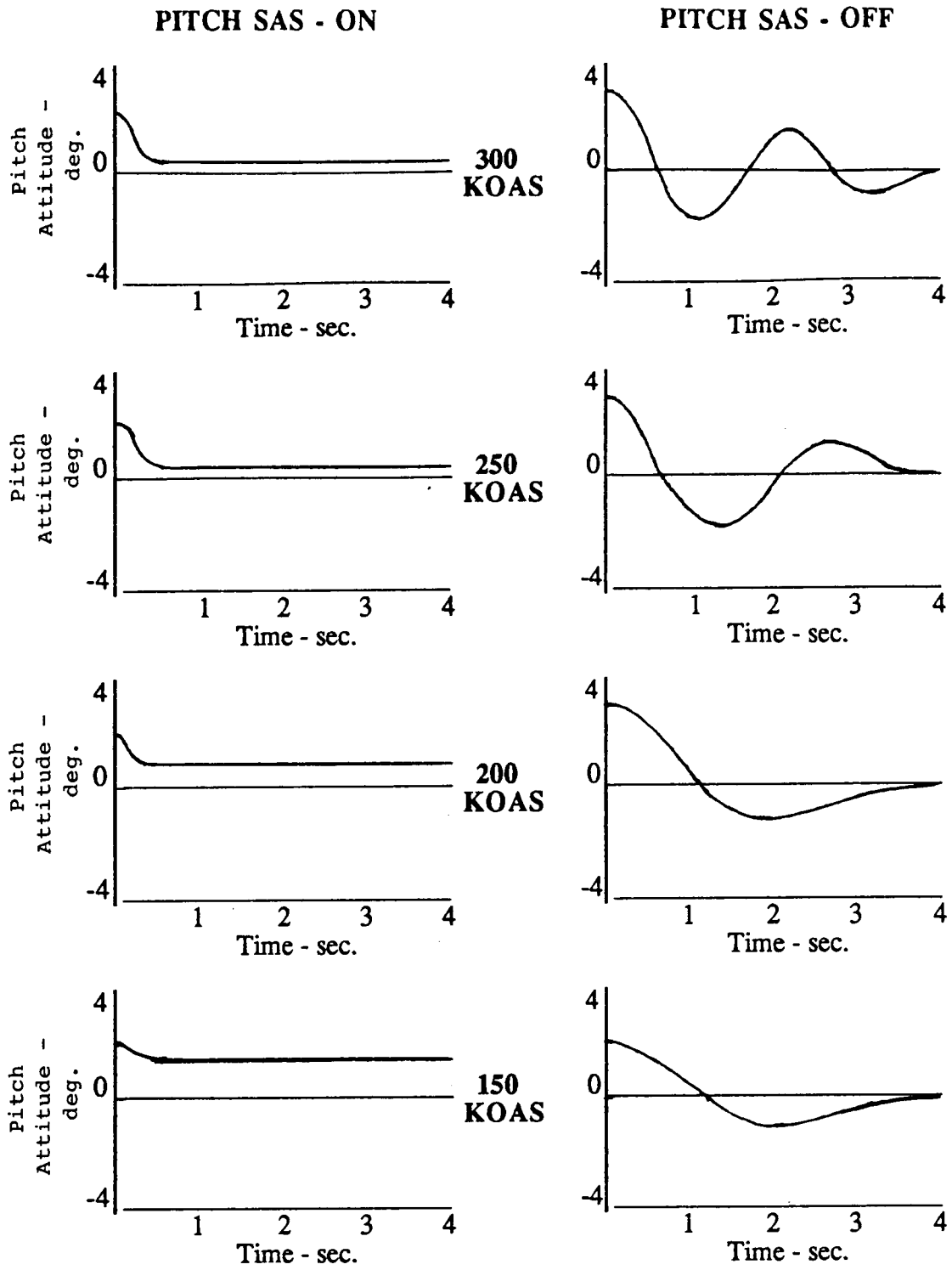

Pitch doublets were conducted at 15,000 ft. MSL and at an average gross weight and CG of 35,800 lb. and 24.0 %MAC. Load A was used.

Figure 35
A-10A CRUISE SHORT PERIOD CHARACTERISTICS

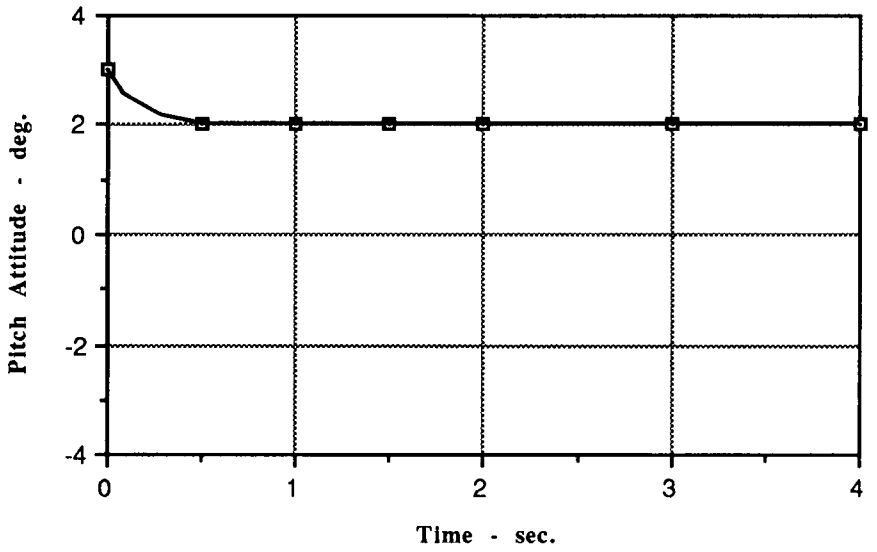

Pitch SAS On

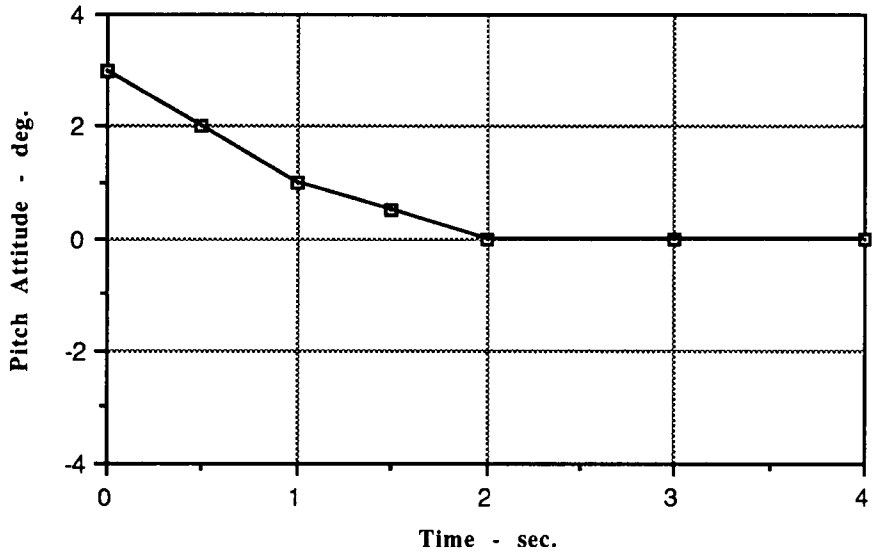

Pitch SAS Off

Pitch doublets were conducted at 8,000 ft. MSL and at an average gross weight and CG of 353,500 lb. and 25.0 %MAC. Load A was used.

Figure 36
A-10A LANDING SHORT PERIOD CHARACTERISTICS

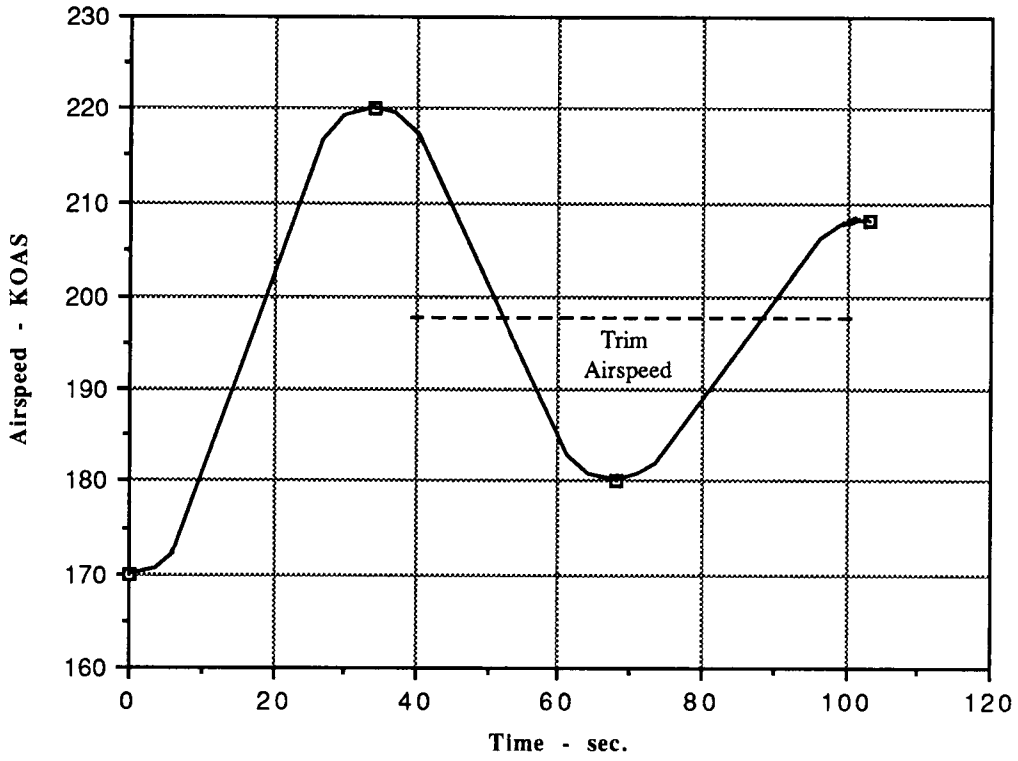

The aircraft was trimmed to approximately 200 KOAS at 15,000 ft. MSL. After being placed out of trim, the aircraft was allowed to seek its own pitch attitude with controls-free. Load A was used and the average gross weight CG was 36,500 lb. and 24.2 %MAC.

Figure 37
A-10A CRUISE PHUGOID CHARACTERISTICS

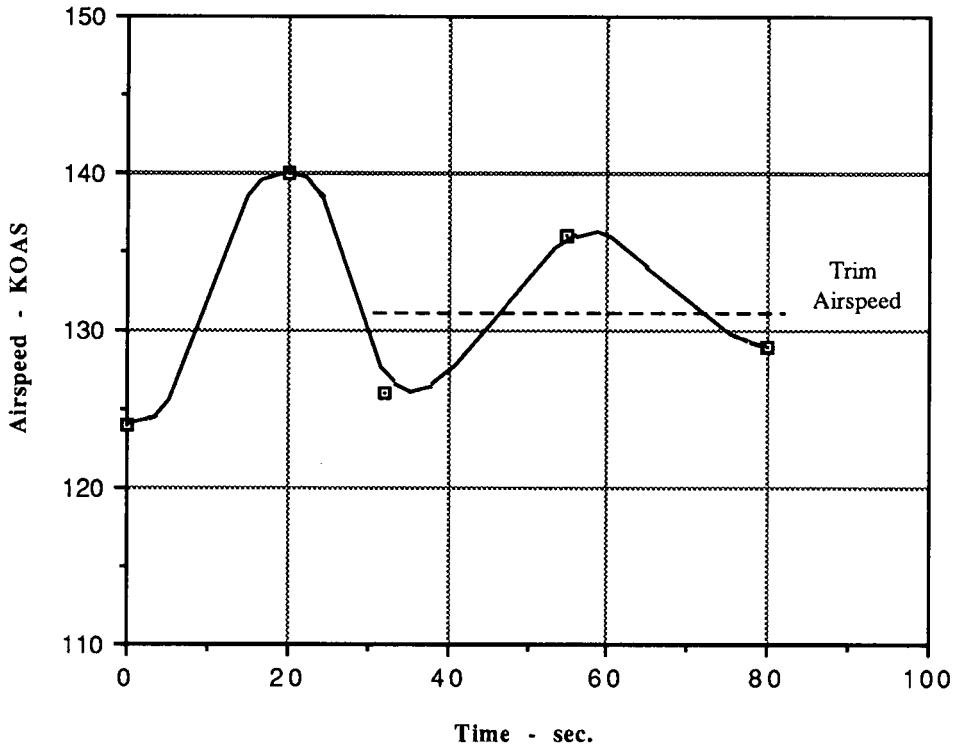

The aircraft was trimmed to approximately 130 KOAS at 8,000 ft. MSL. After being placed out of trim, the aircraft was allowed to seek its own pitch attitude with controls-free. Load A was used and the average gross weight CG was 33,000 lb. and 24.9 %MAC.

Figure 38
A-10A LANDING PHUGOID CHARACTERISTICS

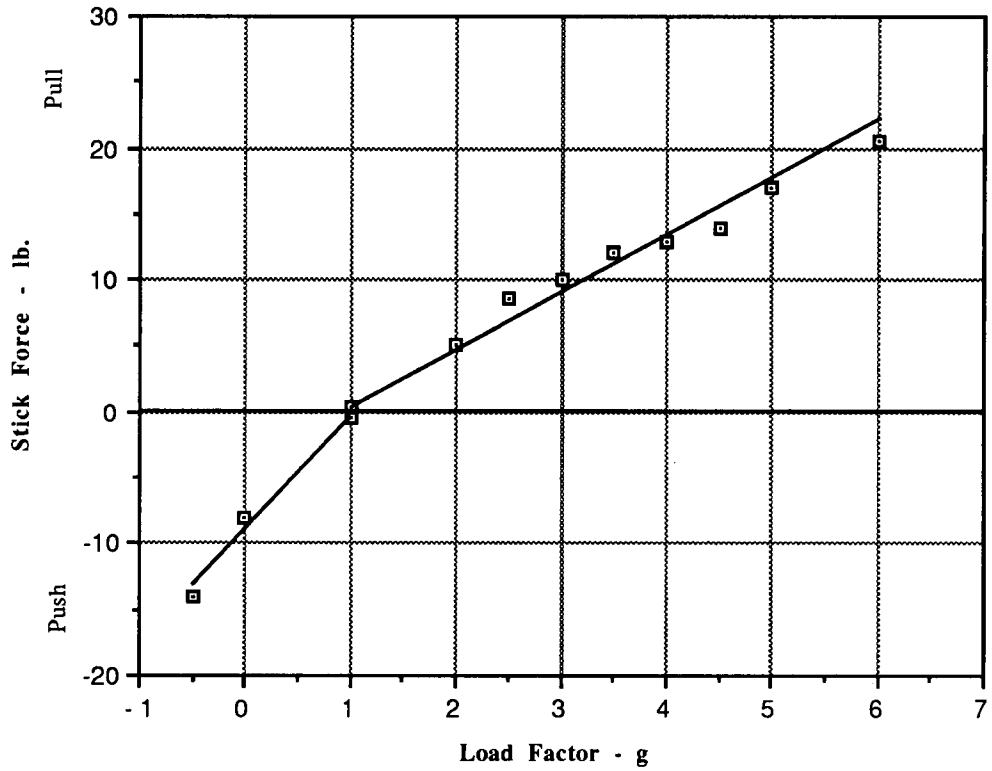

Stabilized, wings-level pulls and pushes were conducted at 8,000 ft. MSL and 325 KOAS. Load A and maximum thrust was used. The average gross weight and CG was 34,500 lb. and 23.6 %MAC.

Figure 39
A-10A CRUISE LONGITUDINAL MANEUVERING STABILITY

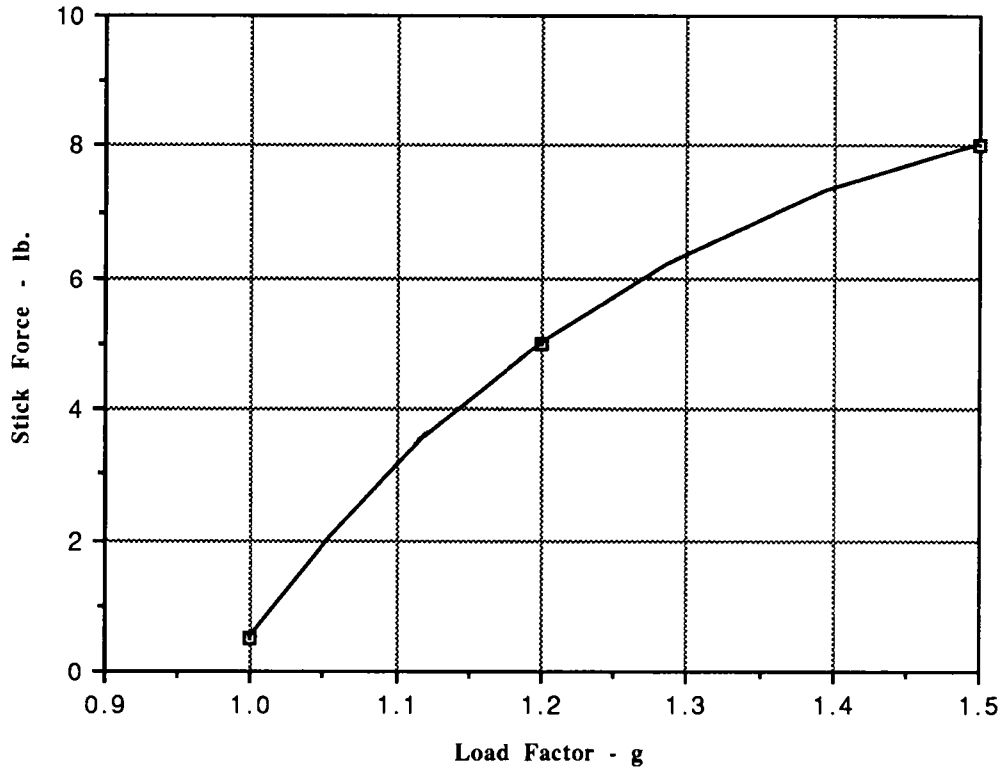

Stabilized, wings-level pulls and pushes were conducted at 8,000 ft. MSL and 140 KOAS. Load B and maximum thrust was used. The average gross weight and CG was 33,000 lb. and 24.9 %MAC.

Figure 40
A-10A LANDING LONGITUDINAL MANEUVERING STABILITY

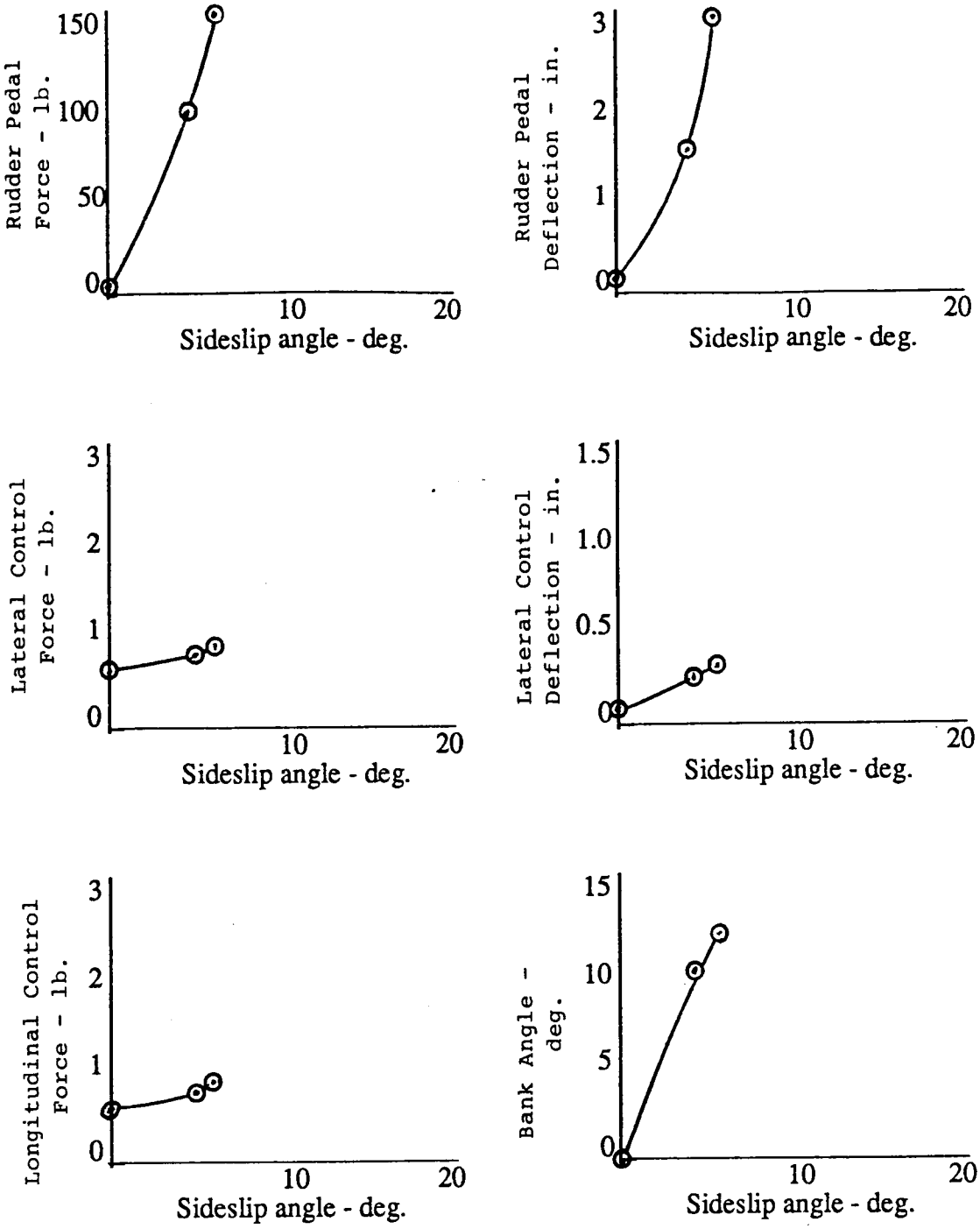

Steady heading sideslips were conducted at 17,000 ft. MSL and at a trim airspeed of 270 KOAS. The average gross weight and CG were 36,000 lb. and 24.1 %MAC. Load A was used.

Figure 41
A-10A CRUISE STATIC LATERAL-DIRECTIONAL STABILITY

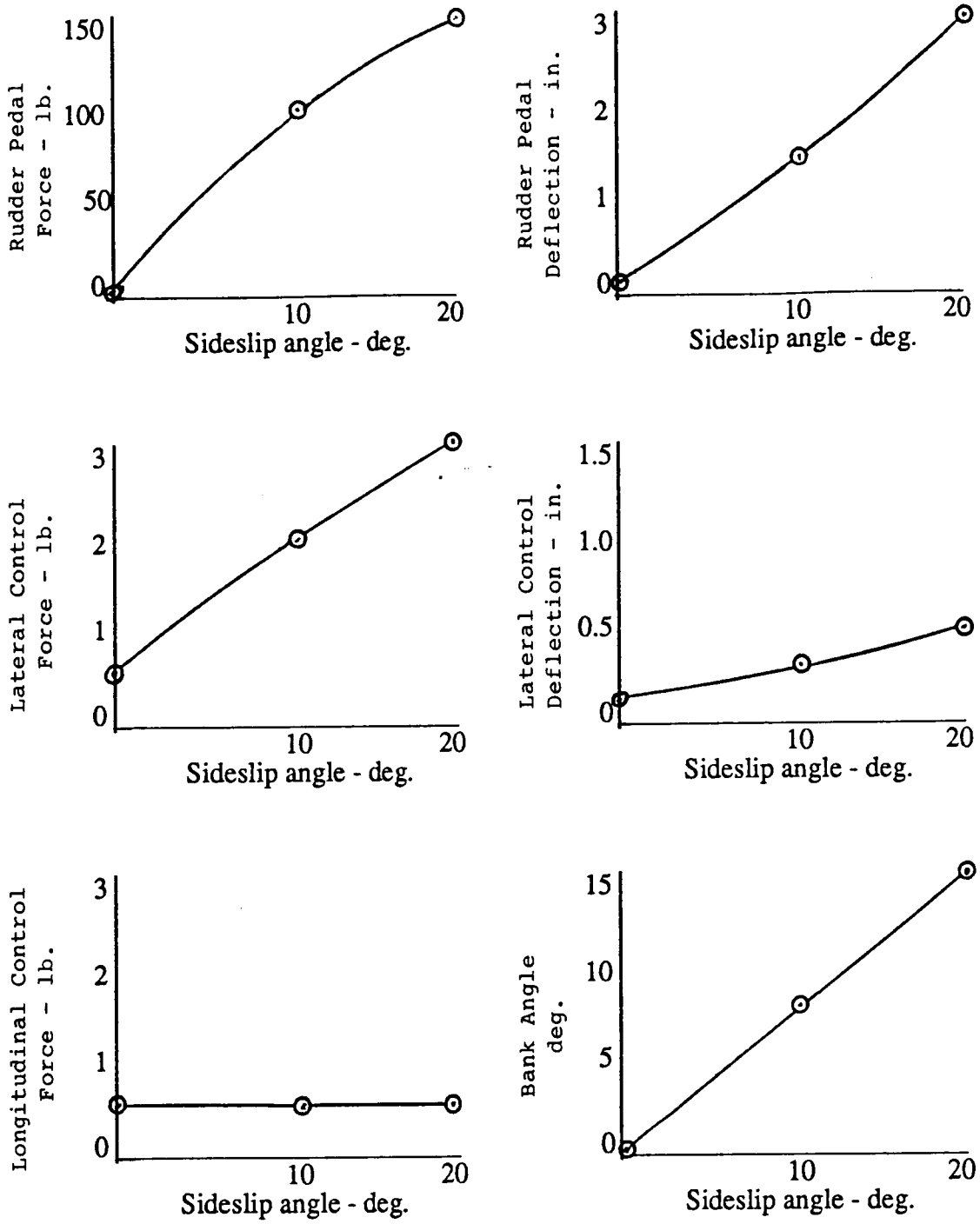

Steady heading sideslips were conducted at 8,000 ft. MSL and at a trim airspeed of 140 KOAS. The average gross weight and CG were 32,900 lb. and 24.9 %MAC. Load A was used.

Figure 42
A-10A LANDING STATIC LATERAL-DIRECTIONAL STABILITY

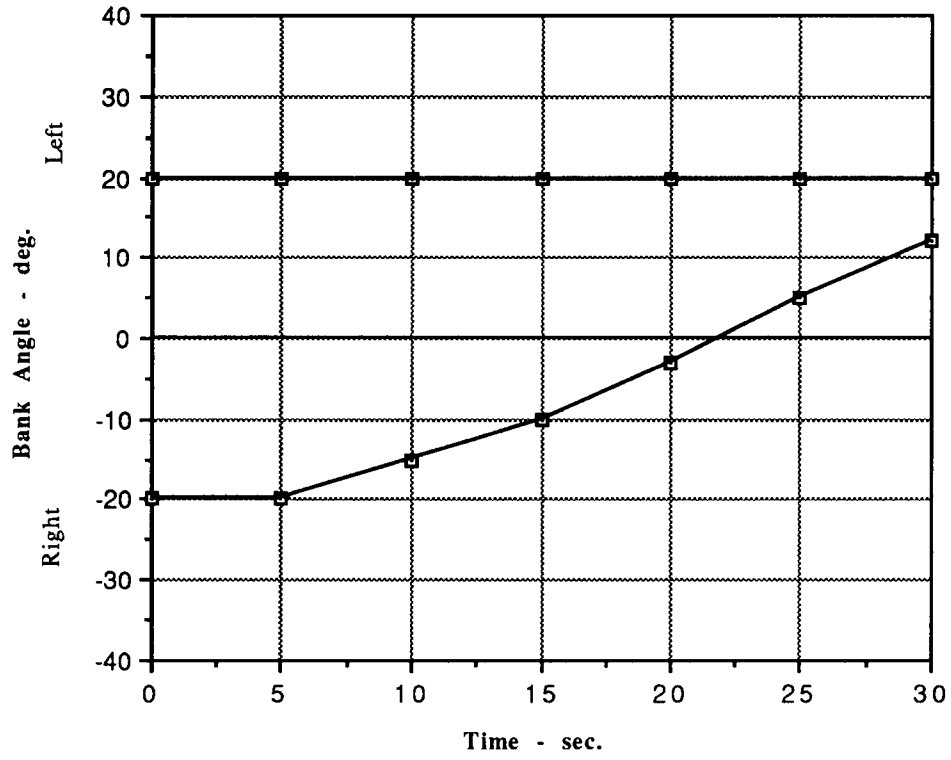

The aircraft was trimmed to 250 KOAS at 15,000 ft. MSL. From a left and a right initial bank angle of 20° the aircraft was allowed to seek its own roll attitude with controls-free. Load A was used and the average gross weight and CG was 36,500 lb. and 24.2 %MAC.

Figure 43
A-10A CRUISE SPIRAL STABILITY

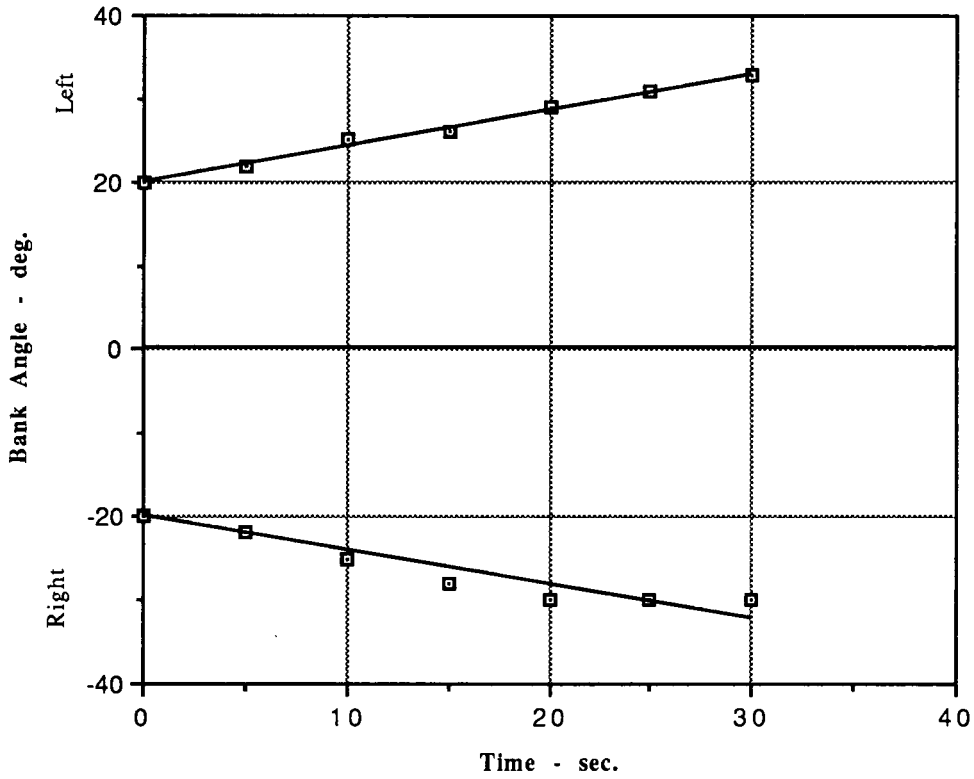

The aircraft was trimmed to 130 KOAS at 8,000 ft. MSL. From a left and a right initial bank angle of 20° the aircraft was allowed to seek its own roll attitude with controls-free. Load A was used and the average gross weight and CG was 33,000 lb. and 24.9 %MAC.

Figure 44
A-10A LANDING SPIRAL STABILITY

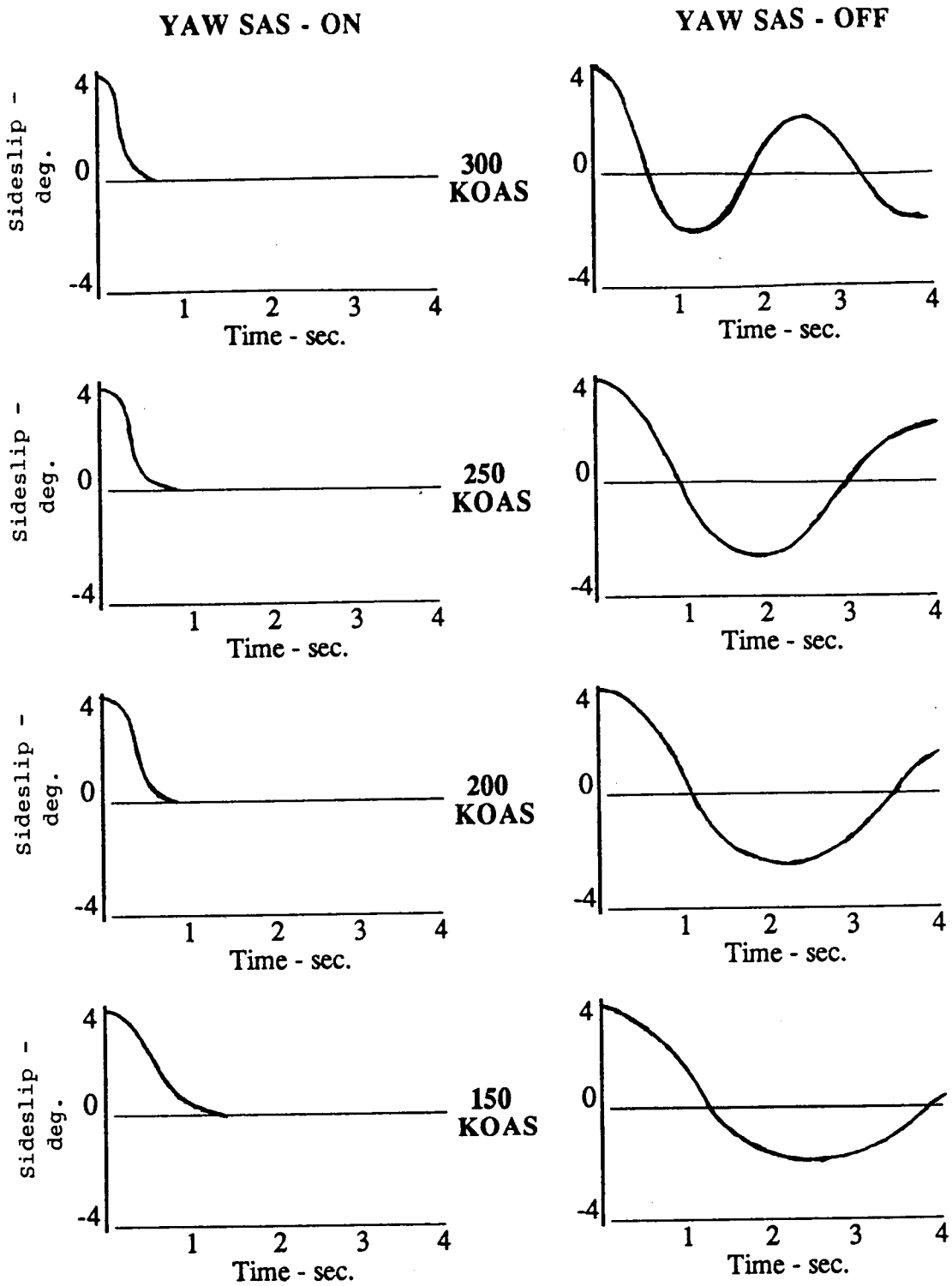

Rudder doublets were conducted at 15,000 ft. MSL and at an average gross weight and CG of 35,800 lb. and 24.0 %MAC. Both A and B loads were used.

Figure 45
A-10A CRUISE DUTCH ROLL CHARACTERISTICS

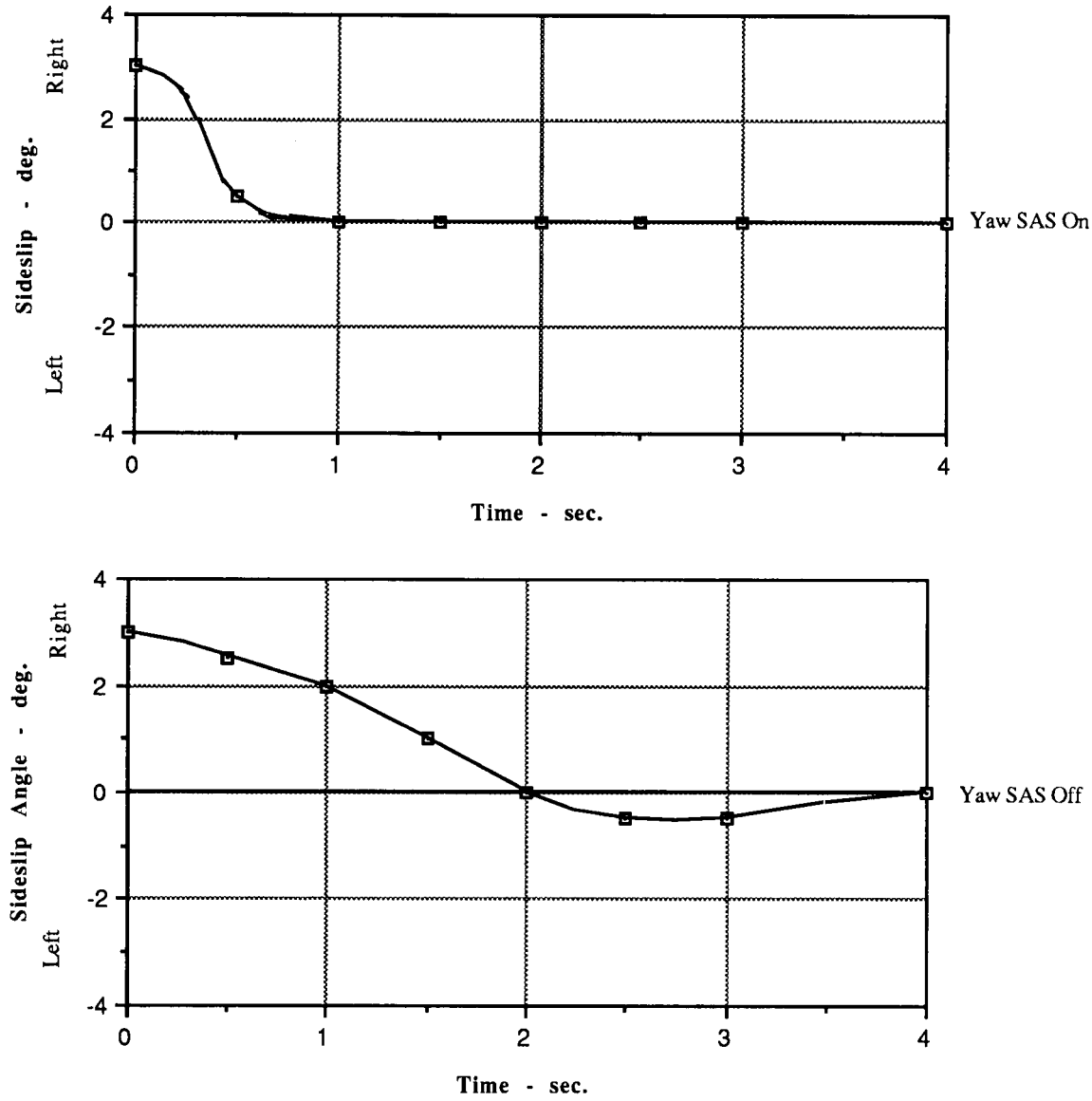

Rudder doublets were conducted at 8,000 ft. MSL and at an average gross weight and CG of 33,500 lb. and 25.0 %MAC. The trim airspeed was 130 KOAS. Both A and B loads were used.

Figure 46
A-10A LANDING DUTCH ROLL CHARACTERISTICS

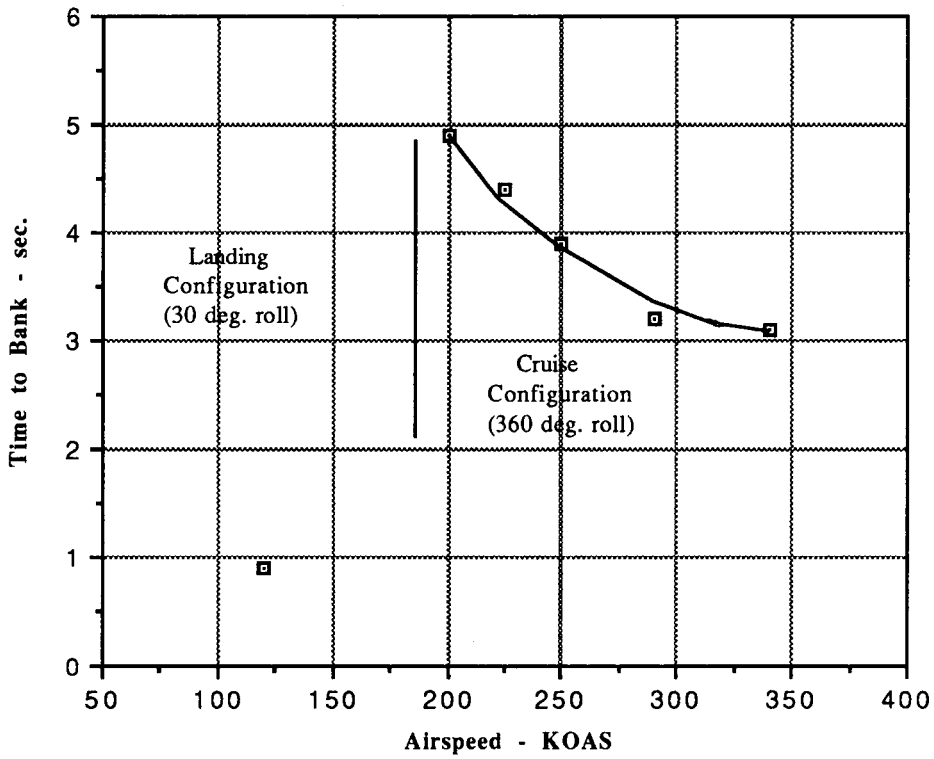

All rolls were performed at 5,000 ft. MSL and full stick deflection was used. Load A was used and the average gross weight and CG was 37,000 lb. and 24.2 %MAC (25.9 %MAC in the landing condition).

Figure 47
A-10A ROLL PERFORMANCE

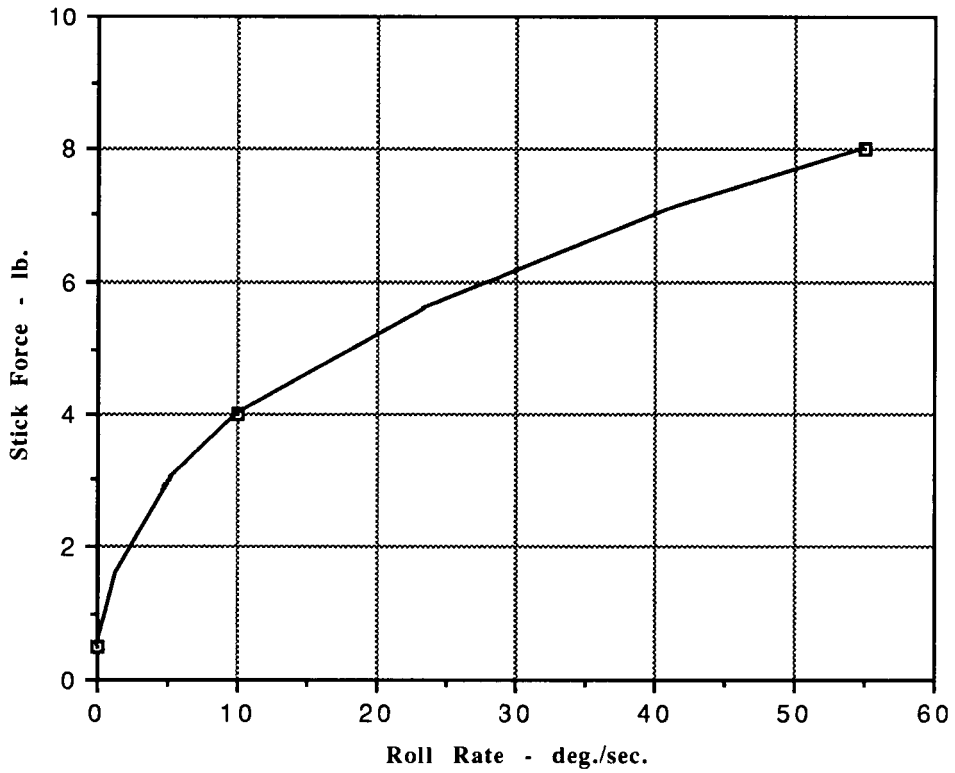

The aircraft was trimmed to 250 KOAS at 15,000 ft. MSL. A steady sideforce was applied to the stick from an initial bank angle of 30°. Roll rate was determined by timing the roll from wings-level to 30° opposite wing down. Load A was used and the average gross weight and CG was 36,500 lb. and 24.2 %MAC.

Figure 48
A-10A CRUISE ROLL SENSITIVITY

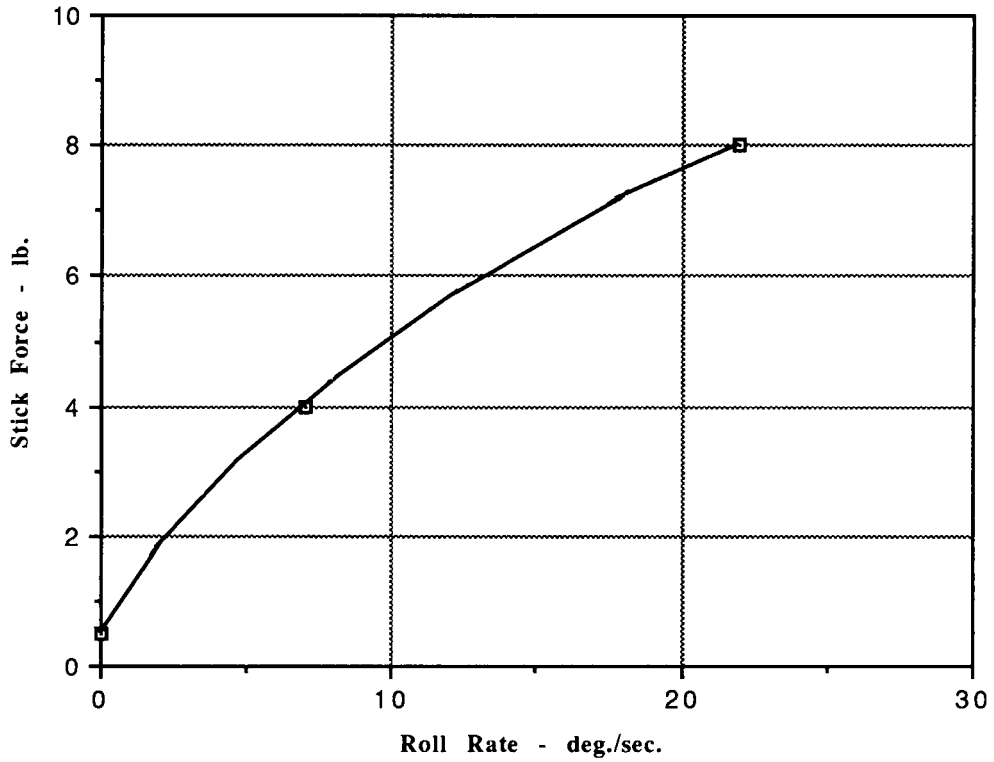

The aircraft was trimmed to 130 KOAS at 10,000 ft. MSL. A steady sideforce was applied to the stick from an initial bank angle of 30°. Roll rate was determined by timing the roll from wings-level to 30° opposite wing down. Load A was used and the average gross weight and CG was 33,000 lb. and 24.9 %MAC.

Figure 49
A-10A LANDING ROLL SENSITIVITY

APPENDIX D

ANALYSIS

1. BASIC ANALYSIS OF A-10A AIRCRAFT CONSTANTS

a. The following is given from the Flight Manual, the NACA standard atmosphere tables, and enclosed descriptions:

$b = 57.5$ ft. (wingspan)
$c = 8.85$ ft. (average wing chord)
$T_1 = 18{,}000$ lb. (original thrust)
$T_2 = 27{,}000$ lb. (improved thrust)
p_a (5,000 ft.) $= 1760$ lb./ft.^{2} (atmospheric pressure)
p_a (15,000 ft.) $= 1190$ lb./ft.^{2}
p_a (25,000 ft.) $= 785$ lb./ft.^{2}
ρ(5,000 ft.) $= 0.00205$ slugs/ft.^{2}
ρ(6,000 ft.) $= 0.00199$ slugs/ft.^{2}

b. The following is derived from standard formulae:

$AR = b/c = 6.50$ (aspect ratio)
$S = bc = 510$ ft.^{2} (wing area)

c. The following formulae will be used throughout as a basis for calculations:

$$D = c_{do}S\rho V^2/2 + (2W^2/\pi eARS\rho V^2) \quad \text{eq. (1)}$$
$$= c_{do}\gamma p_a M^2/2 + (2W^2/\pi eARS\gamma p_a M^2) \quad \text{eq. (2)}$$

$$P_S = V\,(T - D)\,/\,W \quad \text{eq. (3)}$$

d. The following assumptions will be made:

(1) Engine thrust remains constant throughout the aircraft's airspeed envelope.
(2) Engine thrust remains constant from sea level to 6,000 ft. MSL.
(3) Induced drag is negligible at V_{max}.
(4) c_{do} is constant throughout the aircraft's airspeed & altitude envelope.
(5) The drag polar is parabolic.

e. c_{do} will be derived from the V_{max} point (340 KOAS, 370 KTAS, 624 ft./sec.) attained at the end of the acceleration run at 5,000 ft. MSL:

$$D = c_{do}\rho SV^2/2 + (2W^2/\pi eARS\rho V^2) \quad \text{eq. (1)}$$

Since induced drag is negligible:

$$D = c_{do}\rho SV^2/2 \quad \text{eq. (4)}$$

Because the point is a stable one:

$$T = D \quad \text{eq. (5)}$$

So: $T = c_{do}\rho SV^2/2$ eq. (6)

Solving: $c_{do} = 2T/\rho SV^2$ eq. (7)

$= 2\ (18000) / (0.00205)(510)(624)^2$

$= 0.0883$

f. e (wingspan efficiency) varies according to lift coefficient, or more apparently by angle of attack. A rough distribution will be generated by calculation of e at two flight conditions. First, a high lift (23.5 units angle of attack) will be derived from the 200 kt. (338 ft./sec.) maximum sustained turn point at 6,000 ft. MSL and 2.6g:

$D = c_{do}\rho SV^2/2 + 2W^2/\pi eAR S\rho V^2)$ eq. (1)

In this case:

$W = n_z\ W'$ (where W' is the gross weight) eq. (8)

Solving for e:

$e = 2W^2 n_z^2 / (T - (c_{do}\rho SV^2/2))(\pi AR S\rho V^2)$ eq. (9)

$$= \frac{2(34400)^2(2.6)^2}{(18000-((0.0883)(0.00199)(510)(338)^2/2))(\pi(6.5)(510)(0.00199)(338)^2)}$$

$= 0.525$

At a mid-to-high angle of attack (17 units), the minimum drag point is defined by lowest fuel flow required. Efficiency will be computed beginning with the drag distribution of:

$c_d = c_{do} + c_L^2 / \pi eAR$ eq. (10)

Also:

$D = 2D_o$ eq. (11)

so:

$c_{do} = c_L^2 / \pi eAR$ eq. (12)

Furthermore:

$L = c_L\ qS$ eq. (13)

and in level flight:

$L = W$ eq. (14)

Combining:

$c_{do} = W^2 / q^2 S^2 \pi eAR$ eq. (15)

Rearrange:

$e = W^2 / q^2 S^2 \pi AR c_{do}$ eq. (16)

Solve for minimum drag point at 5,000 ft. MSL:

$e = (38000)^2 / ((0.5)(0.00205)(253)^2)^2(510)^2(6.5)(0.0883)$
$e = 0.700$

A presentation of span efficiency versus angle of attack is presented in figure 50.

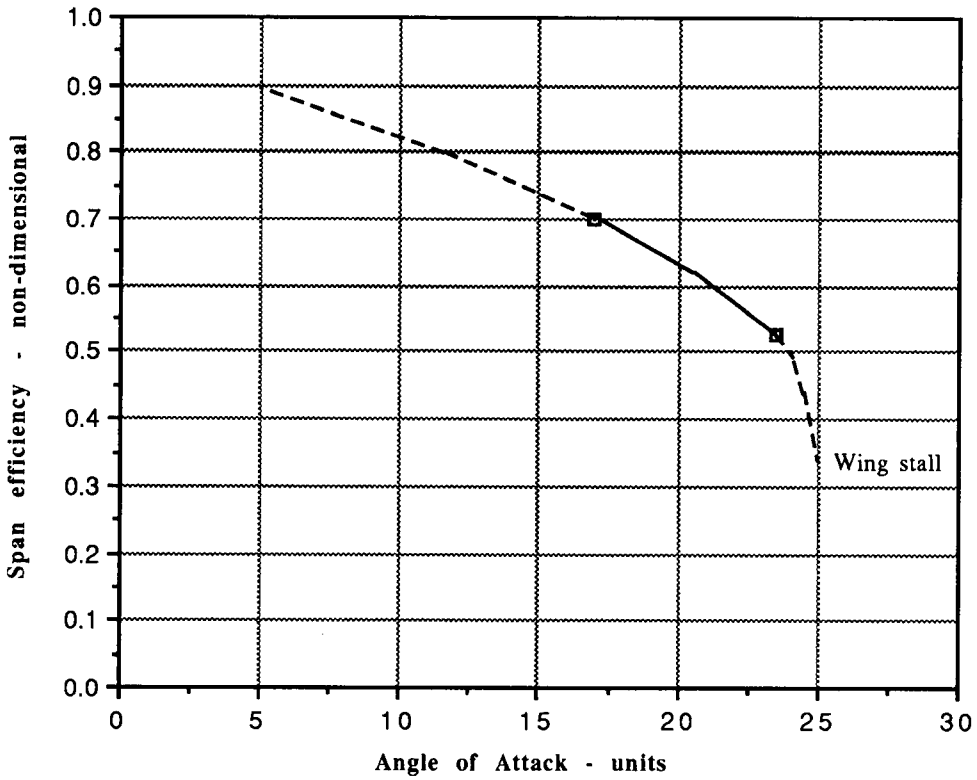

Figure 50
A-10A WINGSPAN EFFICIENCY

In succeeding sections, the following values will be used for e:

Range performance:	0.800
Endurance performance:	0.700
Maneuvering performance:	0.525

2. IMPROVED TAKEOFF DISTANCE

a. Given:

$W = 38{,}000$ lb.
$V_{t/o} = 140$ KOAS (236 ft./sec.)
$d_1 = 2{,}000$ ft. (takeoff distance)
$t_1 = 17$ sec. (takeoff time)
$T_1 = 18{,}000$ lb.
$T_2 = 27{,}000$ lb.

b. Determine aircraft mass:

$$m = W / g \qquad \text{eq. (17)}$$
$$= 38{,}000 / 32.2$$
$$= 1{,}180 \text{ sl.}$$

c. Determine average aircraft acceleration:

$$a = V_{t/o} / t_1 \qquad \text{eq. (18)}$$
$$= 236 \text{ ft./sec.} / 17 \text{ sec.}$$
$$= 13.9 \text{ ft./sec.}^2$$

d. Use: $F = ma$ eq. (19)
and: $F = T - D$ eq. (20)
to form: $T - D = ma$ eq. (21)

e. Solve for average drag during the takeoff roll:

$$D = T - ma \qquad \text{eq. (22)}$$
$$= 18000 - (1180)(13.9)$$
$$= 1600 \text{ lb.}$$

f. Solve for new average takeoff acceleration:

$$T - D = ma \qquad \text{eq. (21)}$$
$$a_2 = (T_2 - D) / m$$
$$= (27000 - 1600) / 1180$$
$$= 21.5 \text{ ft./sec.}^2$$

g. Solve for time to accelerate to takeoff speed:

$$t_2 = V_{t/o} / a_2$$
$$= 236 / 21.5$$
$$= 11.0 \text{ sec.}$$

h. Solve for new takeoff distance:

$$d_2 = V_{avg.}\, t_2$$
$$= (118)(11.0)$$
$$= 1300 \text{ ft.}$$

3. IMPROVED CLIMB PERFORMANCE

a: Given:

$V_{avg.}$ = 190 KOAS (321 ft./sec.)
W_a = 37,000 lb. (load A)
W_b = 37,000 lb. (load B)
t_a = 520 sec. (time from 5,000 to 25,000 ft., load A)
t_b = 205 sec. (time from 3,000 to 15,000 ft., load B)
T_1 = 18,000 lb.
T_2 = 27,000 lb.
FF_a = 4200 lb./hr. (average fuel flow, load A climb)
FF_b = 5000 lb./hr. (average fuel flow, load B climb)

b. Find average drag:

$P_s = V (T - D) / W$ eq. (3)

Knowing: $dh/dt = P_s$

$dh/dt = V (T - D) / W$ eq. (23)

$D = T - (dh\ W)/(dt\ V)$ eq. (24)

Load A: $D = 18000 - ((20000)(37000))/((520)(321))$
$= 13600$ lb.

Load B: $D = 18000 - ((12000)(38500))/((205)(321))$
$= 11000$ lb.

(An interesting note here; that load B shows a lower drag than load A. This is due to the free air temperature being lower during the day of load B flight tests, resulting in much improved engine performance, and the apparently lower drag.)

c. Solve for time to climb (same altitudes):

$dh/dt = V (T - D) / W$ eq. (23)

$dt = (dh\ W) / (V(T - D))$ eq. (25)

Load A: $t = (20000)(37000)/((321)(27000-13600))$
$= 172$ sec.

Load B: $t = (12000)(38500)/(321)(27000-11000))$
$= 90.0$ sec.

d. Solve for fuel to climb (assume same fuel flow):

$Fuel = (FF)(t)$ eq. (26)

Load A: $Fuel = (4200)(172/3600)$
$= 201$ lb.

Load B: $Fuel = (5000)(90/3600)$
$= 125$ lb.

e. Solve for distance to climb (convert KOAS to KTAS at average climb altitude):

$Distance = (V)(t)$

Load A: $Distance = (250)(172/3600)$
$= 11.9$ nm.

Load B: $Distance = (250)(90/3600)$
$= 6.25$ nm.

4. IMPROVED SINGLE-ENGINE PERFORMANCE

a. Given:

$T_1 = 9{,}000$ lb.
$T_2 = 13{,}500$ lb.
$P_{s1(120\ KOAS)} = 475$ ft./min.
$P_{s1(135\ KOAS)} = 490$ ft./min.
$P_{s1(150\ KOAS)} = 400$ ft./min.

b. Convert KOAS to true airspeed in ft./sec.:

120 KOAS = 130 KTAS = 13200 ft./sec.
135 KOAS = 146 KTAS = 14800 ft./sec.
150 KOAS = 163 KTAS = 16500 ft./sec.

c. To find new rates of climb:

$$P_s = V\,(T - D) / W \qquad \text{eq. (3)}$$

Rearrange:

$$W = (T - D) / P_s \qquad \text{eq. (27)}$$

As weight, airspeed, and drag will remain constant, equate original aircraft to improved aircraft parameters:

$$V(T_1 - D) / P_{s1} = V(T_2 - D) / P_{s2} \qquad \text{eq. (28)}$$

Cancelling:

$$T_1 / P_{s1} = T_2 / P_{s2} \qquad \text{eq. (29)}$$

or:

$$P_{s2} = P_{s1}\,(T_2 / T_1) \qquad \text{eq. (30)}$$
$$= P_{s1}\,(13500/9000)$$
$$= P_{s1}\,(1.5)$$

Solving:

$P_{s2(120\ KOAS)} = 712$ ft./min.
$P_{s2(135\ KOAS)} = 735$ ft./min.
$P_{s2(150\ KOAS)} = 600$ ft./min.

d. To solve for new climb angles:

$$\text{Climb Angle} = \sin^{-1}\,(P_s / V_{true}) \qquad \text{eq. (31)}$$

$$\text{Climb Angle.}_{(120\ KOAS)} = \sin^{-1}\,(712/13200)$$
$$= 3.10^{o}$$
$$\text{Climb Angle.}_{(135\ KOAS)} = \sin^{-1}\,(735/14800)$$
$$= 2.85^{o}$$
$$\text{Climb Angle.}_{(150\ KOAS)} = \sin^{-1}\,(600/16500)$$
$$= 2.08^{o}$$

5. IMPROVED RANGE

a: Given: $T_2 = (1.5)\, T_1$

b. For each stabilized point:

$$T = D \qquad \text{eq. (5)}$$

Therefore, the new specific ranges will be where:

$$D_2 = (1.5)\, D_1$$

Simply put, fuel flow will be assumed unchanged for a given throttle setting. With the thrust increase available on the new engines, the new airspeed at which the old fuel flow data was apparent will now occur where the drag has increased by 50%.

c. Use e = 0.8 (approximation for best range conditions).

d. Compute the drag for each flight condition:

$$D = c_{do}\gamma p_a S M^2/2 + (2W^2/\pi e A R S \gamma p_a M^2) \qquad \text{eq. (2)}$$
$$= (0.0883)(1.4)p_a(510)M^2/2 + (2W^2/\pi(0.800)(6.5)(510)(1.4)p_a M^2)$$

Substitute values for p_a, M, and W for each condition:

Flight Condition	Mach	Drag (lb.)
5,000 ft. MSL, load A:	0.23	5600
	0.26	5840
	0.33	7340
	0.41	10200
	0.57	18500
15,000 ft. MSL, load A:	0.30	5450
	0.39	6930
	0.43	7950
15,000 ft. MSL, load B:	0.32	6250
	0.39	7040
	0.50	10200
25,000 ft. MSL, load A:	0.35	5470
	0.38	5640
	0.48	7000
	0.57	8960

d. The drag numbers are graphed on figure 51, on the following page.

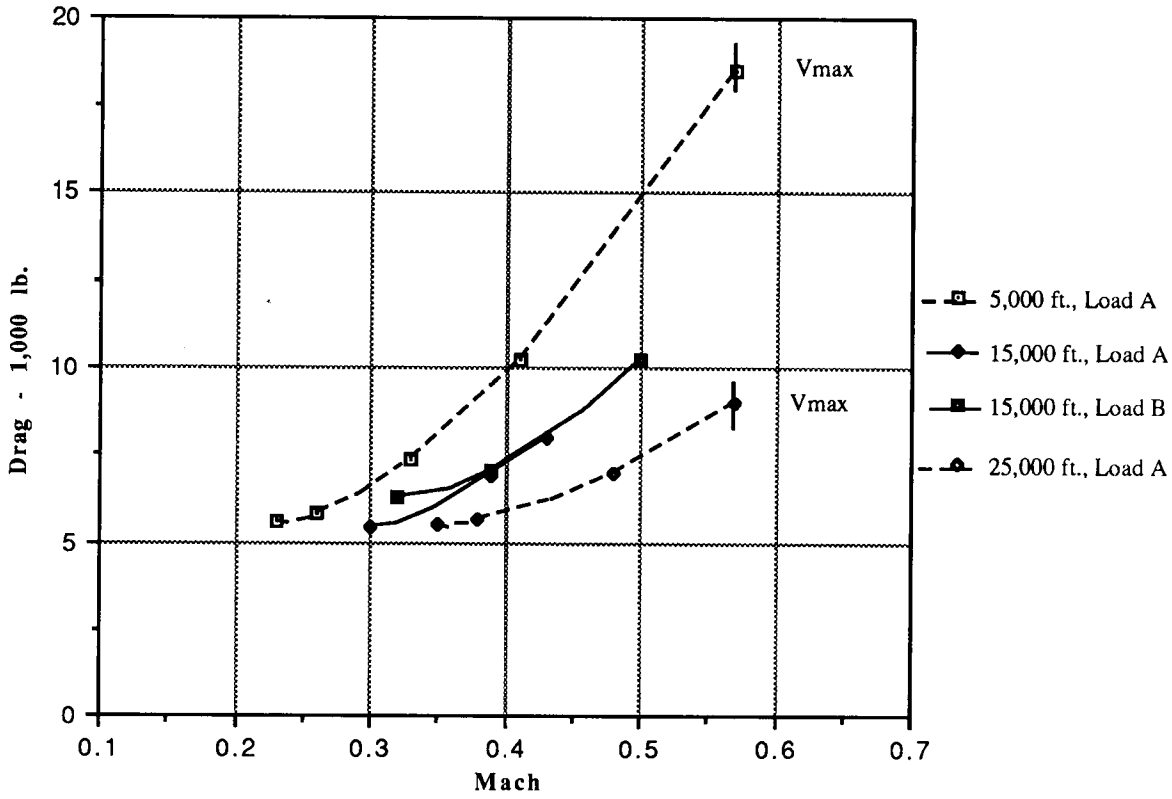

Figure 51
A-10A AIRCRAFT DRAG

f. From section b above, stable point fuel flows are assigned to the Mach number where the drag is 1.5 times higher than at the original point and are as follows:

Flight Condition	Mach	Fuel Flow (lb./hr.)
5,000 ft. MSL, load A:	0.36	2000
	0.38	2000
	0.42	2200
	0.51	2900
	0.68**	5850
15,000 ft. MSL, load A:	0.43	2000
	0.50	2150
	0.56*	2500
15,000 ft. MSL, load B:	0.47	1850
	0.51*	2050
	0.62*	3200
25,000 ft. MSL, load A:	0.54	1700
	0.56	1800
	0.62*	2000
	0.68**	3200

* - Indicates derived from extrapolation.
** - Indicates derived from maximum level airspeed data obtained on page 116.

6. IMPROVED LEVEL ACCELERATION

a: Given: H_{po} = 5000 ft. MSL
T_1 = 18000 lb.
T_2 = 27000 lb.
W = 35100 lb.
t_1 = 45 sec. (time to accelerate from 200 to 300 KOAS)

b. Find the aircraft mass:

$$m = W / g \qquad \text{eq. (18)}$$
$$= 35100 / 32.2$$
$$= 1090 \text{ sl.}$$

c. Determine average aircraft acceleration:

$$a = dV / dt \qquad \text{eq. (32)}$$
$$= 100 \text{ ft./sec./45 sec.}$$
$$= 2.22 \text{ ft./sec.}^2$$

d. Find the average drag:

$$D = T - ma \qquad \text{eq. (23)}$$
$$= 18000 - (1090)(2.22)$$
$$= 15600 \text{ lb.}$$

e. Solve for new acceleration:

$$a_2 = (T_2 - D) / m \qquad \text{eq. (33)}$$
$$= (27000 - 15600) / 1090$$
$$= 10.5 \text{ ft./sec.}^2$$

f. Solve for time from 200 to 300 KOAS:

$$t_2 = dV/a \qquad \text{eq. (34)}$$
$$= 100/10.5$$
$$= 9.52 \text{ sec.}$$

7. IMPROVED MAXIMUM LEVEL AIRSPEED

a: Given:

$T_1 = 18{,}000$ lb.
$T_2 = 27{,}000$ lb.
$W = 35{,}100$ lb.
$V_{max1} = 342$ KOAS (370 KTAS, 624 ft./sec.)

b: Solve for new performance:

$$T = c_{do}\rho S\, V^2/2 \qquad \text{eq. (6)}$$

Rearrange:

$$V = ((2T)/(c_{do}\rho S))^{0.5} \qquad \text{eq. (35)}$$

or:

$$V = ((2T_2)/(c_{do}\rho S))^{0.5}$$
$$= ((2(27{,}000)/(0.0883)(0.00205)(510))^{0.5}$$
$$= 765 \text{ ft./sec.}$$
$$= 453 \text{ KTAS}$$
$$= 415 \text{ KOAS (at 5,000 ft. MSL)}$$
$$= 0.68 \text{ M} \quad \text{(at 5,000 ft. MSL)}$$

8. IMPROVED MAXIMUM SUSTAINED TURN PERFORMANCE

a: Given:

H_{po} = 5000 ft. MSL
T_1 = 18000 lb.
T_2 = 27000 lb.
W = 34400 lb.

n_{z1}(200 KOAS) = 2.6g	(338 ft./sec.)
n_{z1}(250 KOAS) = 2.9g	(422 ft./sec.)
n_{z1}(300 KOAS) = 2.7g	(506 ft./sec.)
n_{z1}(325 KOAS) = 2.1g	(549 ft./sec.)
n_{z1}(338 KOAS) = 1.0g	(570 ft./sec.)

b. To find a way to correct turn performance for a change in thrust, start with:

$$D = c_{do}\rho SV^2/2 + (2W^2/\pi eARS\rho V^2) \quad \text{eq. (1)}$$

and:

$$P_s = V(T - D)/W \quad \text{eq. (3)}$$

In this case:

$$W = n_z W' \text{ (where W' is the gross weight)} \quad \text{eq. (8)}$$

Furthermore, because each point is a stable one:

$$T = D \quad \text{eq. (5)}$$

or:

$$dT = dD \quad \text{eq. (36)}$$

Therefore, find the change in drag:

$$dD = D_2 - D_1 = 2(n_{z2}^2 - n_{z1}^2)/\pi eARS\rho V^2 \quad \text{eq. (37)}$$

Substitute dT for dD and solve for n_{z2}:

$$n_{z2} = (n_{z1}^2 + ((dT\pi eARS\rho V^2)/2W^2))^{0.5} \quad \text{eq. (38)}$$

where dT is the difference in thrust, or:

$T_2 - T_1 = 27000 - 18000$
$= 9000$ lb.

c. Solve for new sustained performance:

$$n_{z2} = (n_{z1}^2 + (((9000)(\pi)(0.525)(6.5)(510)(0.00199)(V^2)/2(34400)^2))^{0.5}$$

Enter the appropriate n_{z1} and V values to get:

n_{z2}(200 KOAS) = 3.35g	
n_{z2}(250 KOAS) = 3.95g	
n_{z2}(300 KOAS) = 4.22g	
n_{z2}(325 KOAS) = 4.13g	
n_{z2}(338 KOAS) = 3.85g	

APPENDIX E

REVISED CURVES

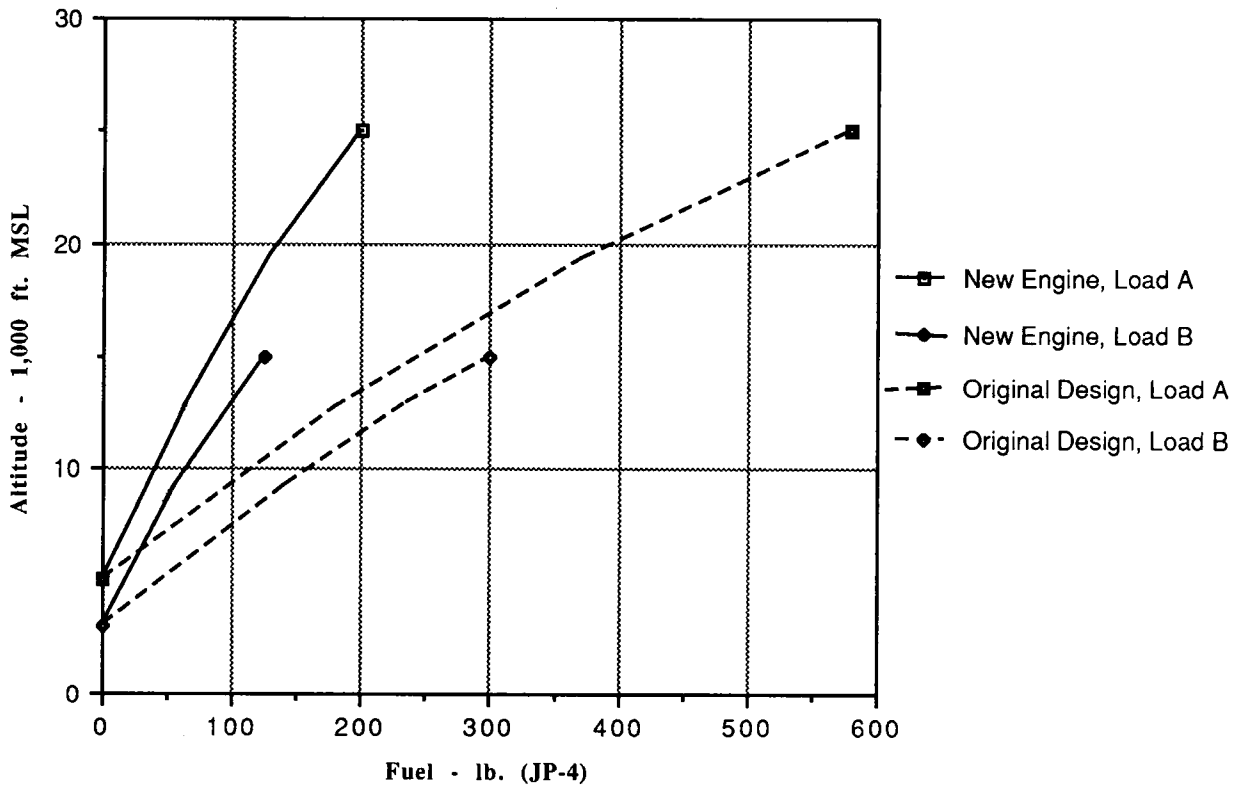

Improved climb performance was analyzed in appendix D, section 3. Ambient conditions and aircraft weight remain the same as presented in Appendix C, figure 4.

Figure 52
IMPROVED FUEL TO CLIMB

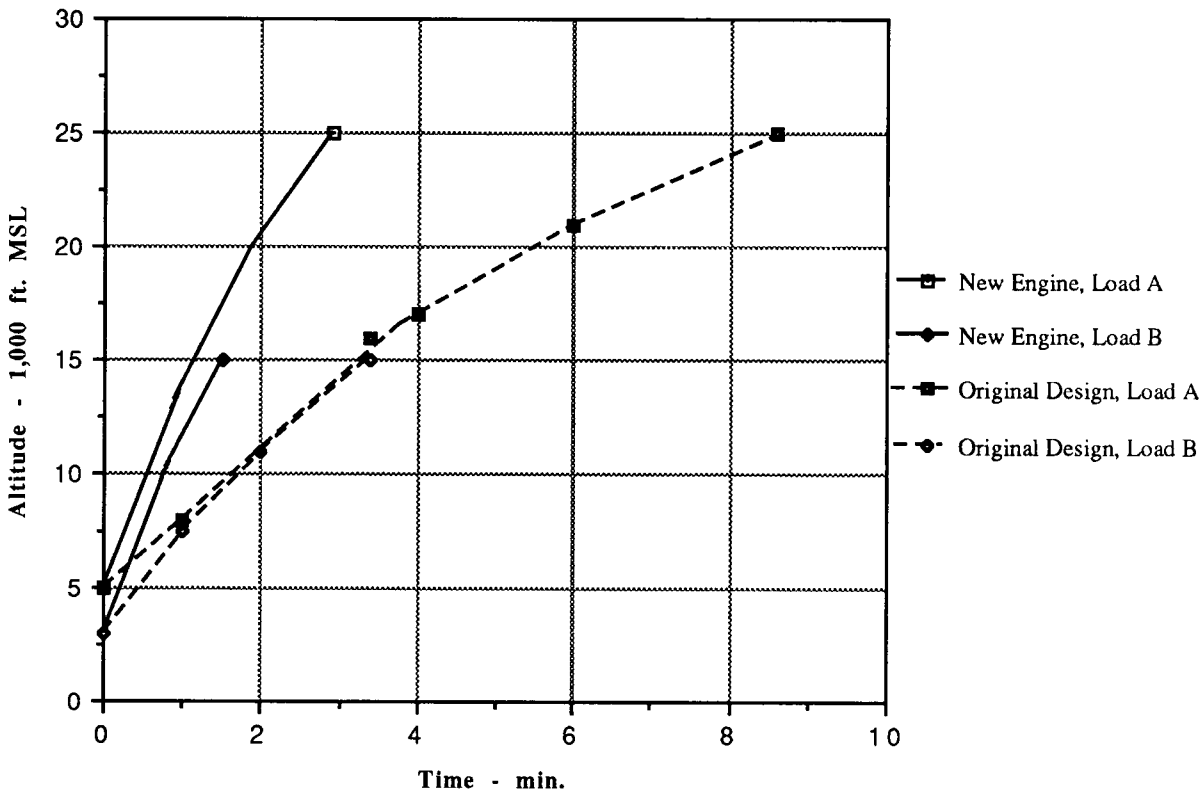

Improved climb performance was analyzed in appendix D, section 3. Ambient conditions and aircraft weight remain the same as presented in Appendix C, figure 5.

Figure 53
IMPROVED TIME TO CLIMB

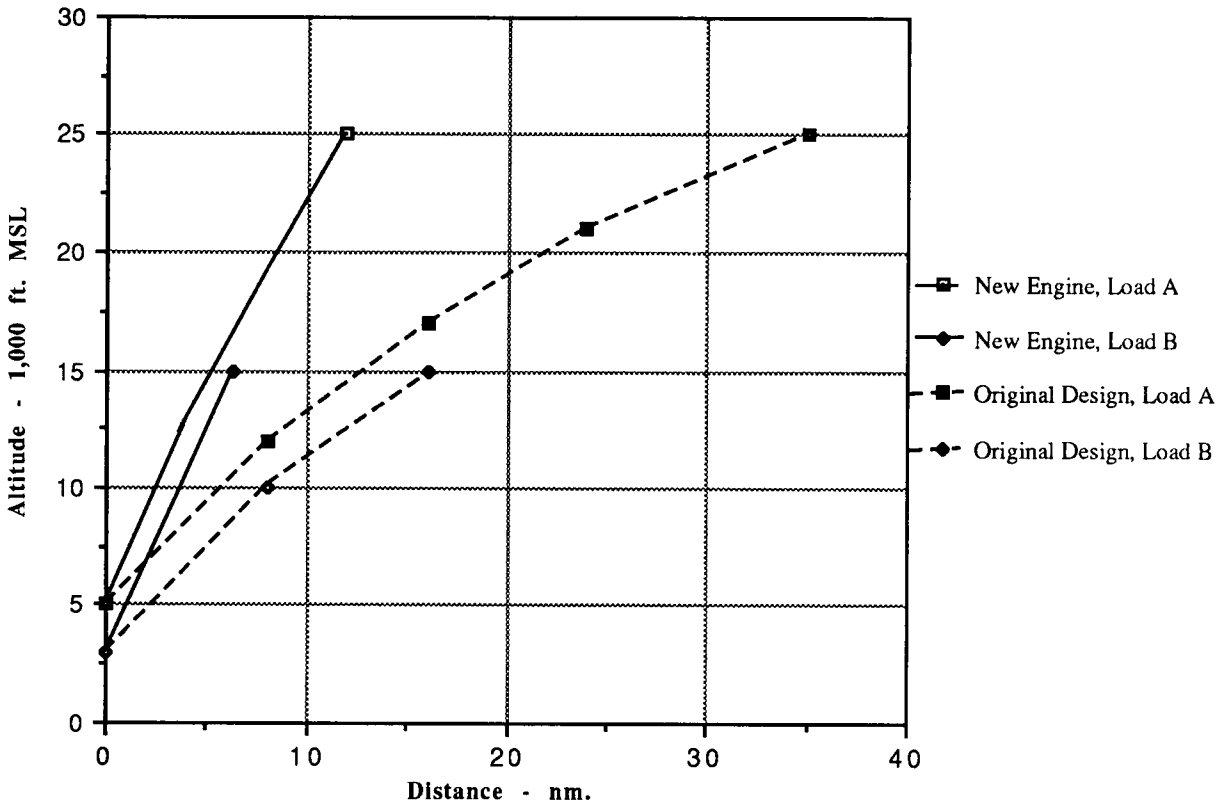

Improved climb performance was analyzed in appendix D, section 3. Ambient conditions and aircraft weight remain the same as presented in Appendix C, figure 6.

Figure 54
IMPROVED DISTANCE TO CLIMB

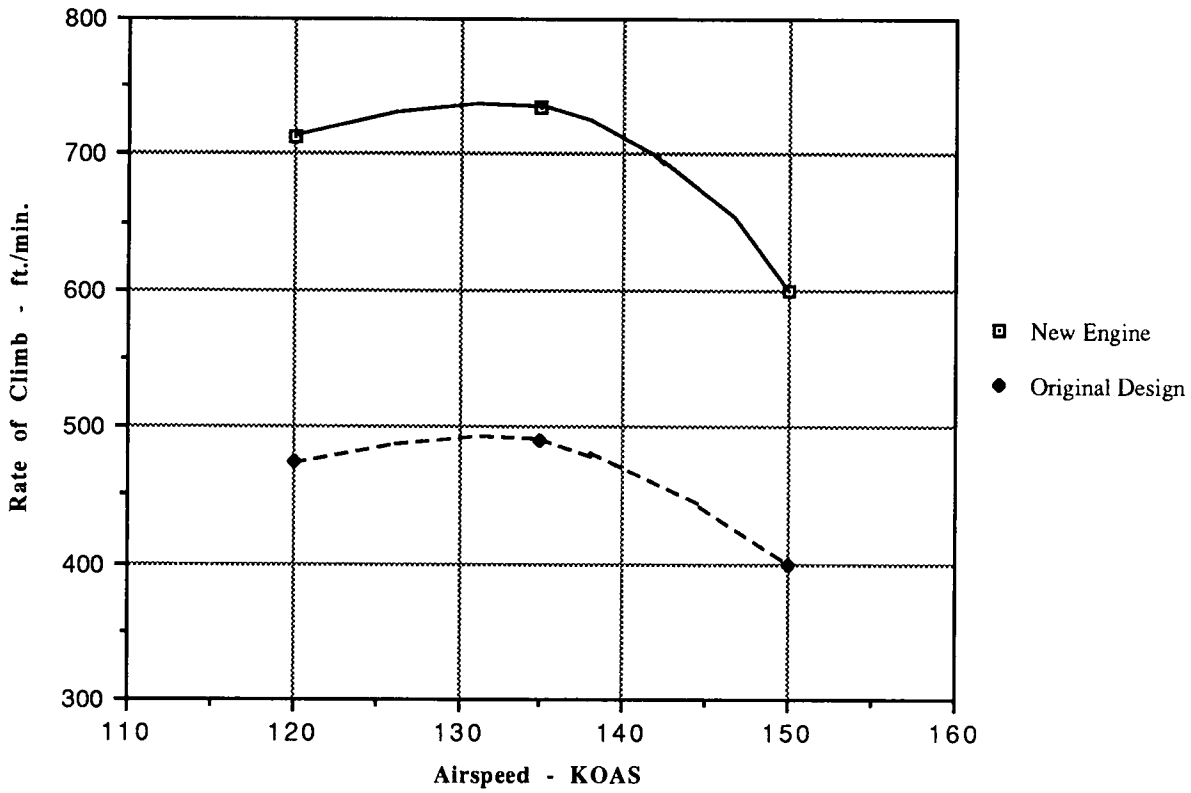

Improved single-engine performance was analyzed in appendix D, section 4. Ambient conditions and aircraft weight remain the same as presented in Appendix C, figure 7.

Figure 55
IMPROVED SINGLE-ENGINE RATE OF CLIMB

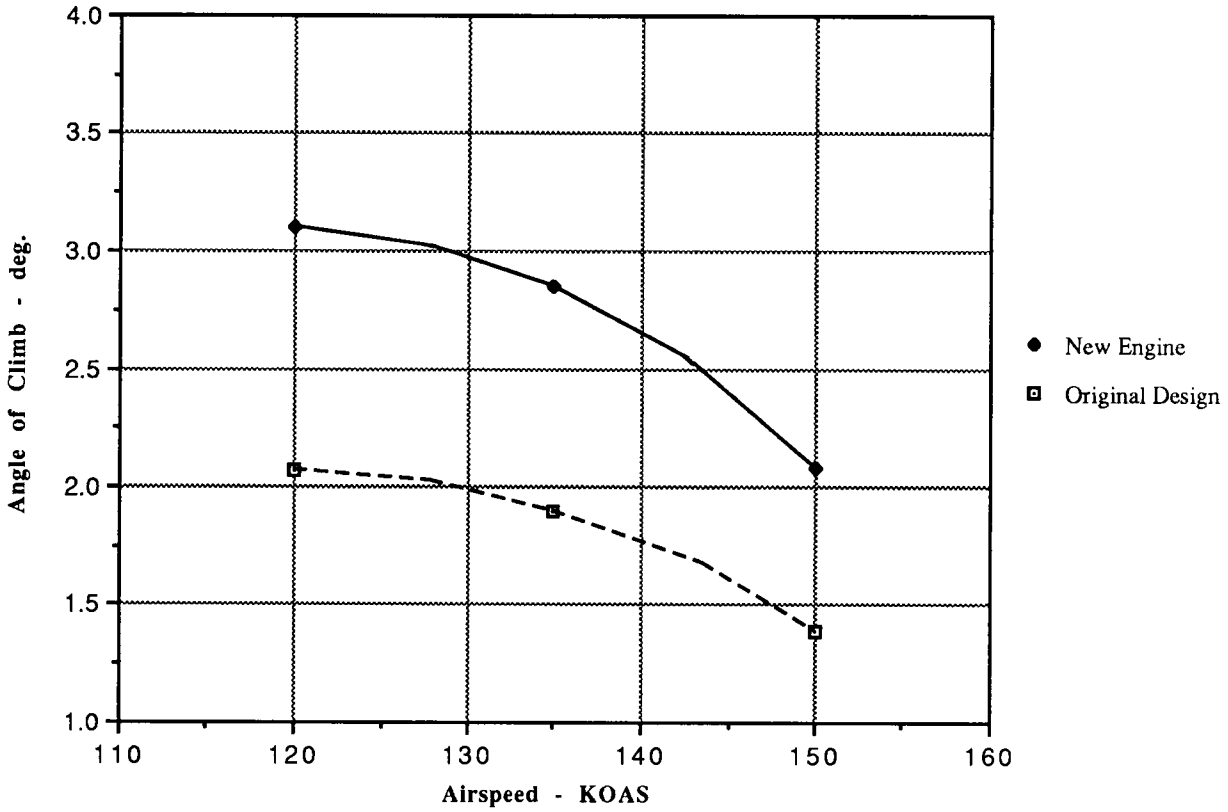

Improved single-engine performance was analyzed in appendix D, section 4. Ambient conditions and aircraft weight remain the same as presented in Appendix C, figure 8.

Figure 56
IMPROVED SINGLE-ENGINE ANGLE OF CLIMB

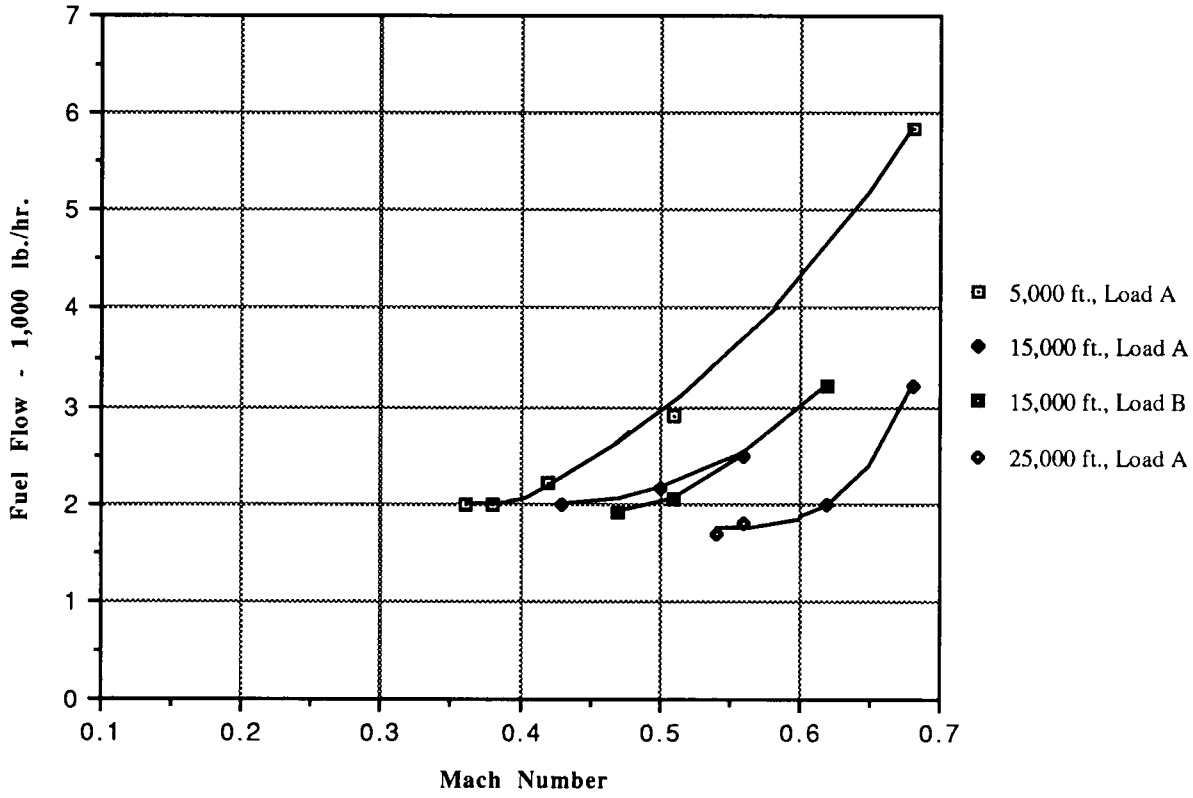

Improved range performance was analyzed in appendix D, section 5. Ambient conditions and aircraft weight remain the same as presented in Appendix C, figure 9.

Figure 57
IMPROVED CRUISE FUEL FLOW

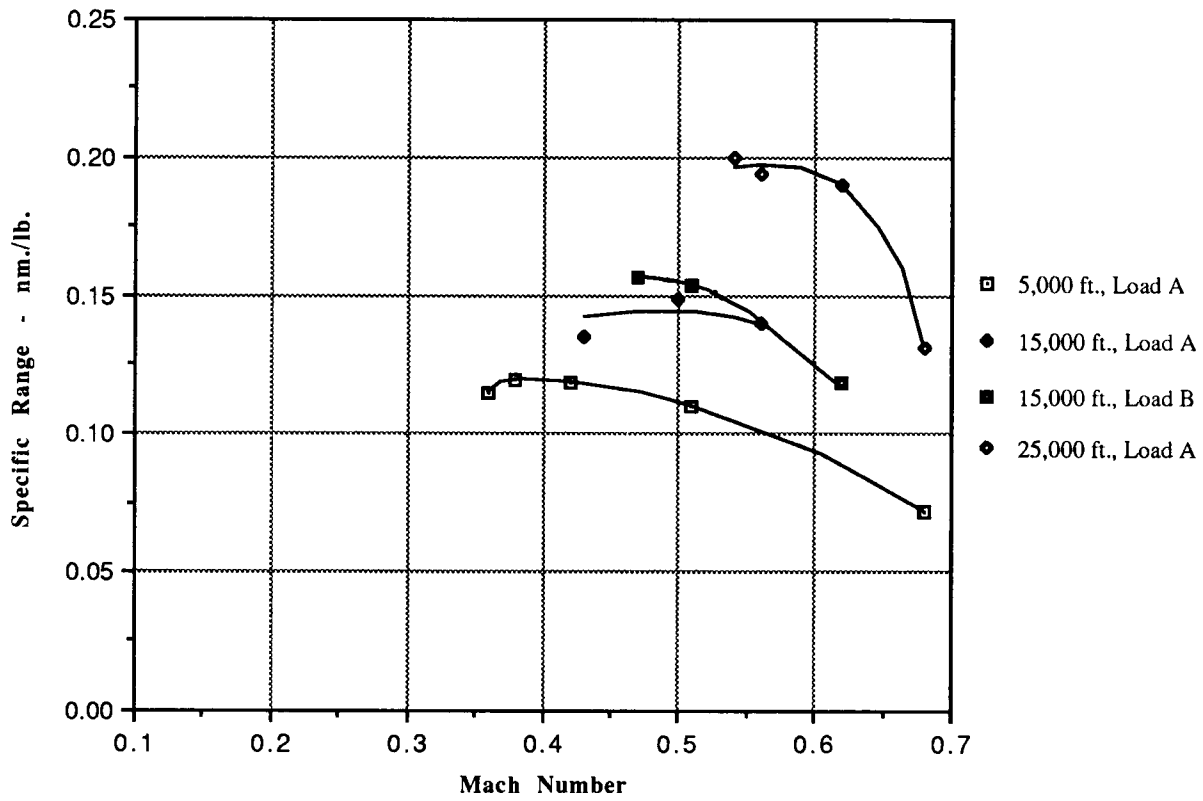

Improved range performance was analyzed in appendix D, section 5. Ambient conditions and aircraft weight remain the same as presented in Appendix C, figure 10.

Figure 58
IMPROVED CRUISE SPECIFIC RANGE

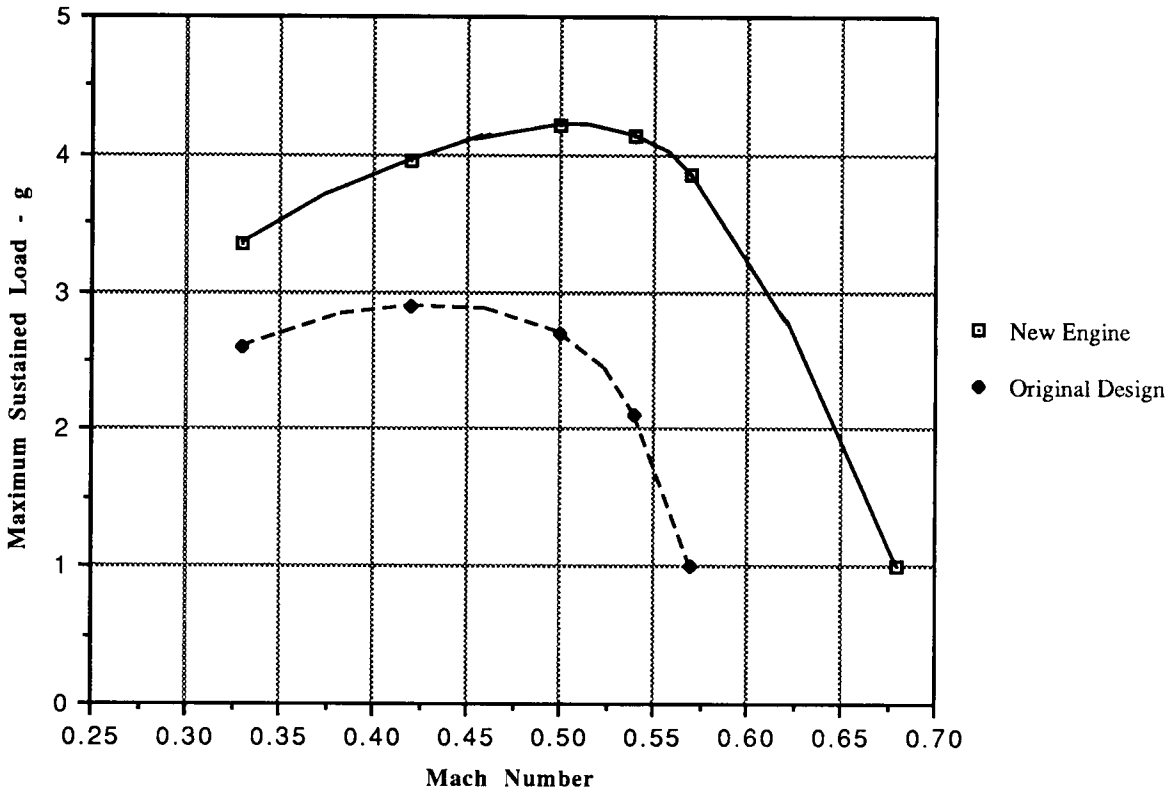

Improved maximum sustained turn performance was analyzed in appendix D, section 8. Ambient conditions and aircraft weight remain the same as presented in Appendix C, figure 14.

Figure 59
IMPROVED MAXIMUM SUSTAINED LOAD FACTOR

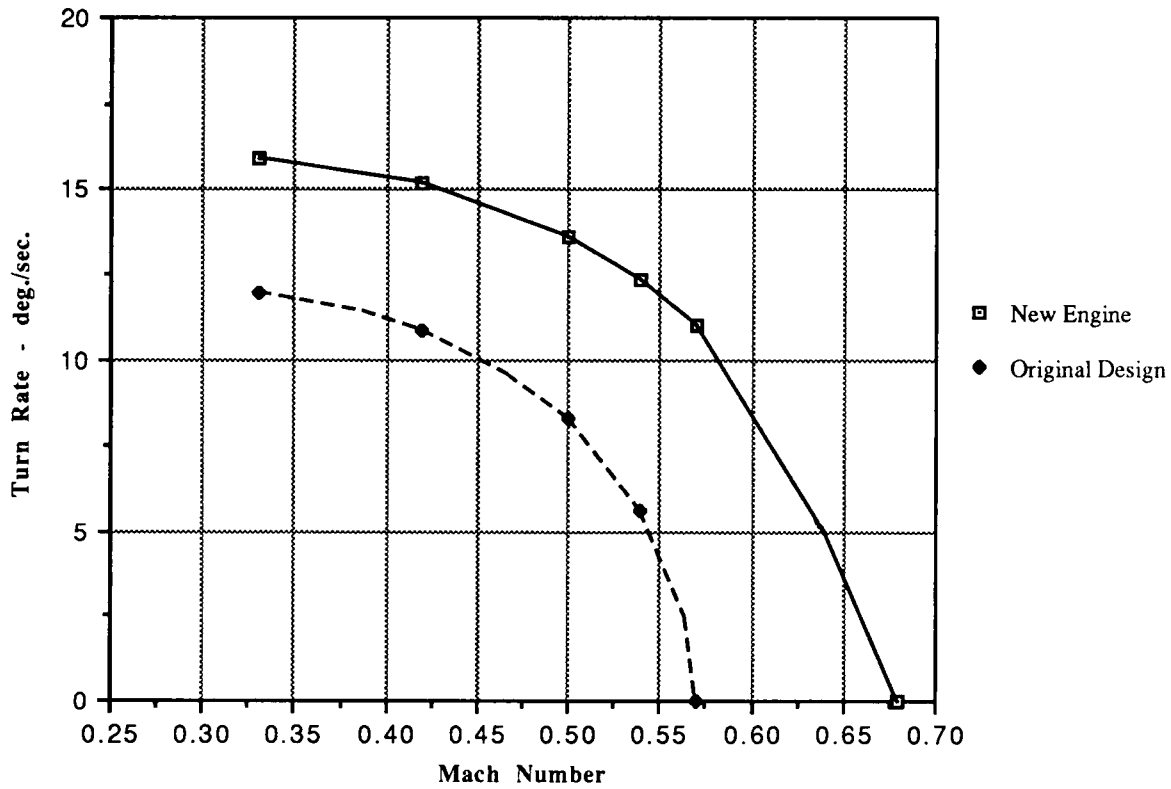

Improved maximum sustained turn performance was analyzed in appendix D, section 8. Ambient conditions and aircraft weight remain the same as presented in Appendix C, figure 15.

Figure 60
IMPROVED MAXIMUM SUSTAINED TURN RATE

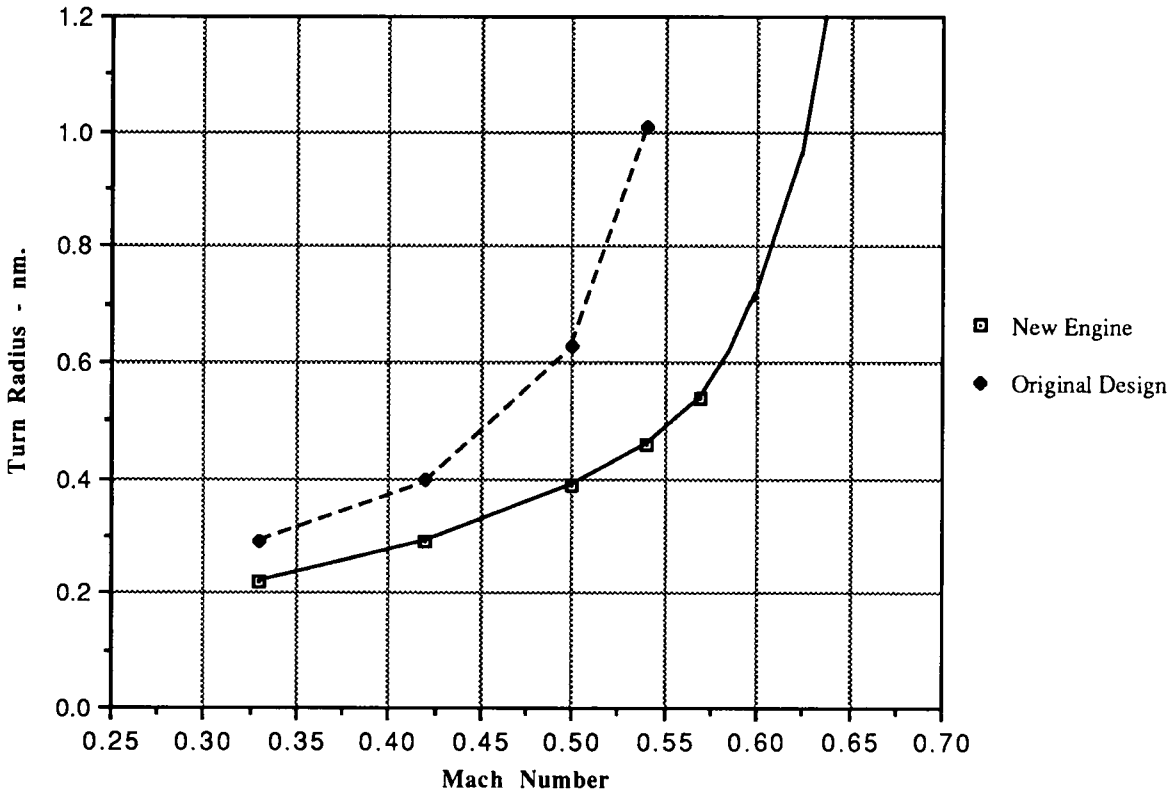

Improved maximum sustained turn performance was analyzed in appendix D, section 8. Ambient conditions and aircraft weight remain the same as presented in Appendix C, figure 16.

Figure 61
IMPROVED MINIMUM SUSTAINED TURN RADIUS

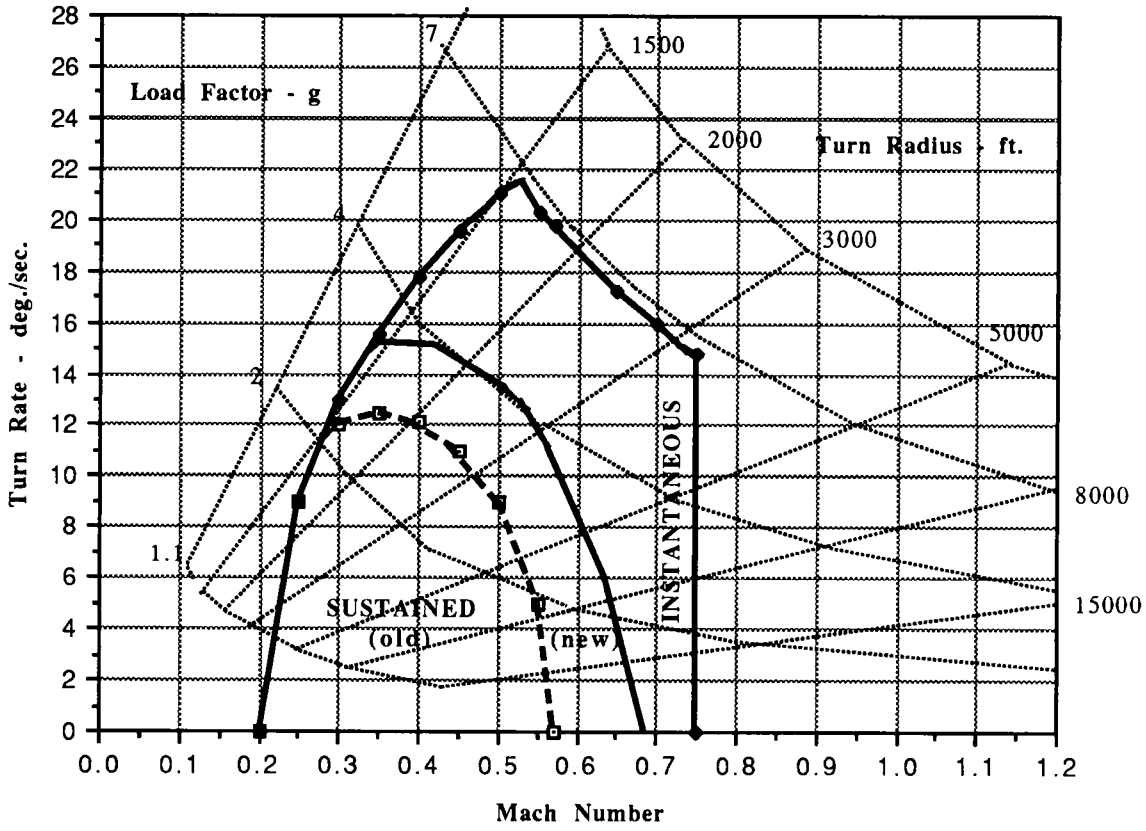

Improved maximum sustained turn performance was analyzed in appendix D, section 8. Ambient conditions and aircraft weight remain the same as presented in Appendix C, figure 26.

Figure 62
IMPROVED TOTAL MANEUVERING ENVELOPE

APPENDIX F

LIST OF SYMBOLS

LIST OF SYMBOLS

AGL	Above Ground Level
AOA	Angle of Attack (units indicated)
c_d	Coefficient of drag
c_{di}	Coefficient of drag (induced portion)
c_{do}	Coefficient of drag (parasitic portion)
c_L	Coefficient of lift
$^oF.$	Degrees Fahrenheit
D	Drag
deg.	Degrees
ft.	Feet
γ	Ratio of specific heats for air (1.4)
hr.	Hours
in.	Inches
KOAS	Knots of Observed Airspeed
Kt.	Knots
KTAS	Knots of True Airspeed
L	Lift
lb.	Pounds of force
M	Mach Number
min.	Minute
MSL	Mean Sea Level
nm.	Nautical Miles
%MAC	Percent Mean Aerodynamic Chord
π	(3.14)
p_a	Atmospheric pressure
psi	Pounds per Square Inch
rad.	Radians
ρ	Atmospheric density
sec.	Seconds
sl.	Slugs
VMC	Visual Meteorological Conditions